



Future Automotive Systems Technology Simulator (FASTSim) Validation Report – 2021

Chad Baker, Matthew Moniot, Aaron Brooker,
Lijuan Wang, Eric Wood, and Jeffrey Gonder

National Renewable Energy Laboratory

**NREL is a national laboratory of the U.S. Department of Energy
Office of Energy Efficiency & Renewable Energy
Operated by the Alliance for Sustainable Energy, LLC**

This report is available at no cost from the National Renewable Energy
Laboratory (NREL) at www.nrel.gov/publications.

Contract No. DE-AC36-08GO28308

Technical Report
NREL/TP-5400-81097
October 2021



Future Automotive Systems Technology Simulator (FASTSim) Validation Report – 2021

Chad Baker, Matthew Moniot, Aaron Brooker,
Lijuan Wang, Eric Wood, and Jeffrey Gonder

National Renewable Energy Laboratory

Suggested Citation

Baker, Chad, Matthew Moniot, Aaron Brooker, Lijuan Wang, Eric Wood, and Jeffrey Gonder. 2021. *Future Automotive Systems Technology Simulator (FASTSim) Validation Report – 2021*. Golden, CO: National Renewable Energy Laboratory. NREL/TP-5400-81097. <https://www.nrel.gov/docs/fy22osti/81097.pdf>.

**NREL is a national laboratory of the U.S. Department of Energy
Office of Energy Efficiency & Renewable Energy
Operated by the Alliance for Sustainable Energy, LLC**

This report is available at no cost from the National Renewable Energy Laboratory (NREL) at www.nrel.gov/publications.

Contract No. DE-AC36-08GO28308

Technical Report
NREL/TP-5400-81097
October 2021

National Renewable Energy Laboratory
15013 Denver West Parkway
Golden, CO 80401
303-275-3000 • www.nrel.gov

NOTICE

This work was authored by the National Renewable Energy Laboratory, operated by Alliance for Sustainable Energy, LLC, for the U.S. Department of Energy (DOE) under Contract No. DE-AC36-08GO28308. Funding provided in part by the U.S. Department of Energy Office of Energy Efficiency and Renewable Energy Vehicle Technologies Office. The views expressed herein do not necessarily represent the views of the DOE or the U.S. Government.

This report is available at no cost from the National Renewable Energy Laboratory (NREL) at www.nrel.gov/publications.

U.S. Department of Energy (DOE) reports produced after 1991 and a growing number of pre-1991 documents are available free via www.OSTI.gov.

Cover Photos by Dennis Schroeder: (clockwise, left to right) NREL 51934, NREL 45897, NREL 42160, NREL 45891, NREL 48097, NREL 46526.

NREL prints on paper that contains recycled content.

Preface

The National Renewable Energy Laboratory's Future Automotive Systems Technology Simulator (FASTSim) captures the most important factors influencing vehicle power demands and performs large-scale fuel efficiency calculations very quickly. These features make FASTSim well suited to evaluate a representative distribution of real-world fuel efficiency over a large quantity of in-use driving profiles, which have become increasingly available in recent years owing to incorporation of Global Positioning System data collection into various travel surveys and studies. In addition, by being open source, computationally lightweight, freely available, and free from expensive third-party software requirements, analyses conducted using FASTSim may be easily replicated and critiqued in an open forum. This is highly desirable for situations in which technical experts seek to reach consensus over questions about what vehicle development plans or public interest strategies could maximize fuel savings and minimize adverse environmental impacts with an evolving vehicle fleet. While FASTSim continues to be refined and improved on an ongoing basis, this report compiles available runs using versions of the tool from the past few years to provide illustrative comparisons of the model results against measured data.

Acknowledgments

The core development and use of FASTSim have been funded for many years by the Vehicle Systems Program, the Analysis Program, and the Energy Efficient Mobility Systems Program at the Vehicle Technologies Office in the U.S. Department of Energy's Office of Energy Efficiency and Renewable Energy. The authors would particularly like to thank the U.S. Department of Energy's David Anderson, Lee Slezak, and Jacob Ward for their support and feedback through the years.

List of Acronyms

AC	air conditioning
ANL	Argonne National Laboratory
DOE	U.S. Department of Energy
EPA	U.S. Environmental Protection Agency
EV	electric vehicle
FASTSim	Future Automotive Systems Technology Simulator
FTP	Federal Test Procedure
HEV	hybrid electric vehicle
HVAC	heating, ventilation, and air conditioning
HWFET	Highway Fuel Economy Test
mpg	miles per gallon
MPGGE	miles per gasoline gallon equivalent
mph	miles per hour
NREL	National Renewable Energy Laboratory
PHEV	plug-in hybrid electric vehicle
PTC	positive temperature coefficient
RMSE	root-mean-square error
UDDS	Urban Dynamometer Driving Schedule

Executive Summary

The National Renewable Energy Laboratory (NREL) has been developing and using the Future Automotive Systems Technology Simulator (FASTSim) for roughly two decades in support of the U.S. Department of Energy’s (DOE’s) transportation research goals. FASTSim produces rapid estimates of vehicle efficiency, performance, cost, and battery life in conventional and advanced powertrain technologies, enabling completion of such analyses using a modest set of publicly available vehicle parameters. This streamlined approach provides accurate results for many types of analysis while increasing speed, ease of use, and value related to finding required inputs, running the model, and interpreting results. FASTSim can also use customized inputs to represent specific vehicles even more precisely if detailed input data are available and the particular analysis warrants such increased fidelity.

As with any model, the most critical aspect of FASTSim is its ability to reflect reality accurately. This is the purpose of validation—the comparison of modeling outputs versus results measured during vehicle or component operation in the laboratory or on the road. This report begins by describing FASTSim and its role within the continuum of available modeling tools, and then focuses on the validation of FASTSim.

FASTSim occupies a “sweet spot” along the continuum of modeling tools based on each tool’s trade-off between accuracy and complexity, where “complexity” includes the required number of input parameters, availability of required input data, time required to obtain the inputs and perform calibration, software requirements, and computational overhead to run (Figure ES-1). FASTSim is designed to balance predictive accuracy with model complexity across a wide range of analytical tasks. Across its range of capabilities, FASTSim is particularly well suited for quickly and conveniently conducting large numbers of simulations over representative real-world driving distributions and/or myriad vehicle design variations. In such analyses, the uncertainties and efficiency impacts from the broad spectrum of operating conditions or design variants far exceed small uncertainties resulting from modeling simplifications within FASTSim.

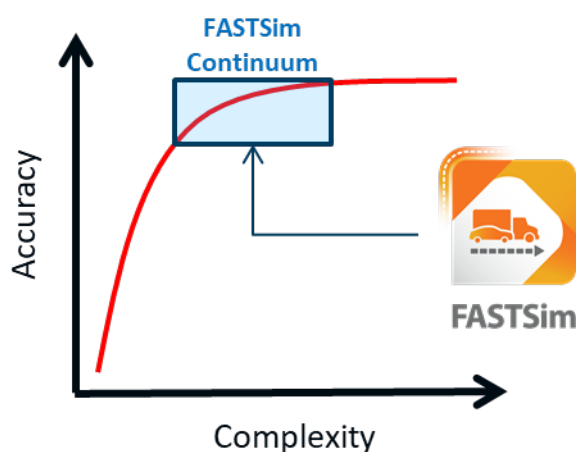


Figure ES-1. Conceptual illustration of the FASTSim continuum on the vehicle modeling continuum

FASTSim’s continuum of modeling capabilities—illustrated by the box in Figure ES-1—can be divided conceptually into different levels (Table ES-1). The base option is suitable for large-scale simulation of hundreds or even thousands of vehicles. It employs generally representative default maps of power versus efficiency for each of the components, which are then scaled based on the component power ratings for a particular modeled vehicle. Thus, the base option has the fastest calibration, only requiring a small amount of publicly available vehicle information, and still captures the most important factors for high-level vehicle comparisons. However, for some targeted studies, more component data details may be available on specific vehicles of interest and/or the studies may seek to investigate scenarios sensitive to factors such as operating temperature or gear selection. For these situations, FASTSim enables further customization and the addition of modeling extensions, moving the model up the trade-off curve of accuracy versus complexity.

Table ES-1. FASTSim Continuum: Modeling Levels and Their Strengths and Limitations

Level of Modeling	Strengths	Limitations
Base Option		
<ul style="list-style-type: none"> • Default power versus efficiency maps for each component • Maps scaled based on component power ratings for modeled vehicle 	<ul style="list-style-type: none"> • Fastest to calibrate, requires small amount of public vehicle information • Suitable for large-scale simulation/evaluation of thousands of vehicle designs 	<ul style="list-style-type: none"> • Captures most important factors for high-level comparisons but lacks detail that may be needed for some focused studies
Customized Option		
<ul style="list-style-type: none"> • Vehicle-specific component calibration 	<ul style="list-style-type: none"> • Provides more precise model of specific vehicle(s) 	<ul style="list-style-type: none"> • Larger calibration burden, requires detailed component-level data from manufacturer or testing
Potential Extensions for Targeted Investigations		
<ul style="list-style-type: none"> • Temperature dependence • Torque versus speed disaggregation • Shift schedules • Transmission impacts 	<ul style="list-style-type: none"> • Even more detail for studies that need it • Precise validation in numerous dimensions and conditions 	<ul style="list-style-type: none"> • Further increases calibration burden • Still not suitable for applications requiring real-time control (e.g., hardware-in-the-loop testing)

At the base level, FASTSim’s power-based engine model provides a well-validated reduction of more intricate and computationally intense torque-versus-speed models, which are higher on the accuracy-complexity continuum. FASTSim’s representative efficiency-power engine maps have been shown to scale well to various engine sizes. FASTSim’s power-based approach works similarly well for modeling other components, such as electric motors.

At the vehicle level, road load and energy consumption results generated using FASTSim’s base option validate well against chassis dynamometer data for conventional gasoline vehicles, hybrid electric vehicles, plug-in hybrid electric vehicles, battery electric vehicles, and fuel cell vehicles. Figure ES-2 gives an example of the fit between measured and modeled results for a Chevrolet

Volt over sections of the high-speed, high-acceleration US06 drive cycle. While the second-by-second validation results for FASTSim’s base option using generic component maps do not agree exactly with the measured data, they do provide reasonable overall agreement.

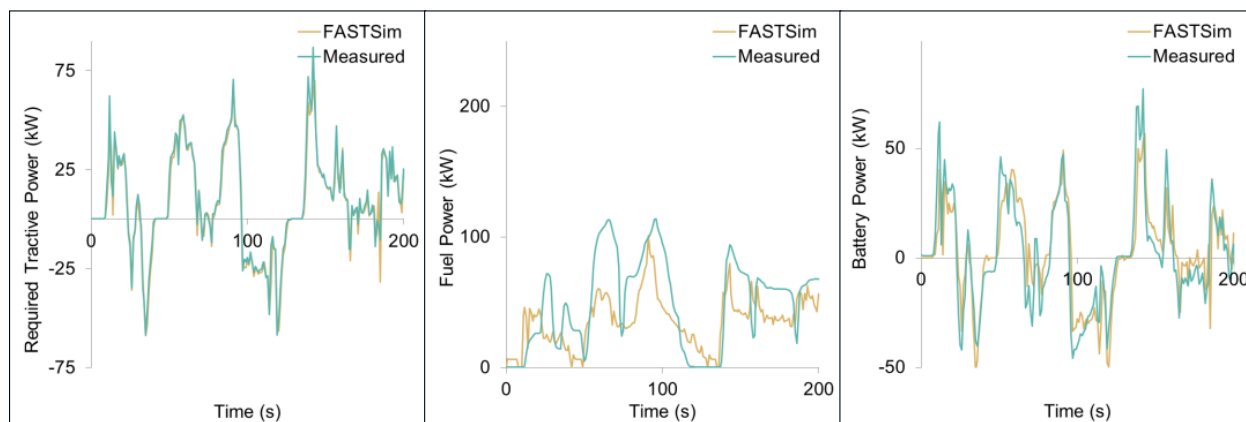


Figure ES-2. Time series validation: Chevrolet Volt, US06

Additionally, full-cycle-level FASTSim base fuel economy and performance results validate well for a wide range of vehicles. Figure ES-3 and Figure ES-4 show the fuel economy and electricity consumption validation for an assortment of conventional, hybrid, fuel cell, and battery electric vehicles. Figure ES-5 shows the FASTSim base acceleration validation for these vehicles. The full report demonstrates equally strong fuel economy, electricity consumption and acceleration validation for a set of roughly 700 existing vehicles, with simulated results typically falling within 10% of measured data and often within 5%.

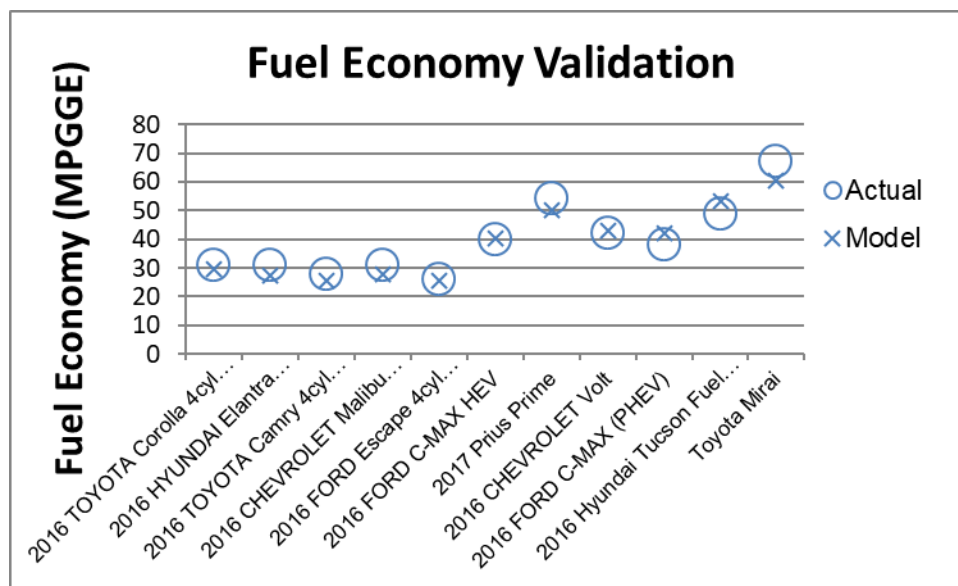


Figure ES-3. FASTSim fuel economy validation versus EPA window sticker data for a range of example vehicles

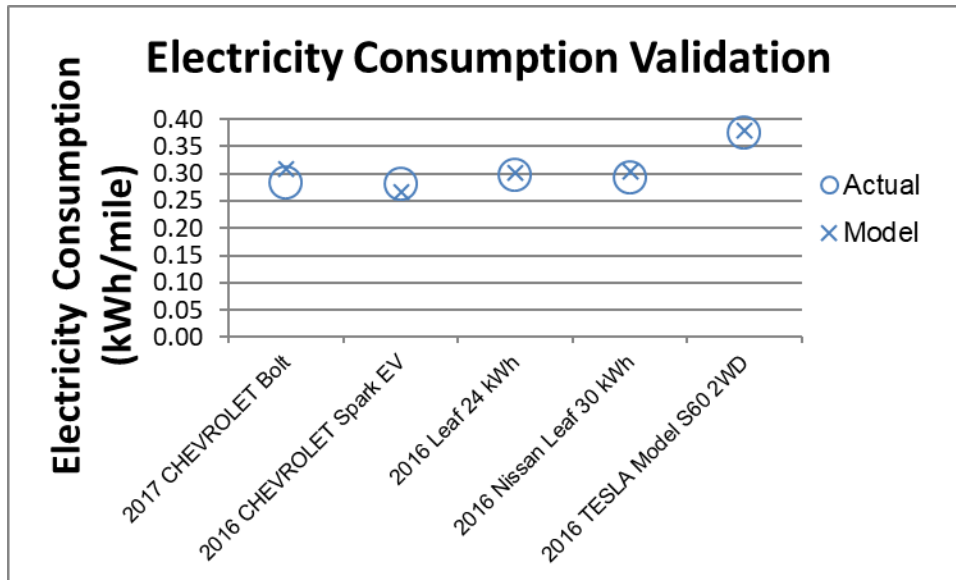


Figure ES-4. FASTSim electricity consumption validation versus EPA window sticker data for example EVs

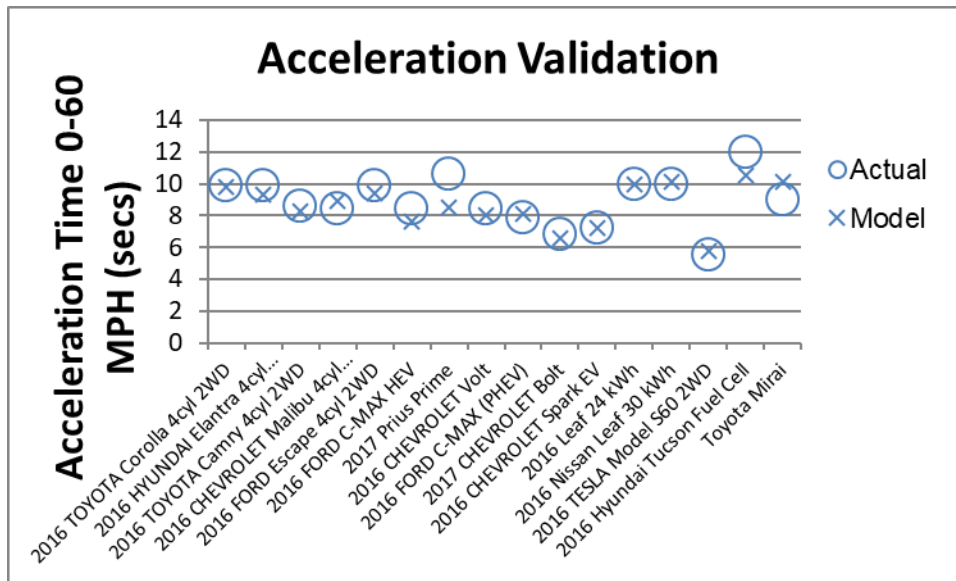


Figure ES-5. FASTSim acceleration validation versus Zeroto60Times website data for a range of example vehicles

Over its development history, NREL has and continues to add various improvements and enhancements to FASTSim. These include maintaining the original Excel platform for the tool, which is approachable by any user regardless of software experience level, along with a more recent Python platform for FASTSim, which facilitates large-scale simulations over real-world driving data and contains a variety of advanced features. This report describes various FASTSim feature enhancements, including efforts to incorporate a generalized thermal modeling capability given the substantial vehicle energy consumption impacts that arise when vehicles are operated over a range of temperature conditions. Figure ES-6 shows example results from a semi-empirical

thermal modeling enhancement to FASTSim (tuned from publicly-available data), and how this enhancement enables the simulation to closely match actual energy consumption measured over a cold temperature chassis dynamometer test—virtually eliminating the discrepancy relative to modeling that does not account for the temperature conditions of the test.

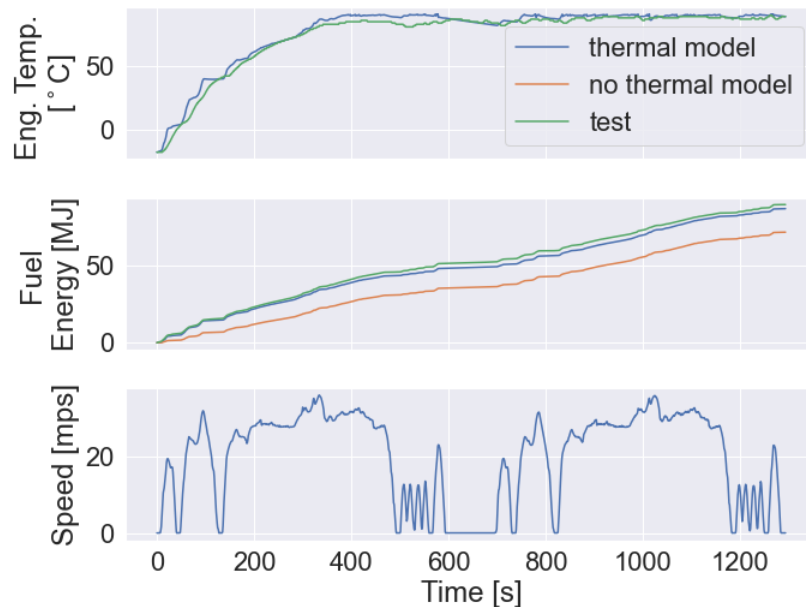


Figure ES-6. (Top) Engine temperature for model and test; (middle) cumulative fuel energy consumed for thermal model, baseline model without any thermal effects, and test; and (bottom) vehicle speed vs. time for repeated US06 tests conducted in 0°F/–17.8°C.

When FASTSim moves beyond generalized component/feature representations scaled for a given vehicle to detailed sub-models individually tailored for a specific application, the modeling is described as moving from FASTSim’s base option to FASTSim’s customized option with potential extensions. Calibrated FASTSim custom models align very closely with second-by-second operating data for a modeled vehicle and its components, as illustrated in Figure ES-7 for a measured versus FASTSim custom modeled fuel consumption profile.

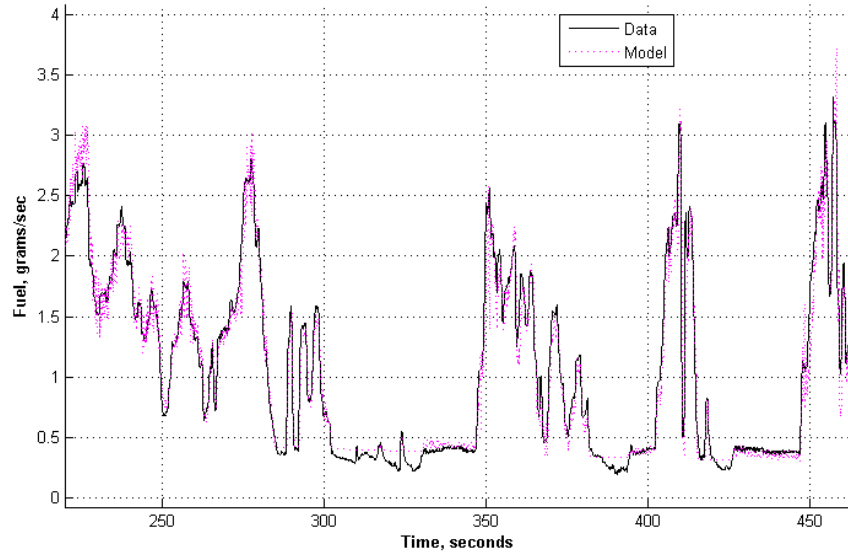


Figure ES-7. Example of precise fuel consumption validation enabled by FASTSim’s customized option with extensions for select components

Example vehicle-level FASTSim custom model validation is demonstrated by a project where NREL and Argonne National Laboratory (ANL) collected detailed test data on a highly instrumented Ford Fusion midsize conventional vehicle. Chassis dynamometer data were used to calibrate a customized FASTSim model of the Fusion, which included estimating impacts from engine oil viscosity and fuel enrichment using lumped thermal models for engine oil/coolant and exhaust catalyst—producing an engine efficiency model sensitive to both engine power and thermal state. The resulting model calculates fuel consumption to within 2.4% root-mean-square error (RMSE) on the chassis dynamometer test cycles, which is within the range of cycle-to-cycle dynamometer test uncertainty. NREL and ANL subsequently performed on-road testing of the highly instrumented Ford Fusion. Figure ES-8 shows the validation of the customized FASTSim model against the on-road data. Overall, the model matches the measured results within a 5.6% RMSE, showing that FASTSim trained on a limited set of dynamometer cycles can perform well over a broad range of real-world conditions (over which trip-level fuel economy varies by more than $\pm 50\%$ from the average for the vehicle).

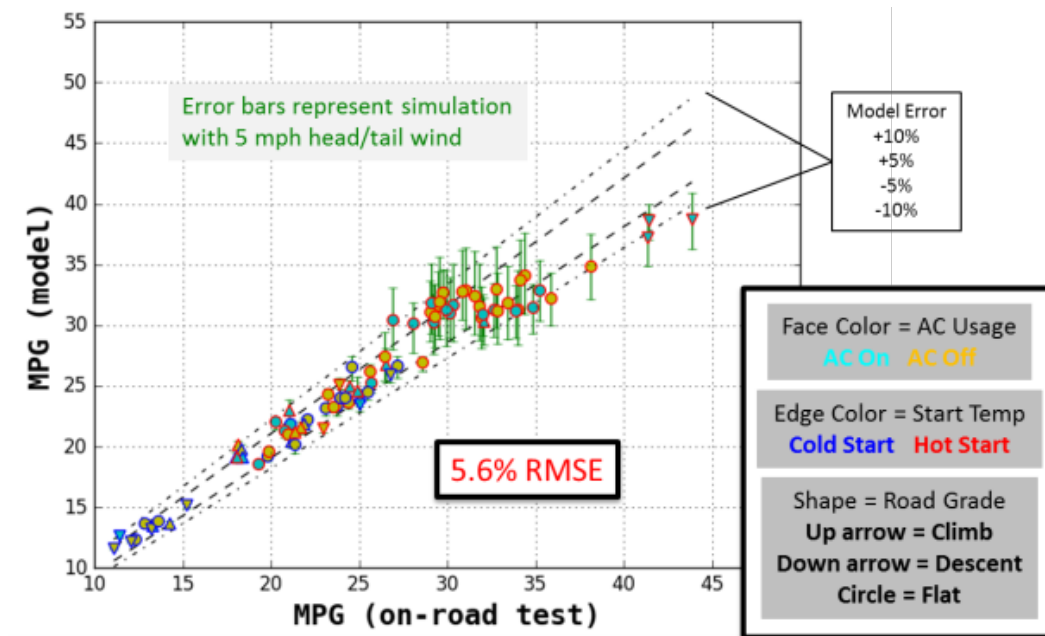


Figure ES-8. Validation of FASTSim custom modeled versus measured fuel economy over on-road driving

This report additionally summarizes the widespread referencing of FASTSim in the literature. Many of the numerous studies that use FASTSim are from NREL, but additional users include DOE, other national laboratories, automakers, the California Air Resources Board, Google, and American and foreign universities and research centers. The publicly released version of FASTSim has been robust, with thousands of unique downloads and no reports of major errors or inaccuracies.

Finally, public sponsorship and open-source code add transparency and credibility to FASTSim, making it well suited for analyses that must be shared and understood among multiple stakeholders, such as automakers and regulatory agencies. In this capacity, it can be a powerful tool for building large-scale future scenarios of the type that might support public interest discussions related to vehicle fuel economy and design.

Table of Contents

Executive Summary	vi
1 Introduction	1
2 FASTSim in the Vehicle Modeling Continuum	2
2.1 The Vehicle Modeling Continuum	2
2.2 The FASTSim Continuum	3
3 Component-Level Modeling and Validation	8
3.1 Generalized Component Modeling	8
3.2 Transmission Impacts on Fuel Converter Efficiency	12
3.3 Generalized Thermal Modeling – FASTSim Hot	14
3.3.1 Thermal Model Structure: Internal Combustion Vehicles and Hybrid Vehicles	15
3.3.2 Thermal Model Structure: Electric Vehicles	20
3.3.3 Thermal Model Structure: Plug-In Hybrid Vehicles	22
3.4 Vehicle Specific Semi-Empirical Thermal Modeling	22
3.4.1 Model Structure and Parameters	23
3.4.2 Temperature and Fuel Consumption Results for a 2011 Ford Fusion	25
3.5 Engine Stop/Start Fuel Saving Feature	27
4 Vehicle-Level Base Modeling and Validation	27
4.1 Vehicle-Level Time Series Validation	27
4.2 Fuel Economy and Performance Validation	30
4.2.1 Validation Results for Vehicles with Vetted Inputs	31
4.2.2 Large-Scale Validation Results for Vehicles with Partially Vetted Inputs	32
5 On-Road/Real-World Validation	37
6 FASTSim Applications and Publications	41
7 Summary	49
References	50
Appendix A: Partially Vetted Vehicle Validation Results	52
Appendix B: Studies Using FASTSim	70
Appendix C: Supplemental Plots	82

List of Figures

Figure ES-1. Conceptual illustration of the FASTSim continuum on the vehicle modeling continuum.....	vi
Figure ES-2. Time series validation: Chevrolet Volt, US06.....	viii
Figure ES-3. FASTSim fuel economy validation versus EPA window sticker data for a range of example vehicles.....	viii
Figure ES-4. FASTSim electricity consumption validation versus EPA window sticker data for example EVs.....	ix
Figure ES-5. FASTSim acceleration validation versus Zeroto60Times website data for a range of example vehicles.....	ix
Figure ES-6. (Top) Engine temperature for model and test; (middle) cumulative fuel energy consumed for thermal model, baseline model without any thermal effects, and test; and (bottom) vehicle speed vs. time for repeated US06 tests conducted in 0°F/−17.8°C.....	x
Figure ES-7. Example of precise fuel consumption validation enabled by FASTSim’s customized option with extensions for select components.....	xi
Figure ES-8. Validation of FASTSim custom modeled versus measured fuel economy over on-road driving.....	xii
Figure 1. Conceptual illustration of the vehicle modeling continuum.....	3
Figure 2. Conceptual illustration of the FASTSim continuum within the vehicle modeling continuum.....	4
Figure 3. Example default gasoline engine efficiency map for FASTSim’s base option	6
Figure 4. Examples of custom engine and transmission efficiency maps for the 2011 Ford Fusion (dynamometer tested) for FASTSim’s customized option.....	6
Figure 5. Examples of thermally sensitive engine and transmission maps for FASTSim’s customized option with extensions for select components	7
Figure 6. Examples of torque-speed component map (left) and shift schedule (right) for FASTSim’s customized option with extensions for select components	7
Figure 7. Example of precise fuel consumption validation enabled by FASTSim’s customized option with extensions for select components.....	7
Figure 8. Torque-speed engine map with shift schedule showing alignment of constant power and efficiency curves	8
Figure 9. FASTSim efficiency-power engine map (black line) developed from torque-speed map operating points (blue stars) transferred from Figure 8.....	8
Figure 10. Validation of simplified FASTSim engine model against a torque-speed model	9
Figure 11. FASTSim efficiency-power engine maps (orange lines) showing fit with torque-speed model (blue and black stars) for engines of various sizes.....	10
Figure 12. FASTSim fuel economy validation against EPA window sticker data (combined UDDS and HWFET drive cycles) for vehicles with engines of different sizes.....	10
Figure 13. Torque-speed electric motor map for the Nissan Leaf	11
Figure 14. Comparison of FASTSim efficiency-power electric motor map with published Nissan Leaf torque-speed map (98% inverter efficiency).....	11
Figure 15. Validation of FASTSim electric motor model against torque-speed model.....	12
Figure 16. Engine efficiency versus output power for two different transmissions	13
Figure 17. FASTSim engine efficiency curves for vehicles with different transmission gear numbers.....	14
Figure 18. Internal combustion vehicle and hybrid vehicle thermal network.....	15
Figure 19. Internal combustion vehicle thermal network	17
Figure 20. FASTSim Hot engine efficiency map	20
Figure 21. Electric vehicle thermal network.....	21
Figure 22. Schematic of semi-empirical approach to engine thermal modeling.....	23
Figure 23. (Top) Engine temperature for model and test; (middle) cumulative fuel energy consumed for thermal model, baseline model without any thermal effects, and test; and (bottom) vehicle	

	speed vs. time for repeated US06 tests conducted in 0°F/−17.8°C. Note that the thermal model greatly improves the ability to match the fueling rate shown in the test data.	26
Figure 24.	(Top) Energy consumption for a simulated vehicle both without stop/start (“base”) and with stop/start modeled. (Bottom) UDDS speed trace and active/inactive status of stop/start and DFCO for the vehicle simulated with these advanced technologies active.	27
Figure 25.	Time series validation: 2012 Ford Fusion, US06	28
Figure 26.	Time series validation: 2014 Chevrolet Cruze, US06	28
Figure 27.	Time series validation: 2010 Toyota Prius, US06	29
Figure 28.	Time series validation: 2013 Toyota Prius Plug-in, US06	29
Figure 29.	Time series validation: 2012 Chevrolet Volt, US06.....	29
Figure 30.	Time series validation: 2013 Nissan Leaf, US06	30
Figure 31.	Time series validation: 2015 Volkswagen e-Golf, US06	30
Figure 32.	FASTSim base fuel economy validation versus EPA window sticker data for subset of vehicles with vetted inputs	31
Figure 33.	FASTSim base electricity consumption validation versus EPA window sticker data for subset of EVs with vetted inputs.....	32
Figure 34.	FASTSim base acceleration validation versus Zeroto60Times website data for subset of vehicles with vetted inputs	32
Figure 35.	Example of FASTSim base fuel economy (versus EPA window sticker data) and acceleration (versus Zeroto60Times website data) validation for conventional gasoline vehicles with partially vetted inputs.....	33
Figure 36.	Histograms of error (difference between FASTSim base modeled and measured fuel consumption) for partially vetted conventional gasoline vehicles	34
Figure 37.	FASTSim base fuel economy (versus EPA window sticker data) and acceleration (versus Zeroto60Times website data) validation for HEVs (with 2015 sales of more 10,000 vehicles) with partially vetted inputs.....	35
Figure 38.	Histograms of fuel consumption percent error (difference between FASTSim base modeled and measured results) for partially vetted HEVs	35
Figure 39.	FASTSim base electricity consumption (versus EPA window sticker data) and acceleration (versus Zeroto60Times website data) validation for EVs (with 2015 sales of more 1,000 vehicles) with partially vetted inputs	36
Figure 40.	Histograms of electricity consumption percent error (difference between FASTSim base modeled and measured results) for partially vetted EVs.....	36
Figure 41.	Instrumentation of Ford Fusion test vehicle	37
Figure 42.	Calibration of FASTSim-modeled Ford Fusion fuel economy to dynamometer data.....	38
Figure 43.	Validation of FASTSim-modeled versus measured fuel economy over on-road driving	39
Figure 44.	Effects on RMSE of incorporating various vehicle and environmental conditions into the FASTSim model	40
Figure 45.	Fuel-efficient routing options in Google Maps	41
Figure 46.	Power transfer profile for a 100-kW, 5-m inductive transmitter, considering vehicle’s position in both travel and lane directions	42
Figure 47.	Comparison of tested and modeled tractive power for the 2018 Toyota Highlander from an example test cycle	43
Figure 48.	Percentage of congested vehicle miles traveled (CVMT) for trips within each of the four road type clusters (a) before and (b) after partitioning by congestion	44
Figure 49.	Pareto plot of average total cost of ownership and greenhouse gas emissions for BEV, PHEV, HEV, and conventional powertrain types and EV-mode ranges for applicable powertrain types. Circle area is indicative of battery size, where applicable.....	44
Figure 50.	Observed change in coefficient of drag × frontal area (CdA) and road load without wind correction	45

Figure 51. Day- and mile-based fleet utility factors for battery electric vehicles as a function of range based upon 2009 National Household Travel Survey data	46
Figure 52. Box plots for reduction in greenhouse gases when switching a conventional vehicle with its equivalent hybrid electric vehicle in different vehicle groups	46
Figure 53. Combined greenhouse gas emissions at 325-GW renewable capacity	47
Figure 54. Effect of driver aggressiveness (trip-averaged forward acceleration and speed) and trip distance on fuel economy for HEV powertrain.....	48
Figure C-1. Four repeated UDDS cycles with 0°F ambient/start temperature.....	82
Figure C-2. Two repeated US06 cycles with 20°F ambient/start temperature.....	82
Figure C-3. Four repeated UDDS cycles with 20°F ambient/start temperature.....	83
Figure C-4. Two repeated UDDS cycles with 72°F ambient/start temperature.....	83
Figure C-5. Three repeated UDDS cycles with 72°F ambient/start temperature.....	84

List of Tables

Table ES-1. FASTSim Continuum: Modeling Levels and Their Strengths and Limitations.....	vii
Table 1. FASTSim Continuum: Modeling Levels and Their Strengths and Limitations.....	5
Table 2. Dynamometer Drive Cycles Used To Obtain Data for Tuning and Validation of the 2011 Ford Fusion Engine Thermal Model.....	25
Table 3. Tuned Parameters for Engine Thermal Model To Match Test Data for Both Fueling Rate and Temperature	26
Table 4. Matrix of Dynamometer Tests	38
Table 5. On-Road Testing Characteristics	39

1 Introduction

The National Renewable Energy Laboratory (NREL) transportation research team has decades of experience with vehicle powertrain modeling. This extensive history includes development of the ADVISOR (Advanced Vehicle Simulator) model from 1994 to 2004. ADVISOR has been one of the most frequently used vehicle modeling software packages in the United States and abroad. Even after NREL ended formal development of ADVISOR, the tool spun off into an open-source development community and has been downloaded thousands of times each year.

Since 2004, NREL has built on the foundational work with ADVISOR to develop, use, and refine the Future Automotive Systems Technology Simulator (FASTSim) in support of the U.S. Department of Energy's (DOE's) transportation research goals and to meet the needs of multiple industry stakeholders through collaborative analysis. FASTSim produces very rapid estimates of vehicle efficiency, performance, cost, and battery life in conventional and advanced powertrain technologies. The tool enables completion of such analyses using only a few publicly available vehicle parameters, such as peak power output of the engine and hybrid/electric components, vehicle mass, frontal area, and rolling resistance. This simplified approach provides accurate results for many types of analyses while increasing speed, ease, and accuracy related to finding required inputs, running the model, and interpreting results. When appropriate, FASTSim also can use customized inputs to represent specific vehicles even more precisely if detailed input data are available.

In addition, FASTSim has the advantage of being publicly accessible and transparent. FASTSim's graphical user interface is available to step users through selecting a vehicle to run, choosing drive cycles to simulate, and viewing the results. Although many simulations do not require it, FASTSim's open-source approach also allows for customization to capture temperature-dependent characteristics, component speed-related variations, and other detailed aspects. The publicly released version has been robust, with thousands of unique downloads across both Excel and Python versions with no reports of major errors or inaccuracies.

Primary applications of FASTSim include evaluating the impact of technology improvements on efficiency, performance, cost, and battery life in conventional vehicles, hybrid electric vehicles (HEVs), plug-in hybrid electric vehicles (PHEVs), and all-electric vehicles (EVs). FASTSim helps answer questions such as:

- Which battery sizes are most cost effective for a PHEV or EV?
- At what battery prices do PHEVs and EVs become cost effective?
- On average, how much fuel does a PHEV with a 30-mile electric range save compared with a conventional vehicle?
- How much fuel does an HEV save compared with a conventional vehicle over a given drive cycle?
- How do lifetime costs and petroleum use compare for conventional vehicles, HEVs, PHEVs, fuel cell vehicles, and EVs?

FASTSim models vehicle components at as high a level as possible while maintaining accuracy. Simulations over standard city and highway time-versus-speed fuel economy drive cycles take less than 1 second for most vehicles. FASTSim is also capable of running a large number of drive cycles at once. It has been used to estimate the benefits of changing a fleet of vehicles to an

advanced powertrain and to capture a more realistic representation of light-duty vehicle real-world driving by using data sets from NREL’s Transportation Secure Data Center (NREL 2017). More information about FASTSim is available from Brooker et al. (2015-0973) and www.nrel.gov/fastsim.¹

As with any model, the most critical aspect of FASTSim is its ability to reflect reality accurately. This is the purpose of validation—the comparison of modeled results versus results measured during vehicle or component operation in the laboratory or on the road. FASTSim’s high-level vehicle simulation results have been validated against test data for hundreds of different vehicles and most existing powertrain options. In addition, detailed validation of individual vehicles has been performed via both chassis dynamometer and on-road testing of highly instrumented vehicles.

This report focuses on the validation of FASTSim. Section 2 explains FASTSim’s place in the continuum of vehicle modeling options and discusses the continuum of capabilities within FASTSim itself. Sections 3 and 4 analyze modeling and validation of FASTSim at the component and vehicle levels. Recent modeling enhancements are expanded upon, namely generalized thermal component models and adjustments to the engine map based on transmission information. Section 5 details on-road, real-world validation. Section 6 describes how various users have applied FASTSim, and Section 7 summarizes this report’s findings.

2 FASTSim in the Vehicle Modeling Continuum

This section describes the continuum of vehicle modeling options, FASTSim’s place within that continuum, and the continuum of capabilities within FASTSim itself.

2.1 The Vehicle Modeling Continuum

Many software tools have been developed for vehicle/powertrain modeling. For example, Mahmud and Town (2016) reviewed 125 tools available for EV modeling, yet even their long list is not comprehensive and excludes many proprietary tools developed by automakers and others.

Modeling tools can be categorized conceptually into a continuum based on each tool’s trade-off between accuracy and complexity, where “complexity” includes the required number of input parameters, availability of required input data, time required to obtain the inputs and perform calibration, software requirements, and computational overhead to run. Figure 1 shows a qualitative, illustrative representation of the modeling continuum. Importantly, the relationship between accuracy and complexity shown here is nonlinear: The greatest returns in accuracy are gained with the initial advances in complexity, whereas further marginal increases in accuracy come at the cost of greatly increasing complexity, which entails increased data discovery, setup, calibration, and computational and runtime requirements.

¹ This website also links to the latest publicly available version of FASTSim.

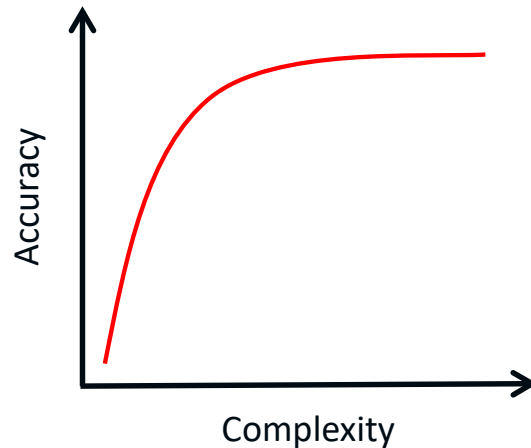


Figure 1. Conceptual illustration of the vehicle modeling continuum

Approaches at the low complexity/low accuracy end of the full vehicle modeling continuum include simply taking vehicles’ U.S. Environmental Protection Agency (EPA) “window sticker” composite fuel economy ratings and multiplying these by the number of miles the vehicles are driven to estimate the total fuel consumed by each vehicle. One step up the accuracy/complexity curve is to consider each vehicle’s “city” and “highway” fuel economy ratings and multiply these by the driving conducted on roads categorized as “city” and “highway.” These approaches may give fair estimates of total fuel consumption by a large population of vehicles, but they are inadequate for studies seeking to represent the distribution of fuel efficiency for a given vehicle technology over a range of customer driving profiles, weather conditions, and (for electrified vehicles) charging behaviors.

Approaches at the high complexity/high accuracy end of the full vehicle modeling continuum include models that call for hundreds of input specifications per vehicle, multidimensional efficiency maps for each component, and computational time steps on the order of 1/100 of a second throughout a vehicle’s exact driving profile. Such approaches can provide accurate representations of vehicle operating behavior and are useful for applications requiring real-time computations, such as development of control code to implement in a production vehicle or completion of hardware-in-the-loop testing. However, the modeling complexity and computational burden for these approaches can be excessive for many applications, limiting the breadth of different operating characteristics and vehicle configurations that could otherwise be explored as a result. In short, the suitability of tools across this continuum depends on the analytical task being performed.

2.2 The FASTSim Continuum

FASTSim occupies a “sweet spot” along the vehicle modeling continuum. It is designed to balance predictive accuracy with model complexity (including data, calibration, computation, and runtime requirements) across a wide range of analytical tasks. Figure 2 locates FASTSim along the continuum. As shown, FASTSim encompasses a sizable segment of the curve—its own continuum—providing moderately high accuracy with low complexity (for standard, high-level analyses) on one end and providing high accuracy with moderate complexity (for customized vehicle-specific analyses) on the other. Across this full range, FASTSim is particularly well suited

for quickly and conveniently conducting large numbers of simulations over representative real-world driving distributions and/or myriad vehicle design variations. In such analyses, the uncertainties and efficiency impacts from the broad spectrum of operating conditions or design variants far exceed any small uncertainties resulting from modeling simplifications within FASTSim.

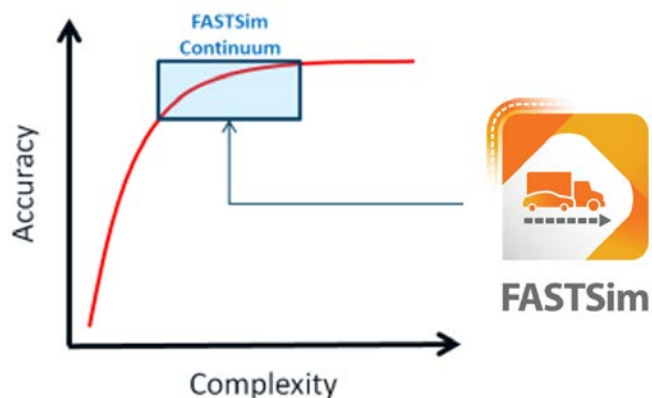


Figure 2. Conceptual illustration of the FASTSim continuum within the vehicle modeling continuum

Several elements are common to FASTSim across its continuum of capabilities and requirements:

- Backward/forward calculation structure²
 - Requires a full driving trajectory but can run using 1-second time steps (enabling fast run times)
- Modeling performed over a variety of drive cycle simulations
 - Certification test cycles (with and without standard adjustments to improve “real-world” representativeness)
 - Best-effort acceleration tests
 - Real-world simulations (leveraging Transportation Secure Data Center data and/or on-road testing)
- Different user interface options
 - Microsoft Excel (simple and user-friendly; has been externally posted for many years)
 - Python (scripting language for even faster run times and streamlined large database integration; has been externally posted for a few years)
- Variety of model validation examples
 - Some coverage in existing publications

² The backward/forward calculation structure starts with power requirements at the vehicle’s wheels as dictated by the road-load equation for a particular driving trajectory, then moves backwards up the driveline to confirm that each component can satisfy the required power before moving forward back down the driveline to apply the identified operating points for each component.

- More comprehensive presentation in this report.

Beyond those common elements, FASTSim can be used across a continuum of modeling levels (Table 1). FASTSim’s base option is suitable for large-scale simulation of hundreds or even thousands of vehicles. It employs generally representative default maps of power versus efficiency for each of the components (such as the standard gasoline engine map shown in Figure 3), which are then scaled based on the component power ratings for a particular modeled vehicle. Thus, the base option has the fastest calibration, only requiring a small amount of publicly available vehicle information, and it still captures most important factors for high-level vehicle comparisons. However, for some targeted studies, more component data details may be available on specific vehicles of interest, or the studies may seek to investigate scenarios sensitive to factors such as operating temperature or gear selection. For these situations, FASTSim enables further customization and the addition of modeling extensions—moving the model up the accuracy-versus-complexity trade-off curve.

Table 1. FASTSim Continuum: Modeling Levels and Their Strengths and Limitations

Level of Modeling	Strengths	Limitations
Base Option		
<ul style="list-style-type: none"> • Default power versus efficiency maps for each component • Maps scaled based on component power ratings for modeled vehicle 	<ul style="list-style-type: none"> • Fastest to calibrate, requires small amount of public vehicle information • Suitable for large-scale simulation/evaluation of thousands of vehicle designs 	<ul style="list-style-type: none"> • Captures most important factors for high-level comparisons but lacks detail that may be needed for some focused studies
Customized Option		
<ul style="list-style-type: none"> • Vehicle-specific component calibration 	<ul style="list-style-type: none"> • Provides more precise model of specific vehicle(s) 	<ul style="list-style-type: none"> • Larger calibration burden, requires detailed component-level data from manufacturer or testing
Potential Extensions for Targeted Investigations		
<ul style="list-style-type: none"> • Temperature dependence • Torque versus speed disaggregation • Shift schedules • Transmission impacts 	<ul style="list-style-type: none"> • Even more detail for studies that need it • Precise validation in numerous dimensions and conditions 	<ul style="list-style-type: none"> • Further increases calibration burden • Still not suitable for applications requiring real-time control (e.g., hardware-in-the-loop testing)

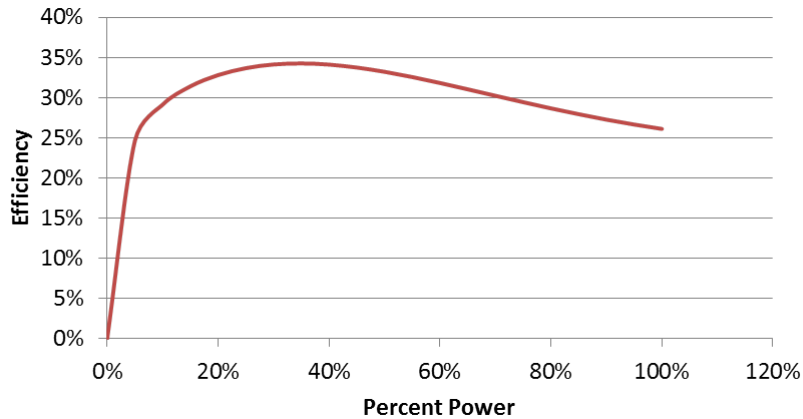


Figure 3. Example default gasoline engine efficiency map for FASTSim's base option

The customized option provides more precise modeling of a specific vehicle or vehicles. The vehicle-specific component calibration (Figure 4) entails a larger calibration burden because detailed component-level data from the manufacturer or from testing are required.

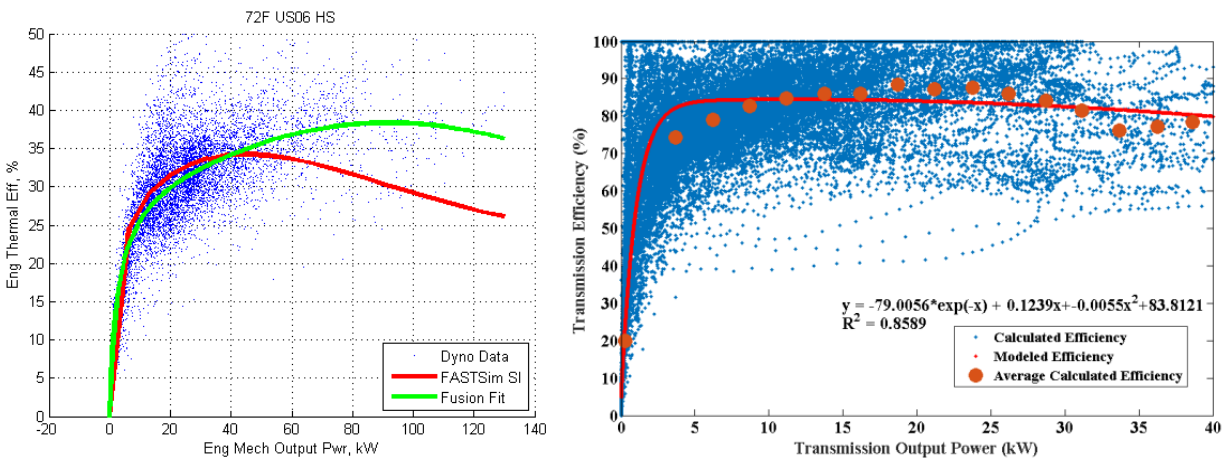


Figure 4. Examples of custom engine and transmission efficiency maps for the 2011 Ford Fusion (dynamometer tested) for FASTSim's customized option

Finally, the customized option can accept extensions for targeted investigations, accounting for factors such as the temperature dependence of efficiency maps for the engine and/or other components, torque-versus-speed disaggregation for select components, and consideration of shift schedules and torque converter lock-up (Figures 5 and 6). Such extensions can provide even more detail for studies that require it and offer precise validation in numerous dimensions and conditions (Figure 7), although at the cost of higher input data requirements and calibration burden. An example FASTSim extension that models thermal impacts on powertrain performance is detailed in Section 3.2.

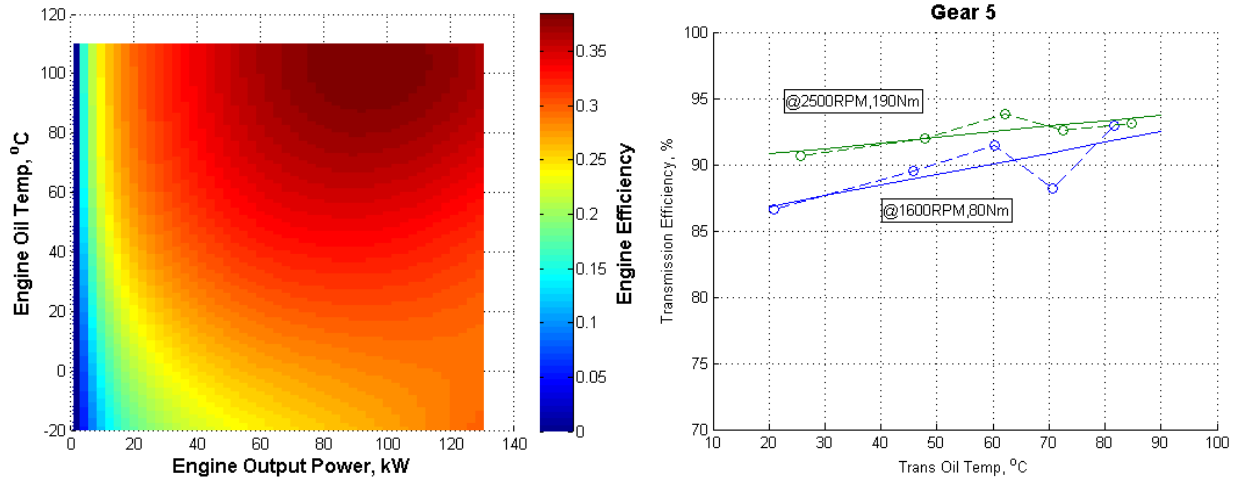


Figure 5. Examples of thermally sensitive engine and transmission maps for FASTSim's customized option with extensions for select components

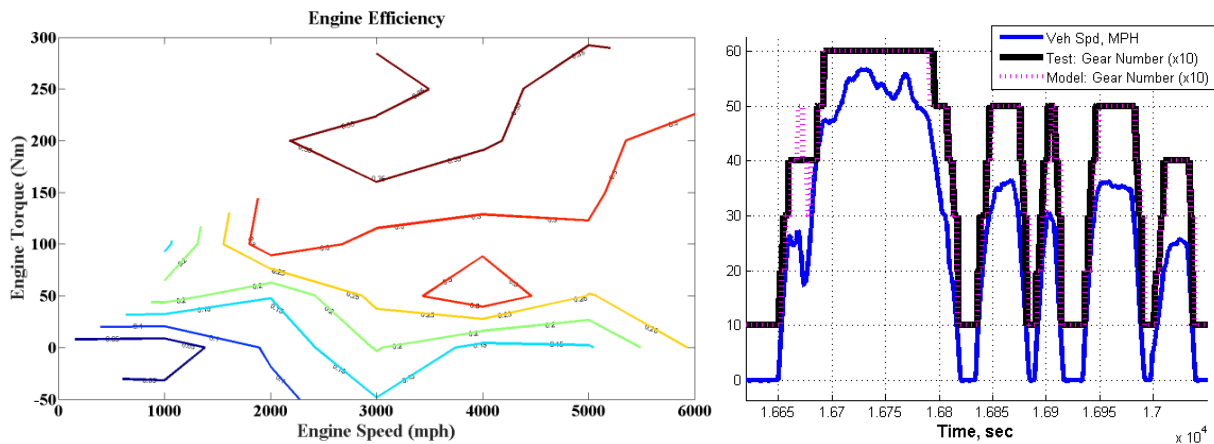


Figure 6. Examples of torque-speed component map (left) and shift schedule (right) for FASTSim's customized option with extensions for select components

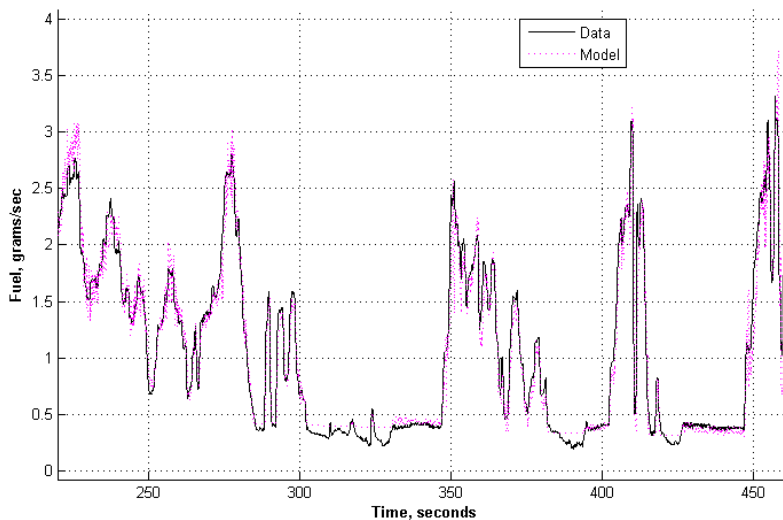


Figure 7. Example of precise fuel consumption validation enabled by FASTSim's customized option with extensions for select components

3 Component-Level Modeling and Validation

3.1 Generalized Component Modeling

This section focuses on component-level modeling and validation within FASTSim’s base option (see Table 1). FASTSim’s standard power-based engine model is a well-validated reduction of more computationally intense torque-versus-speed models (that are higher on the accuracy-complexity continuum). By design, modern automatic transmissions with high gear counts limit engine operation to a relatively narrow band of torque/speed combinations (Figure 8). Within the band of typical engine operation, contours of constant efficiency and constant power tend to be well aligned—particularly at low power, where the engine predominantly operates. Limited operational bands and the alignment of engine power and efficiency make FASTSim’s power-based model of engine efficiency an effective approximation (Figures 9 and 10).

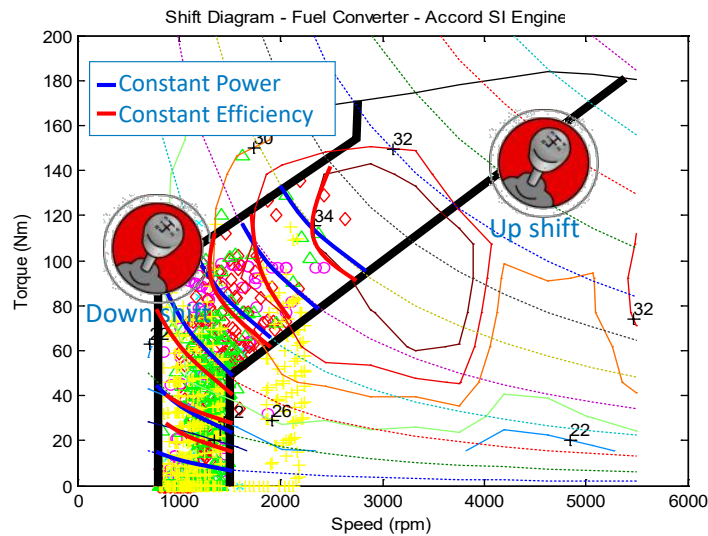


Figure 8. Torque-speed engine map with shift schedule showing alignment of constant power and efficiency curves

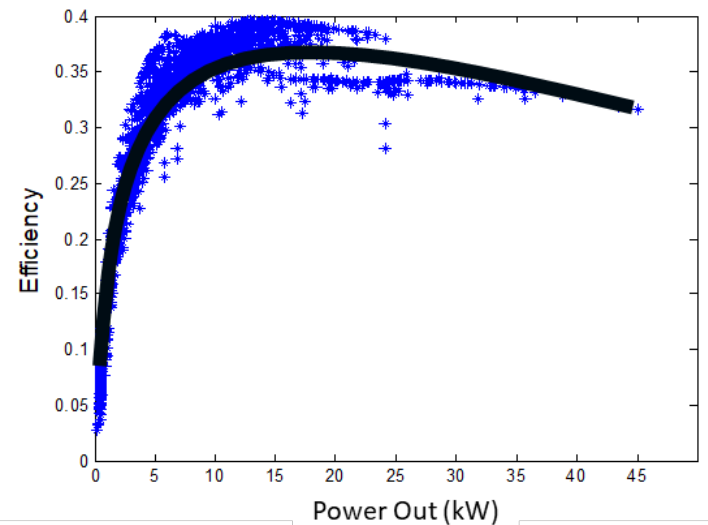


Figure 9. FASTSim efficiency-power engine map (black line) developed from torque-speed map operating points (blue stars) transferred from Figure 8

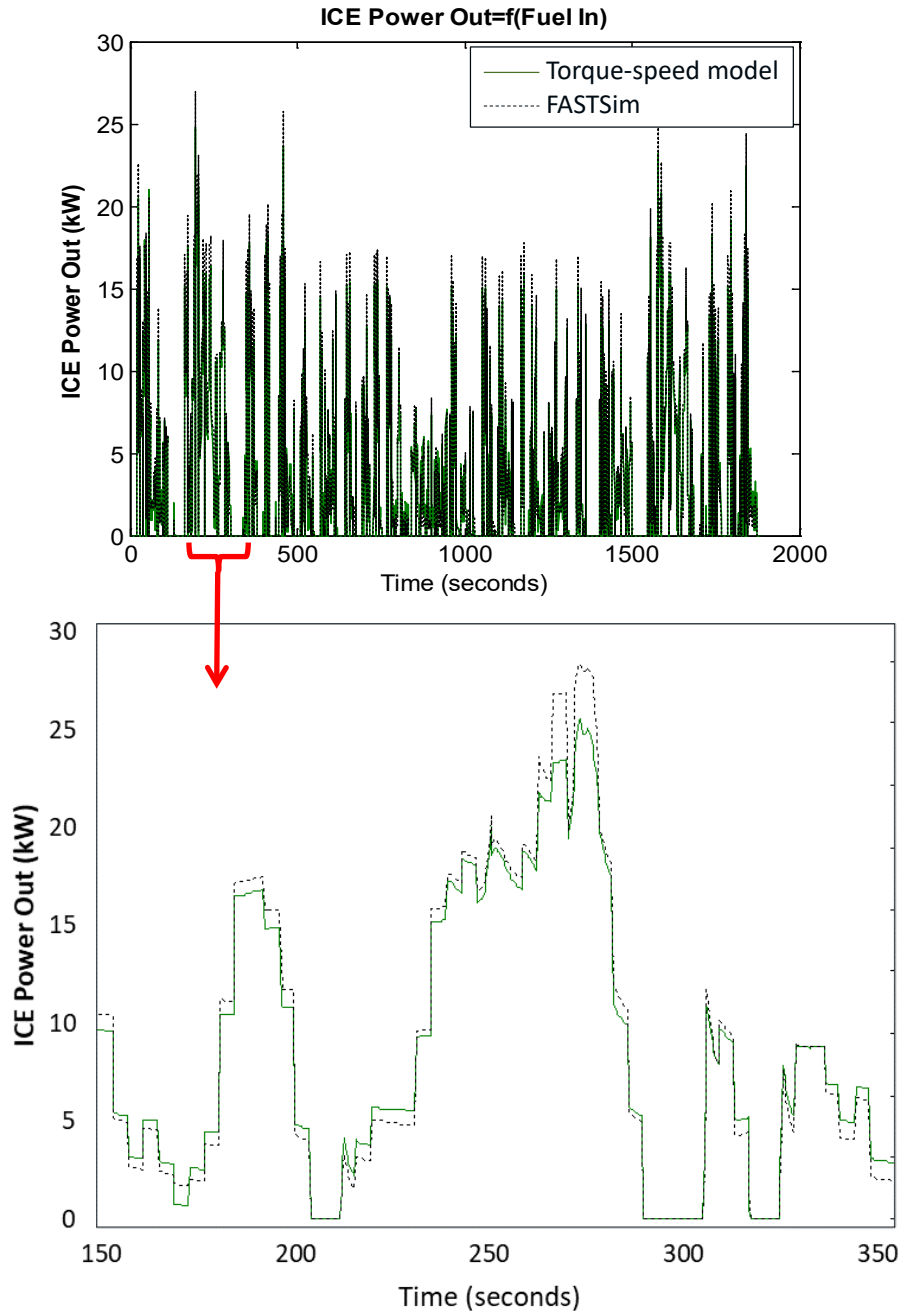


Figure 10. Validation of simplified FASTSim engine model against a torque-speed model

The single FASTSim efficiency-power engine map scales well to various engine sizes. Figure 11 shows the engine map superimposed on data points from a torque-speed model for a 100-kilowatt (kW) and a 125-kW engine, demonstrating a good fit for both. The effectiveness of FASTSim’s engine scaling approach translates well into fuel economy validation for vehicles with engines of different sizes. Figure 12 shows good matches between FASTSim’s modeled fuel economy results and EPA window sticker data for vehicles with engines sizes ranging from 112 to 241 kW.

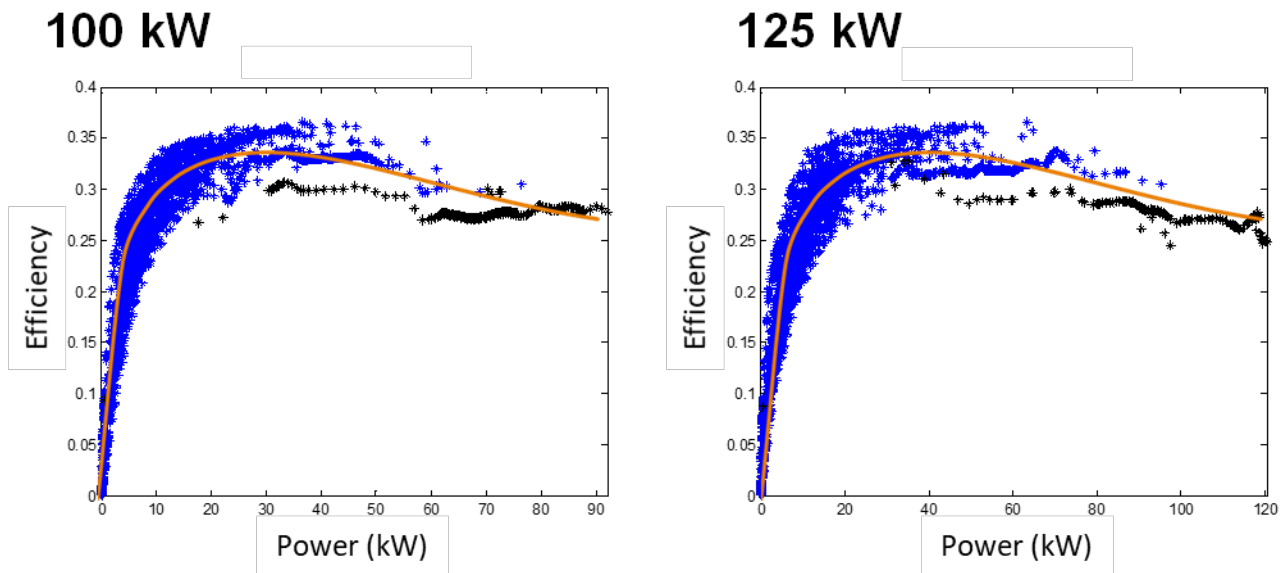


Figure 11. FASTSim efficiency-power engine maps (orange lines) showing fit with torque-speed model (blue and black stars) for engines of various sizes

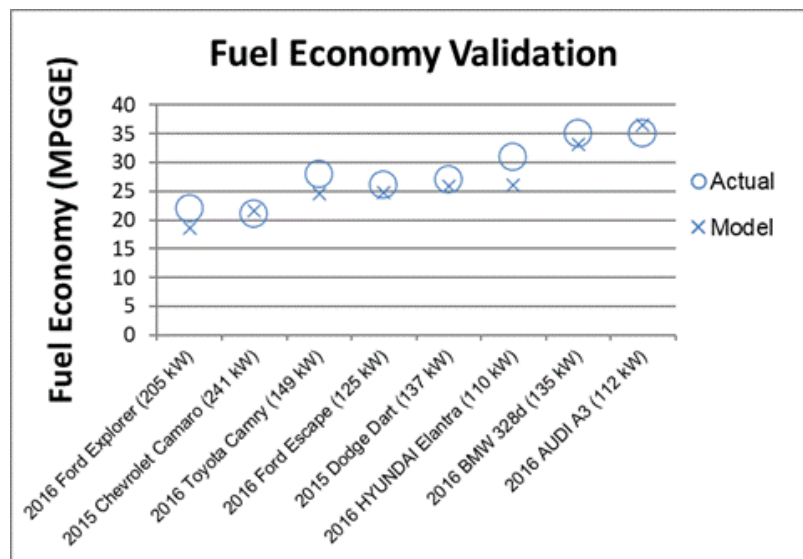


Figure 12. FASTSim fuel economy validation against EPA window sticker data (combined UDDS and HWFET drive cycles)³ for vehicles with engines of different sizes

FASTSim’s power-based approach works similarly well for electric motor modeling. Figure 13 shows a torque-speed electric motor map for the Nissan Leaf. Figure 14 demonstrates a good fit between FASTSim’s efficiency-power approximation and published Nissan Leaf torque-speed data. Finally, Figure 15 shows that FASTSim’s simplified model of efficiency versus power matches well with the torque-speed model.

³ HWFET ≡ Highway Fuel Economy Test; UDDS ≡ Urban Dynamometer Driving Schedule.

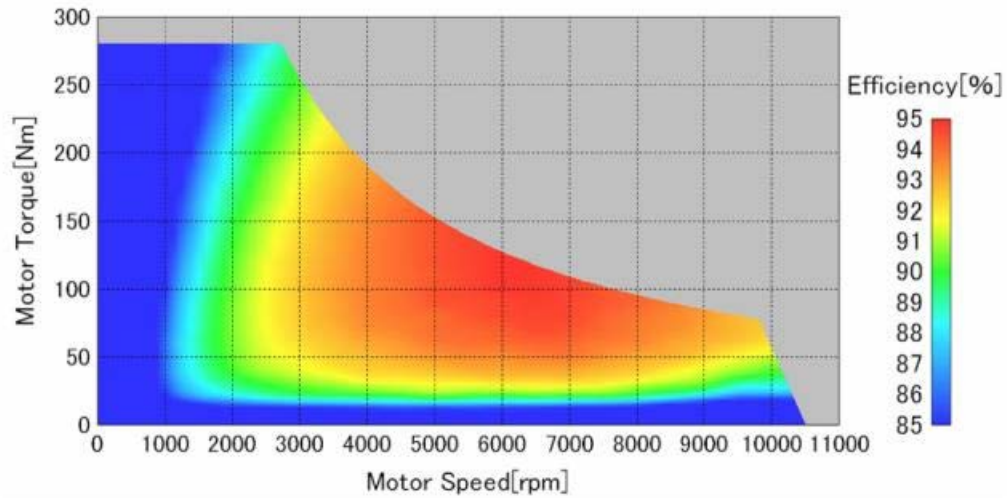


Figure 13. Torque-speed electric motor map for the Nissan Leaf

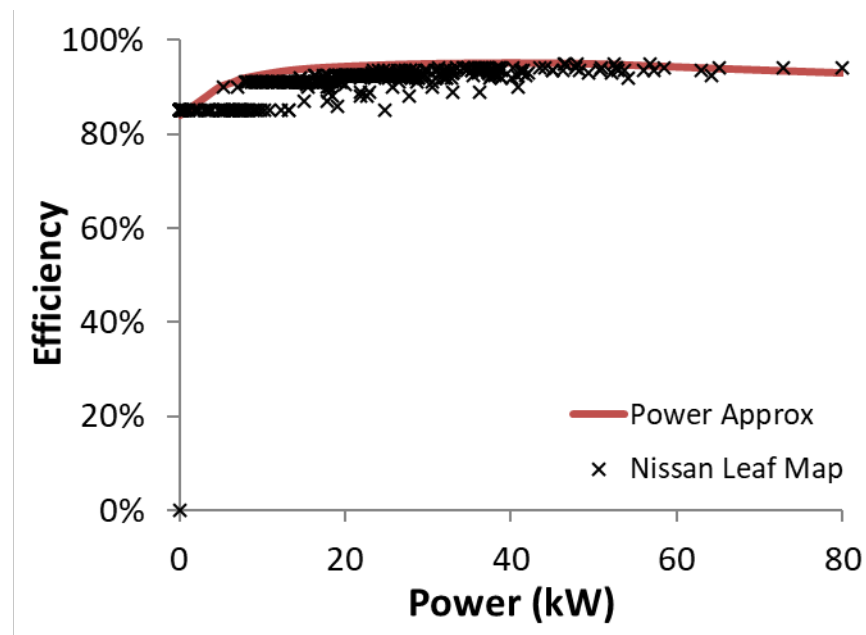


Figure 14. Comparison of FASTSim efficiency-power electric motor map with published Nissan Leaf torque-speed map (98% inverter efficiency)

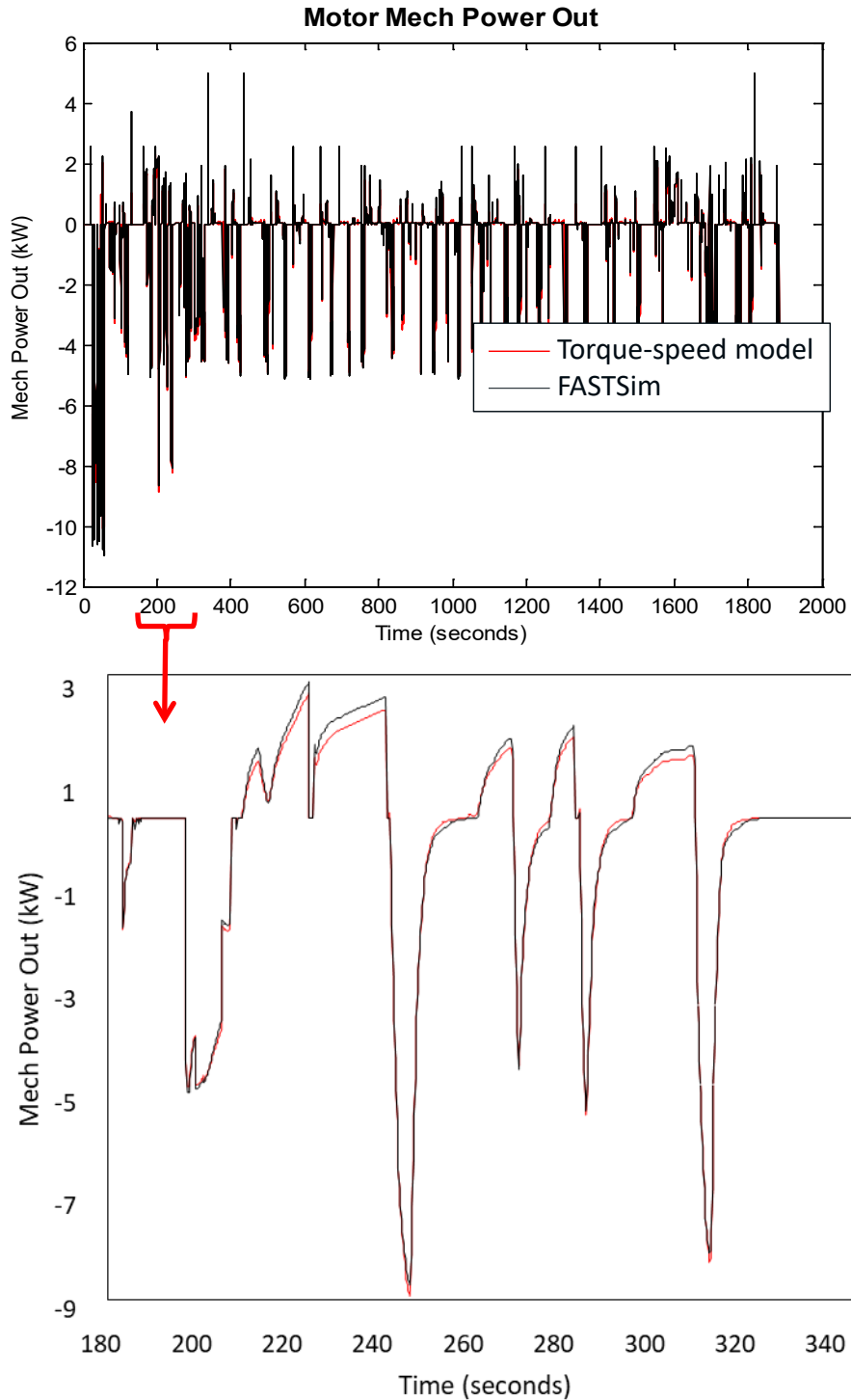


Figure 15. Validation of FASTSim electric motor model against torque-speed model

3.2 Transmission Impacts on Fuel Converter Efficiency

The base version of FASTSim utilizes the engine efficiency map previously introduced in Figure 11, which is scaled based on maximum engine power. However, real-world engine efficiency

varies beyond just instantaneous power output; engine operating points are heavily influenced by the vehicle transmission. Transmissions with a high quantity of gears are capable of improving vehicle fuel economy through increased control of the gear ratio. Improvements in engine operating efficiency can be observed in vehicle dynamometer data. Figure 16 depicts engine operating data from two dynamometer tests. The two tests were consistent in all aspects—including the vehicle engine, vehicle make/model, and drive schedule—except for the transmission. One test featured a vehicle with a six-speed transmission, whereas the other featured a vehicle with an eight-speed transmission. Analysis of the engine performance versus operating power between these cases reveals the engine efficiency improvements associated with increased transmission gears.

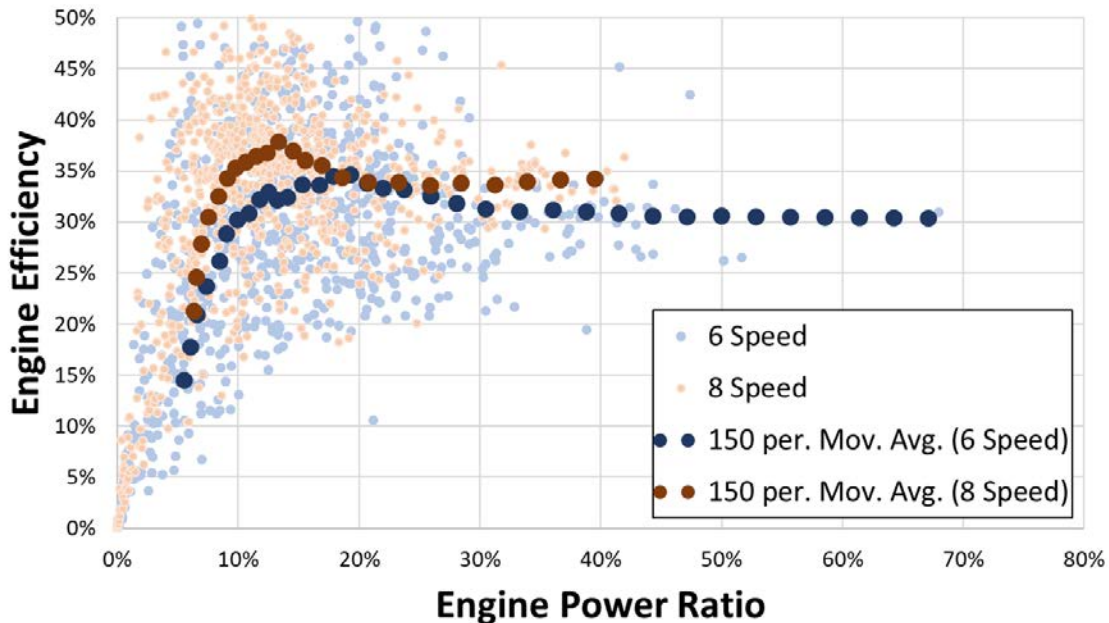


Figure 16. Engine efficiency versus output power for two different transmissions

The default engine efficiency map is adjusted to account for the positive relationship between transmission gear number and improved engine performance. The engine efficiency map is adjusted in a manner consistent with the observed transmission impacts; engine efficiency is improved for moderate and high power levels, although the engine efficiency is similar during operation points at roughly 20% of engine output power. Engine efficiency map adjustments for transmissions with four gears to nine gears were obtained empirically by relating FASTSim modeling results with real-world values. The resulting transmission-sensitive engine efficiency maps are illustrated in Figure 17.

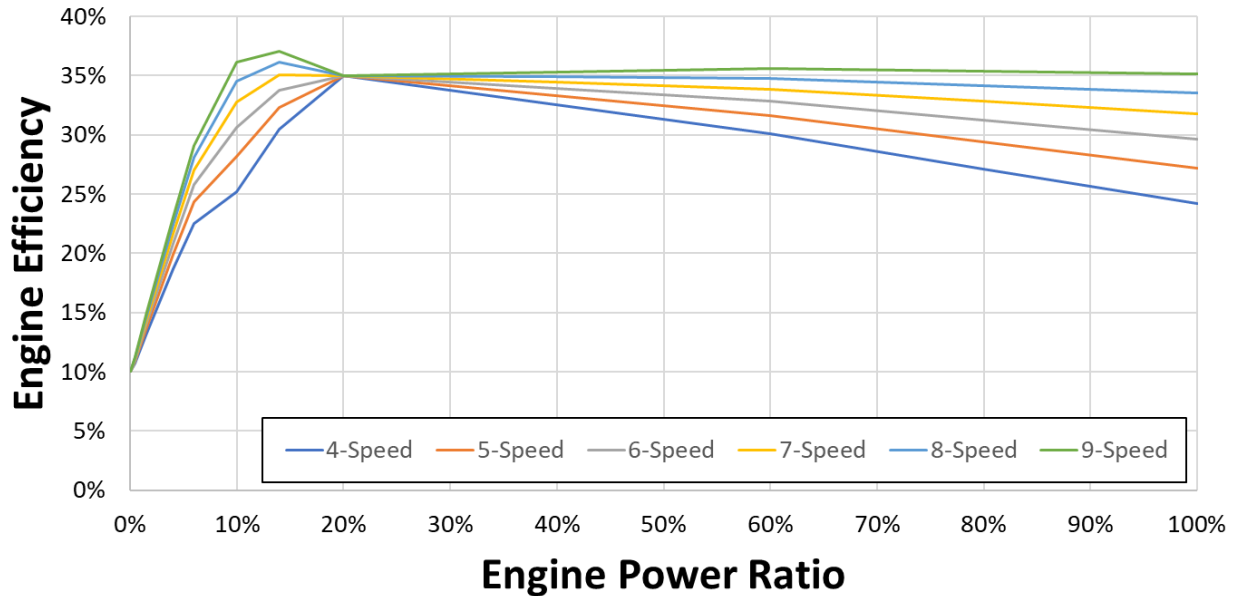


Figure 17. FASTSim engine efficiency curves for vehicles with different transmission gear numbers

3.3 Generalized Thermal Modeling – FASTSim Hot

Multiple prior studies using FASTSim have required explicitly capturing the thermal states of powertrain components and adjusting their performance accordingly. These studies explored the real-world benefits associated with vehicle technologies—transmission preheating on a Ford Fusion (Jehlik et al. 2017) and a cabin comfort technology on a Lexus RX350 (Jehlik et al. 2018)—that influence vehicle performance primarily by affecting its thermal state. Real-world vehicle testing was performed through a collaboration with Argonne National Laboratory (ANL) and corresponding thermal networks were created that accurately captured the technology influence on system-level fuel economy. The thermal networks used within each study were calibrated against the validation data and, until recently, were not available for the full suite of vehicles supported within FASTSim. This section summarizes efforts taken since the publication of these studies to generalize the thermal networks across a greater number of vehicles. Versions of FASTSim that track thermal state and adjust component efficiency accordingly will be referred to as “FASTSim Hot” throughout the remainder of the report.

Ambient conditions may influence vehicle energy consumption through a variety of channels. Cold oil temperature is associated with lower engine efficiency, and extreme temperatures generate large auxiliary loads to maintain cabin comfort. Moreover, the thermal states of individual components often interact. For example, warm oil transfers heat to cold engine coolant, and the vehicle cabin cannot be heated until the engine coolant is sufficiently warm. Accurately characterizing the system-level impacts arising from ambient conditions thus requires sufficiently relating component performance with component temperature and also modeling thermal pathways between components. Finally, the powertrain type influences the architecture of the thermal network due to the presence or absence of certain components (e.g., a conventional gasoline vehicle having an engine but not a traction battery, versus an EV where the reverse is

true). Unique thermal networks for pure internal combustion vehicles along with HEVs, PHEVs, and EVs are described in the following sections. In all cases, the emphasis of the modeling effort is to improve FASTSim simulation results by accurately capturing critical thermal impacts on system-level energy consumption, while maintaining a commitment to limited required inputs and only requiring publicly accessible information. Obscure details, such as manufacturer-specific heating, ventilation, and air-conditioning (HVAC) control strategies are not explicitly modeled.

3.3.1 Thermal Model Structure: Internal Combustion Vehicles and Hybrid Vehicles

Vehicle components present in the internal combustion vehicle thermal network include the engine oil, engine coolant, engine catalyst, and vehicle cabin. These components are related as depicted in the thermal network shown in Figure 18. Each of the modeled vehicle components also interacts with the ambient environment, which is typically modeled as a fixed condition throughout driving events. In addition, each component—absent the vehicle cabin—is influenced by a unique share of the excess thermal generation by the engine, calculated as the amount of fuel energy that is not mechanically output (efficiency loss).

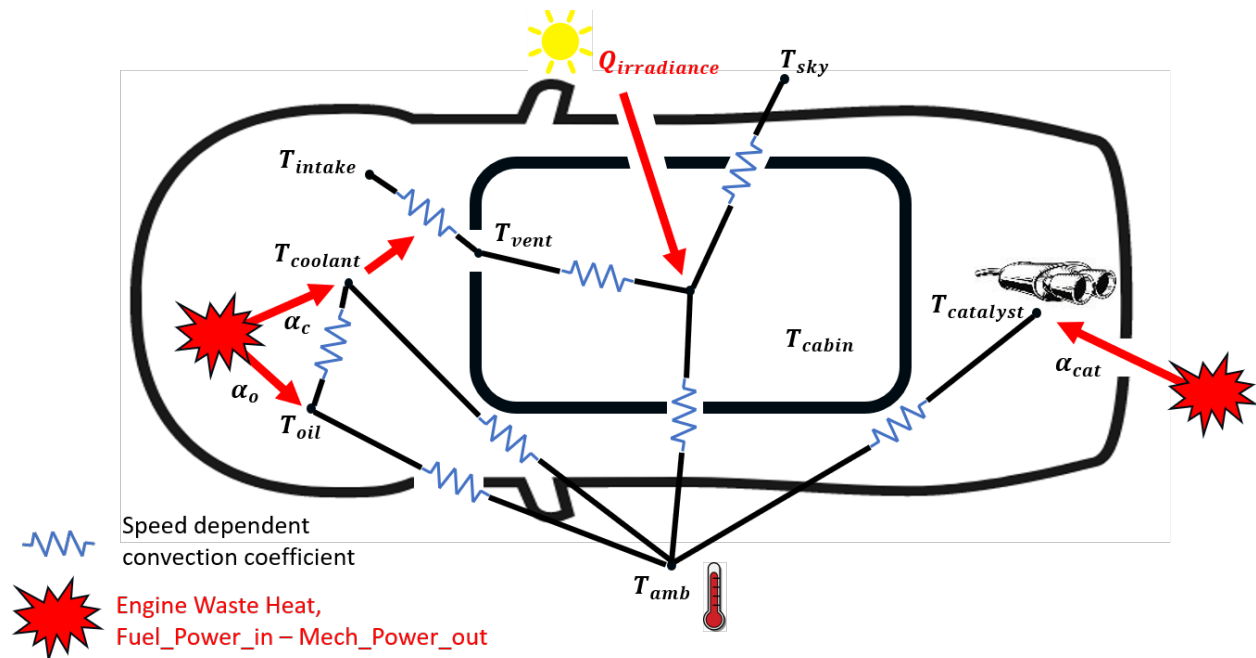


Figure 18. Internal combustion vehicle and hybrid vehicle thermal network

Equations 1–20 depict the component-level temperature models that arise from the internal combustion vehicle thermal network. Thermal coefficients are included for each term within most of the equations; these coefficients were calibrated against a large number of dynamometer tests performed by ANL. The dynamometer data used for model validation, sourced from the Downloadable Dynamometer Database (D³), spanned many conventional and hybrid vehicles operating under varying thermal conditions and driving schedules (ANL 2021). The data set is assumed to represent typical thermal behavior exhibited by conventional and hybrid vehicles. Discussion of each of the thermal network equations follows by component.

3.3.1.1 Engine Oil

The engine oil model includes convective heat transfer from the oil to the environment, convective transfer between the oil and coolant, and the difference between the power in (fuel mass flow rate) and engine power out. The convective heat transfer term for the engine oil includes a vehicle velocity-based function to reflect forced convection as vehicle speed increases. For each time step, the derivative of the oil temperature, \dot{T}_{oil} , is calculated as a function of the current oil temperature and associated component models (e.g., engine coolant, current engine output power). T_{oil} is used in conjunction with the time step length to calculate the oil temperature at the beginning of the subsequent time step. This process is repeated throughout the cycle duration.

$$\dot{T}_{oil} = \frac{h_{1o}(T_{amb} - T_{oil}) + h_2(T_{cool} - T_{oil}) + \alpha_o(P_{out} - P_{in})}{m_{oil}} \quad (1)$$

$$h_1 = a_{1oil}v_{veh} + a_{2oil} \quad (2)$$

where $\dot{T}_{oil} \equiv$ oil temperature rate of change

$a_x \equiv$ lumped coefficients empirically determined

$h_x \equiv$ lumped convective heat transfer coefficients

$m_x \equiv$ component thermal mass

$P_{in} \equiv$ engine input power (fuel rate lower heating value)

$P_{out} \equiv$ engine output power (brake power)

$T_{amb} \equiv$ ambient temperature

$T_{cool} \equiv$ coolant temperature

$T_{oil} \equiv$ oil temperature

$\alpha_o \equiv$ fraction of engine waste heat received by oil

$v_{veh} \equiv$ vehicle velocity.

These variable definitions will be used throughout Sections 3.3 and 3.4. Each of the thermal coefficients, a_x , is calibrated by minimizing the error between modeled temperature values and dynamometer test data containing engine oil data over time. Once calibrated, the same coefficients are used across all internal combustion vehicle powertrains. The mass of the oil is calculated using the oil capacity noted in each vehicle's manufacturer-provided owner's manual. A comparison between FASTSim Hot engine oil results and dynamometer test data for a vehicle driving over the same time step is shown in Figure 19, showing the effectiveness of the simplified lumped capacitance model.

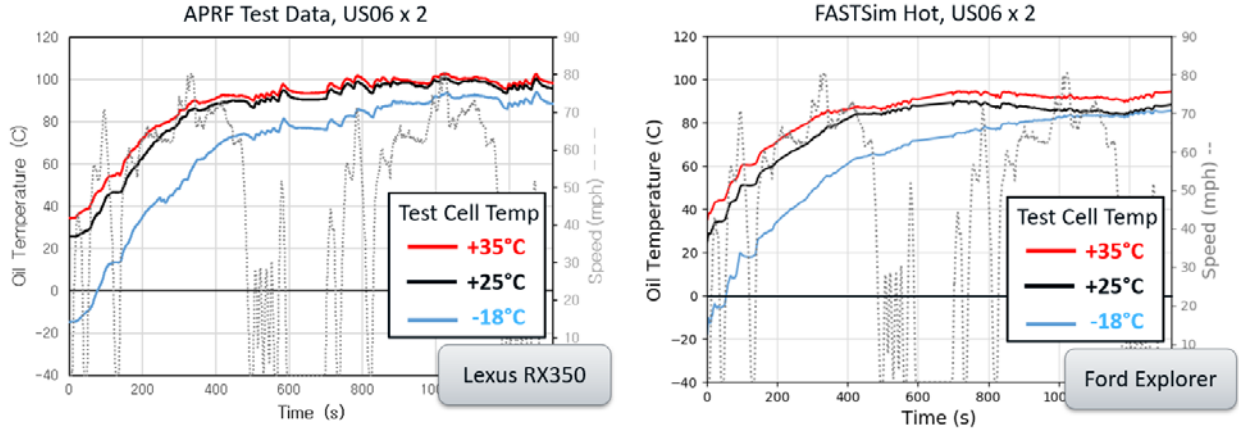


Figure 19. Internal combustion vehicle thermal network

3.3.1.2 Engine Coolant

Similar to the engine oil model, a simplified lumped capacitance model of engine coolant temperature was developed. This model includes convective heat transfer from the coolant to the environment, between the coolant and oil, fractional engine power loss, and heat transfer between the coolant and the intake air to be heated for passenger comfort. A logical operator is included that accounts for the thermostat opening, which increases heat transfer from the coolant to the ambient environment and accounts for vehicle velocity and forced convective heat transfer. An additional logical operator controls the temperature of the intake air forced through the heater core, which is dependent upon the current HVAC setting. Equations 3–5 describe the engine coolant model dynamics. Similar to the engine oil, the mass of the engine coolant is calculated using the oil capacity noted in each vehicle’s manufacturer-provided owner’s manual.

$$\dot{T}_{cool} = \frac{h_{1_{cool}}(T_{amb} - T_{cool}) + h_{2_{cool}}(T_{oil} - T_{cool}) + h_{3_{cool}}(T_{intake} - T_{cool}) + \alpha_c(P_{out} - P_{in})}{m_{cool}} \quad (3)$$

$$\begin{aligned} \text{if } T_{cool} < T_{set}: h_{1_{cool}} &= a_{1_{cool}}v_{veh} + a_{2_{cool}} \\ \text{else: } h_{1_{cool}} &= a_{3_{cool}}v_{veh} + a_{4_{cool}} \end{aligned} \quad (4)$$

$$T_{intake} = (1 - c)T_{amb} + cT_{cab} \quad (5)$$

where $\dot{T}_{cool} \equiv$ coolant temperature rate of change
 $T_{intake} \equiv$ intake air to the coolant heater coil
 $T_{cab} \equiv$ cabin temperature
 $c \equiv$ percent HVAC recirculation
 $\alpha_c \equiv$ fraction of engine waste heat received by coolant.

3.3.1.3 Exhaust Catalyst

A catalyst thermal model was also created to account for fueling rate enrichment prior to catalyst light-off. A simplified lumped capacitance method was applied that included a convective term accounting for heat transfer away from the catalyst to the ambient environment, as well as a fraction of the difference in power between the energy into and out of the engine. As was the case with the coolant and oil, a vehicle velocity term is added to account for forced convection. The

catalyst also receives fractional waste heat from the engine. The engine catalyst mass is obtained through parameter calibration, similar to the procedure for identifying a_x values.

$$\dot{T}_{cat} = \frac{h_{1cat}(T_{amb} - T_{cat}) + \alpha_{cat}(P_{out} - P_{in})}{m_{cat}} \quad (6)$$

$$h_{1cat} = a_{h1cat}v_{veh} + a_{h2cat} \quad (7)$$

$$\alpha_{cat} = a_{\alpha1cat}T_{cat} + a_{\alpha2cat} \quad (8)$$

where $\dot{T}_{cat} \equiv$ catalyst temperature rate of change
 $T_{cat} \equiv$ catalyst temperature
 $\alpha_{cat} \equiv$ fraction of engine waste heat received by catalyst.

3.3.1.4 Vehicle Cabin

Finally, a thermal model was created to describe the cabin temperature versus time to account for the impact of the HVAC setting on vehicle fuel consumption. Lumped capacitance relationships are included that relate the cabin air temperature to the ambient air and the register outlet air. Similar to the previous thermal models, a vehicle velocity term is included to account for forced convection. Cabin heating is modeled as a function of the coolant heater coil, which heats intake air. Heated intake air, T_{vent} , is used to heat the cabin when the cabin temperature is below the cabin setpoint, $T_{CabSetpoint}$, which is set to 22°C by default. Air conditioning (AC) is demanded when the cabin temperature is warmer than the setpoint temperature. AC heat transfer is back-calculated as the amount of cooling needed to maintain the cabin setpoint, limited by q_{ACmax} , the AC cooling limit. Vehicle cabin mass values are calculated using the amount of interior air volume. Typical values are prescribed for each vehicle class (e.g., sedan, SUV).

$$\dot{T}_{Cab} = \frac{(h_{1Cab}(T_{amb} - T_{Cab}) + h_{2Cab}(T_{vent} - T_{Cab}) + q_{AC} + q_{sky} + q_{rad})}{m_{Cab}} \quad (9)$$

$$h_{1Cab} = a_{1Cab}v_{veh} + a_{2Cab} \quad (10)$$

$$\begin{aligned} \text{if } T_{Cab} < T_{CabSetpoint}: h_{2Cab} &= a_{3Cab} \\ \text{else: } h_{2Cab} &= 0 \end{aligned} \quad (11)$$

$$\dot{T}_{intake} = \frac{h_{3cool}(T_{cool} - T_{intake})}{m_{intake}} \quad (12)$$

$$T_{vent} = T_{intake} + T_{intake} \dot{\Delta}t \quad (13)$$

$$\begin{aligned} q_{AC} = \min \left(0, \max \left(- \left(h_{1cab}(T_{amb} - T_{CabSetpoint}) + q_{sky_{setpoint}} + q_{rad} \right) \right. \right. \\ \left. \left. + \min \left(0, \frac{a_{4cab}(T_{CabSetpoint} - T_{Cab})}{m_{Cab}} \right), q_{ACmax} \right) \right) \end{aligned} \quad (14)$$

$$q_{sky} = \sigma((T_{sky} + 273.15)^4 - (T_{Cab} + 273.15)^4) \quad (15)$$

$$q_{Sky_{setpoint}} = \sigma((T_{sky} + 273.15)^4 - (T_{Cab_{setpoint}} + 273.15)^4) \quad (16)$$

$$Aux_{AC} = \frac{q_{AC}}{COP_{AC}} \quad (17)$$

where \dot{T}_{Cab} ≡ vehicle cabin temperature rate of change
 T_{Cab} ≡ vehicle cabin temperature
 T_{vent} ≡ vehicle vent temperature
 q_{AC} ≡ heat transfer from AC
 q_{sky} ≡ black-body radiation between vehicle cabin and the sky
 q_{rad} ≡ solar radiation experienced by the vehicle
 $T_{CabSetpoint}$ ≡ cabin setpoint temperature
 Δt ≡ time step length
 T_{intake} ≡ temperature change over the coolant heater coil
 $q_{sky_{setpoint}}$ ≡ black-body radiation experienced by the vehicle at the setpoint temperature
 $q_{AC_{max}}$ ≡ AC cooling limit
 σ ≡ Stefan-Boltzmann constant
 Aux_{AC} ≡ auxiliary load increase demanded from the engine
 COP_{AC} ≡ AC coefficient of performance.

3.3.1.5 Thermally Sensitive Engine Efficiency

The base engine efficiency curve, as shown in Figure 9, relates engine efficiency to the current output power percentage. This one-dimensional relationship produces accurate values at the system level for warm operating conditions but is not influenced by component temperatures. FASTSim Hot adjusts the base engine curve by applying an adjustment to the engine efficiency as a function of the engine oil temperature using an additional one-dimensional relationship. Equations 18–20 describe the base FASTSim engine efficiency curve and the FASTSim Hot engine efficiency curve. Coefficients relating the engine oil temperature to the engine operating efficiency are determined numerically by minimizing the error between modeling results and dynamometer data.

$$P_{out\%} = \frac{P_{out}}{P_{out_{max}}} \quad (18)$$

$$\eta_{eff_{base}} = f_{emp}(P_{out\%}) \quad (19)$$

$$\eta_{eff_{Hot}} = \eta_{eff_{base}} * (\alpha T_{oil} + \beta) \quad (20)$$

where $P_{out\%}$ ≡ vehicle cabin temperature rate of change
 P_{out} ≡ instantaneous engine output power
 $P_{out_{max}}$ ≡ rated engine output power

f_{emp} \equiv empirical relationship between output power percentage and engine efficiency
 $\eta_{eff_{base}}$ \equiv engine efficiency in the base version of FASTSim
 α, β \equiv engine oil coefficients relating temperature to engine efficiency.

Equation 20 relates engine efficiency both to engine output power and engine oil temperature. The relationship between these two variables on the component efficiency is visualized in Figure 20. The black line shows the engine efficiency curve contained in FASTSim base, which assumes a warm engine operating at 95°C.

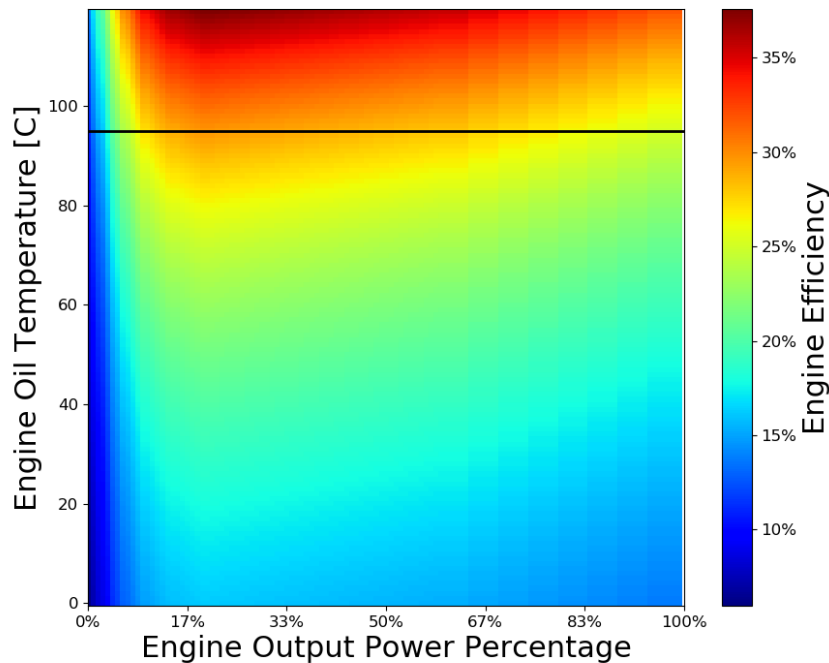


Figure 20. FASTSim Hot engine efficiency map

3.3.2 Thermal Model Structure: Electric Vehicles

Incorporation of thermal factors influencing system-level performance for electric vehicles is also modeled using a thermal network with components depicted as lumped thermal masses (Figure 21). The EV thermal network includes a battery, an electric motor, and the vehicle cabin. These components each primarily interact with the ambient surroundings; there is minimal component-to-component interaction due to the absence of engine waste heat and a dedicated coolant loop. Formulations describing how the temperature for each component changes during vehicle operation are elaborated upon in the subsequent sections. However, note that the current implementation of the EV thermal network does not relate these component temperatures to component performance (as was done in the prior section relating engine oil temperature and engine efficiency). This modeling simplification is due to data limitations associated with battery and motor efficiency versus temperature. While there is an abundance of literature relating engine efficiency to operating temperature, minimal data sets are available relating instantaneous temperature and efficiency for batteries and motors. Although the performance of the motor and

battery component models do not change due to temperature in this construct, auxiliary loads for cabin heating and cooling do explicitly impact vehicle energy consumption.

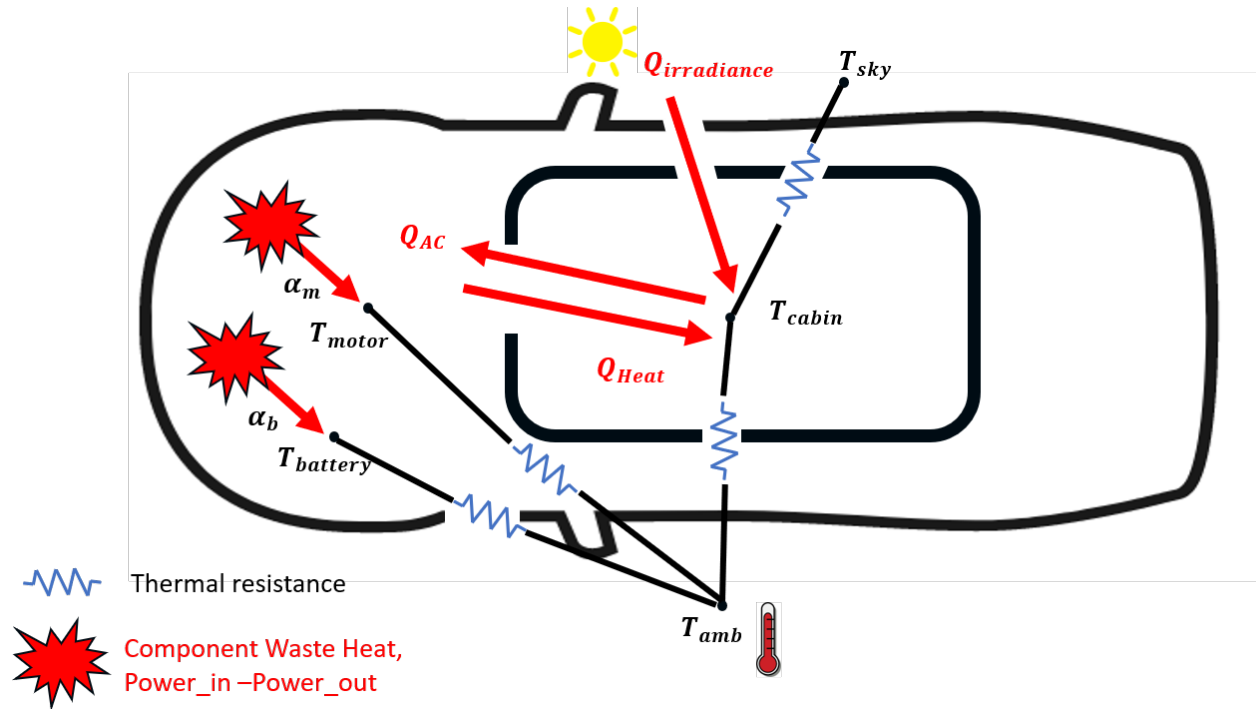


Figure 21. Electric vehicle thermal network

3.3.2.1 Battery and Electric Motor

The battery and motor component models resemble the lumped capacitance model for the engine in the prior section. The following equations describe the temperature changes resulting from convection with the ambient environment and a term associated with internal temperature rise due to heat generation during operation. Heat generation associated with battery performance is modeled using the “round-trip” efficiency, which captures heat generation occurring during charging and discharging events (Equation 21). Electric motor heat generation is modeled as the difference between the component input power and output power. In both cases, a fraction of the generated waste heat influences the component temperature. The remainder of the waste heat is lost to the ambient environment.

$$\dot{T}_{bat} = \frac{h_{1bat}(T_{amb} - T_{mot}) + \alpha_{bat} \left((1 - \eta_{rt}) * \sqrt{|P_{bat}|} \right)}{m_{bat}} \quad (21)$$

$$h_{1bat} = a_{1bat} v_{veh} + a_{2bat} \quad (22)$$

$$\dot{T}_{mot} = \frac{h_{1mot}(T_{amb} - T_{mot}) + \alpha_{mot}(P_{motin} - P_{motout})}{m_{mot}} \quad (23)$$

$$h_{1mot} = a_{1mot} v_{veh} + a_{2mot} \quad (24)$$

where η_{rt} is the round-trip efficiency of the battery. Additional component variables are named consistently with Section 3.3.1.1.

3.3.2.2 EV Vehicle Cabin

The EV vehicle cabin model closely resembles the cabin model formulated for internal combustion powertrains. The EV cabin model interacts with the ambient environment through convective heat transfer and solar radiation. A key difference between the EV cabin model and the cabin model previously introduced is the lack of engine waste heat available for cabin heating. Instead, cabin heat is delivered through a combination of an electric heat pump and an electric positive temperature coefficient (PTC) heater. The coefficient of performance of the heat pump reduces at lower temperatures; when the heat pump coefficient of performance drops below 1, the heat pump is turned off and the PTC heater is used instead. Equation 28 describes the relationship between the air temperature and the coefficient of performance of the combined heating system. The amount of heating or cooling power demanded is calculated by relating the current cabin temperature and the cabin temperature setpoint.

$$\dot{T}_{cab} = \frac{h_{1cab}(T_{amb} - T_{cab}) + Q_{Heat} + Q_{AC} + Q_{Rad} + Q_{Sky}}{m_{cab}} \quad (25)$$

$$h_{1cab} = a_{1cab}v_{veh} + a_{2cab} \quad (26)$$

$$Aux_{Heat} = \frac{Q_{Heat}}{COP_{Heat}} \quad (27)$$

$$COP_{Heat} = \max(1, c_1T_{amb} + c_2) \quad (28)$$

where Q_{Heat} \equiv heat transfer from the heater

COP_{Heat} \equiv combined heat pump and PTC heater coefficient of performance

Aux_{Heat} \equiv auxiliary power needed to satisfy heating load

c_1, c_2 \equiv heat pump efficiency coefficients.

3.3.3 Thermal Model Structure: Plug-In Hybrid Vehicles

The thermal model structure for plug-in vehicles uses concepts from both the conventional vehicle thermal network and the EV thermal network. Component temperatures are tracked for the engine oil, engine coolant, battery, and the electric motor consistent with the equations introduced in the previous sections. A unique feature of the PHEV model is the cabin comfort model. PHEV vehicles are modeled as using an electric air conditioner powered by the battery during both EV and engine-on modes. However, the cabin comfort model differs from the EV implementation due to the absence of electric heating elements. The vehicle engine is commanded to turn on when heat is demanded, even in situations where sufficient battery energy is available to meet driving demand. This assumption is informed by real-world operation of many PHEV models and the energy demand of PTC heaters and heat pumps in cold conditions.

3.4 Vehicle Specific Semi-Empirical Thermal Modeling

An additional approach to thermal modeling makes use of semi-empirical convection heat transfer correlations from literature to provide a more robust match to time series data for a specific vehicle

over a range of operating conditions. A schematic of the heat transfer processes being modeled is shown in Figure 22. This approach has been applied only to the engine temperature in a conventional vehicle and its impact on engine efficiency without accounting for cabin heating auxiliary load. This is useful for understanding how transient warmup affects vehicle fuel consumption. In future FASTSim improvements, this approach will be extended to model thermal behavior of the high-voltage battery (if present), cabin (with both heating and cooling and their effects on auxiliary loads), and possibly other vehicle components. Currently, the model for engine thermal behavior during warmup and steady-state cool weather operation has been validated for a single vehicle over multiple drive cycles with various ambient and starting temperatures.

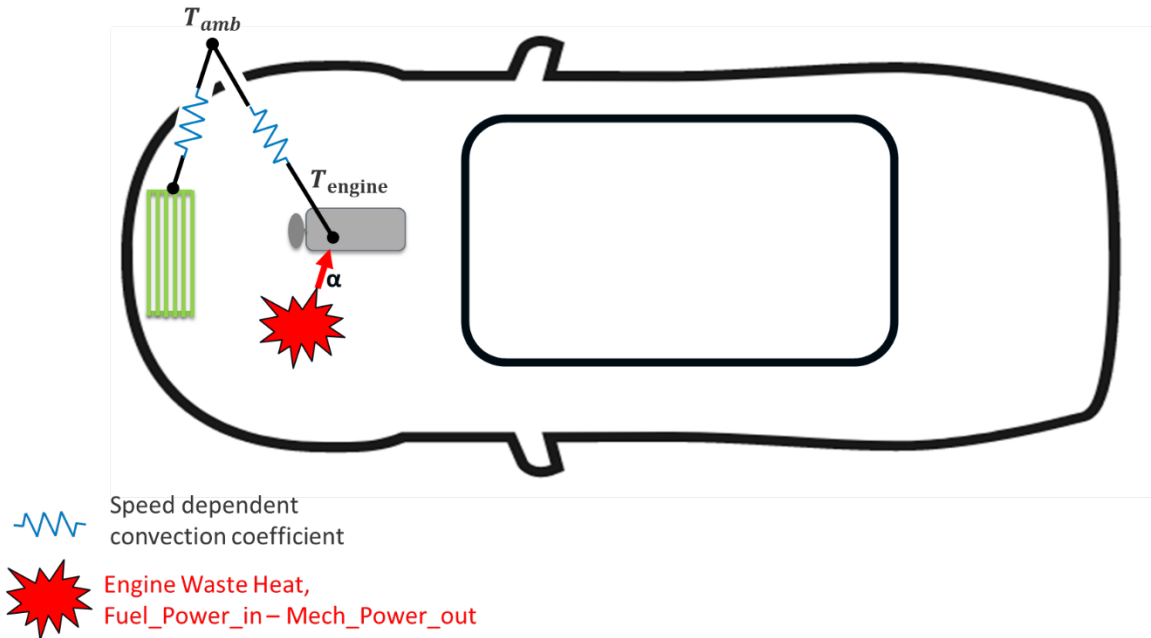


Figure 22. Schematic of semi-empirical approach to engine thermal modeling

3.4.1 Model Structure and Parameters

This model approach requires nine parameters that can be tuned such that engine temperature and instantaneous fuel consumption for a particular vehicle match test data over a wide range of warmup operating conditions (e.g., a vehicle starting at 0°C with an outside ambient temperature of 0°C). These parameters are engine thermal mass (J/K), effective length (m) of engine for convection calculations, fraction of combustion energy lost to engine block, convection coefficient from engine to ambient when the vehicle is stopped, radiator fin effectiveness, linear slope and offset parameters for temperature-dependent efficiency coefficient, temperature at which thermostat opening begins, and temperature at which thermostat is fully open.

The governing equation and constitutive equations for engine temperature are defined as follows:

$$mc_{eng} \frac{dT_{eng}}{dt} = \dot{Q}_{comb-eng} + \dot{Q}_{eng-amb} \quad (29)$$

$$\dot{Q}_{comb-eng} = \alpha(P_{fuel} - P_{crank}) \quad (30)$$

$$\dot{Q}_{eng-amb} = -h_{eng-amb}A_{eng}(T_{eng} - T_{amb}) \quad (31)$$

$$h_{eng-amb} = \begin{cases} (1 - x_{stat}) * h_{stop} + x_{stat} * h_{stop}, v < 2.2 \text{ mph} \\ (1 - x_{stat}) * h_{move} + x_{stat} * h_{move}, v \geq 2.2 \text{ mph} \end{cases} \quad (32)$$

where $mc_{eng} \equiv$ thermal capacitance of the engine

$T_{eng} \equiv$ engine temperature

$\dot{Q}_{comb-eng} \equiv$ heat from combustion to the engine block

$\dot{Q}_{eng-amb} \equiv$ heat transfer from engine to ambient

$\alpha \equiv$ fraction of combustion heat that enters engine thermal mass (adjustable parameter)

$P_{fuel} \equiv$ thermal power of fuel combustion

$P_{crank} \equiv$ mechanical power of engine crankshaft

$h_{eng-amb} \equiv$ heat transfer coefficient from engine to ambient

$A_{eng} \equiv$ effective heat transfer area of engine (based on adjustable effective engine diameter parameter)

$T_{amb} \equiv$ ambient temperature

$x_{stat} \equiv$ fraction of thermostat opening

$h_{stop} \equiv$ coefficient of convection when vehicle is nominally stopped (adjustable parameter)

$h_{move} \equiv$ coefficient of convection when vehicle is moving.

Heat transfer from the engine to ambient is modeled in six modes:

1. Direct cooling of engine to ambient air when the vehicle is stopped (below 2.2 mph or 1 m/s) and the thermostat is fully closed. In this mode, a tunable heat transfer coefficient parameter is used.
2. Direct cooling of engine to ambient air when the vehicle is moving and the thermostat is fully closed. In this mode, the heat transfer from the engine to ambient is modeled with the engine approximated as a sphere with a tuned diameter undergoing external convection using equation 7.44 from Incropera and DeWitt (2002).
3. Fully enhanced cooling of engine to ambient air when the vehicle is stopped (below 2.2 mph or 1 m/s) and the thermostat is fully open. In this mode, heat transfer from the radiator is modeled as if the engine is a finned surface with a tunable parameter for radiator fin efficiency. The constant heat transfer coefficient mentioned in mode 1 is multiplied by this effectiveness.
4. Fully enhanced cooling of engine to ambient air when the vehicle is moving and the thermostat is fully open. In this mode, heat transfer from the radiator is modeled as if the engine is a finned surface with a tunable parameter for radiator fin efficiency. The calculated heat transfer coefficient mentioned in mode 2 is multiplied by this effectiveness.
5. Partially enhanced cooling of engine to ambient air when the vehicle is stopped (below 2.2 mph or 1 m/s) and the thermostat is partially open. In this mode, the heat transfer

rates calculated in modes 1 and 3 are linearly blended based on interpolating the engine temperature between the thermostat start-to-open temperature and the fully open temperature, emulating the behavior of the thermostat.

6. Partially enhanced cooling of engine to ambient air when the vehicle is moving and the thermostat is partially open. In this mode, the heat transfer rates calculated in modes 2 and 4 are linearly blended based on interpolating the engine temperature between the thermostat start-to-open temperature and the fully open temperature, emulating the behavior of the thermostat.

Engine efficiency is calculated using Equation 20.

3.4.2 Temperature and Fuel Consumption Results for a 2011 Ford Fusion

The nine parameters for the engine thermal model were tuned such that temperature and instantaneous fuel consumption matched test data using the Non-dominated Sorting Genetic Algorithm III (NSGA-III) multi-objective algorithm from the pymoo (Blank and Deb 2020) Python package. Tests sourced from the Argonne National Lab Downloadable Dynamometer Database (D³) were conducted with a conventional powertrain 2011 Ford Fusion for the drive cycles in Table 2.

Table 2. Dynamometer Drive Cycles Used To Obtain Data for Tuning and Validation of the 2011 Ford Fusion Engine Thermal Model

Initial/Ambient Temperature	Cycle	Usage
-17.8°C (0°F)	UDDS repeated four times	Tuning
	US06 repeated four times	Validation
-6.67°C (20°F)	US06 repeated two times	Tuning
	UDDS repeated four times	Validation
22.2°C (72°F)	UDDS repeated three times	Tuning
	US06 repeated two times	Validation

The data in Table 2 are organized such that for each temperature, one UDDS-based and US06-based cycle are used for tuning and validation, or vice versa. Thus, each temperature has both a tuning and validation cycle, and both cycles are used for both tuning and validation. For both temperature and fueling rate, Equation 33 was used to calculate the minimization objective values:

$$\omega = \frac{\int abs(x_{model} - x_{test}) dt}{t} \quad (33)$$

where $\omega \equiv$ the value of the objective to be minimized

$x_{model} \equiv$ the value of the variable provided by the model

$x_{test} \equiv$ the value of the variable from the test data

$t \equiv$ time.

Running the optimizer for 100 generations with a population size of 200 yields the values in Table 3 for the engine thermal model parameters.

Table 3. Tuned Parameters for Engine Thermal Model To Match Test Data for Both Fueling Rate and Temperature

Engine thermal mass [kJ/K]	50.2
Engine diameter for convection model [m]	0.109
Combustion to engine heat fraction	0.248
Stopped convection coefficient [W/(m ² ·K)]	62.3
Radiator fin effectiveness	46.1
Efficiency coefficient offset	0.382
Efficiency coefficient slope [K ⁻¹]	6.31 × 10 ⁻³
Thermostat start-to-open temperature [°C]	89.4
Thermostat fully open temperature [°C]	90.9

Note that the values shown in Table 3 are the result of tuning the semi-empirical model to match publicly available test data without the need for any proprietary manufacturer details and are not necessarily exact matches for the real vehicle. A sample plot of results generated from these parameters is shown in Figure 23.

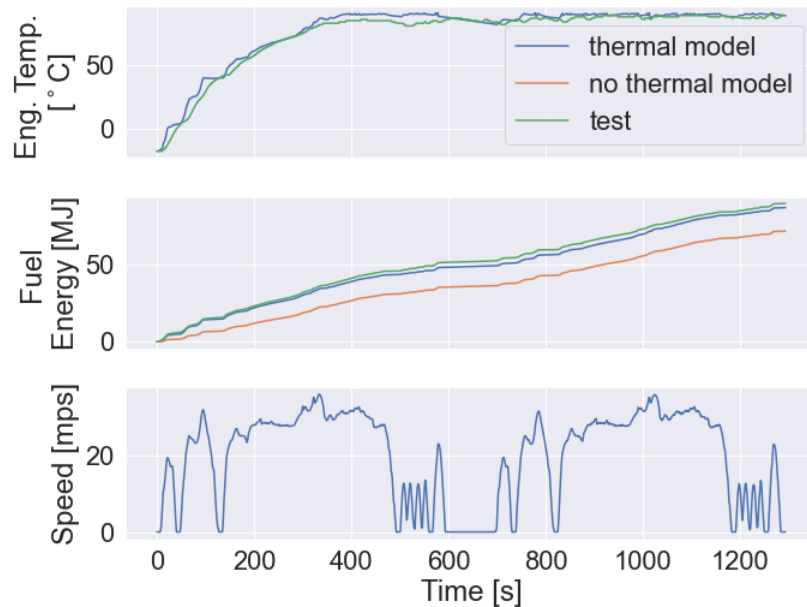


Figure 23. (Top) Engine temperature for model and test; (middle) cumulative fuel energy consumed for thermal model, baseline model without any thermal effects, and test; and (bottom) vehicle speed vs. time for repeated US06 tests conducted in 0°F/−17.8°C. Note that the thermal model greatly improves the ability to match the fueling rate shown in the test data.

Thermal tuning and validation results for all the remaining drive cycles in Table 2 are shown in Appendix C.

3.5 Engine Stop/Start Fuel Saving Feature

Over 30% of vehicles sold in the United States now have stop/start and deceleration fuel cutoff (DFCO) capabilities (EPA 2020), in which the engine can completely shut off during what would otherwise be idle periods (e.g., at a traffic light) or stop fueling during deceleration events to save fuel. In typical real-world driving conditions, stop/start saves around 5% in a range of driving conditions (Simmons et al. 2015).

To implement engine stop/start in FASTSim, the standard full HEV controls and battery capacity were modified to prevent the motor/generator from providing any assistance with forward propulsion. This enables fueling of the engine to shut off during a vehicle stop or deceleration event, but no other changes occur relative to a conventional vehicle. Resulting fuel energy consumption for a hypothetical 2016 Toyota Corolla both with and without stop/start are shown in Figure 24, producing fuel energy savings of 5.4%, consistent with values found in the literature.

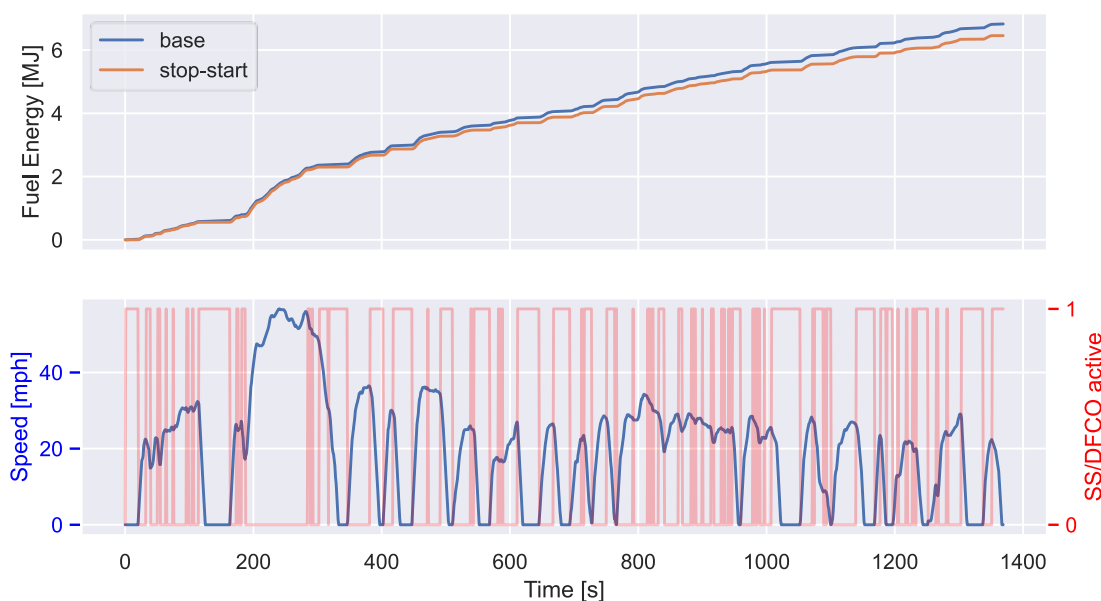


Figure 24. (Top) Energy consumption for a simulated vehicle both without stop/start (“base”) and with stop/start modeled. (Bottom) UDDS speed trace and active/inactive status of stop/start and DFCO for the vehicle simulated with these advanced technologies active.

4 Vehicle-Level Base Modeling and Validation

This section focuses on vehicle-level modeling and validation within FASTSim’s base option (see Table 1). Section 4.1 addresses vehicle-level time series validation. Section 4.2 addresses fuel economy and performance validation.

4.1 Vehicle-Level Time Series Validation

The time series validations shown here compare FASTSim road load and energy consumption rates (fuel power and battery power, both in kilowatts) against data from ANL chassis

dynamometer testing. All time series plots are shown over sections of the high-speed, high-acceleration US06 drive cycle.

Figure 25 and Figure 26 show results for the midsize Ford Fusion and the compact Chevrolet Cruze conventional gasoline vehicles. Both demonstrate good FASTSim fits to measured data for required tractive power and fuel power over time.

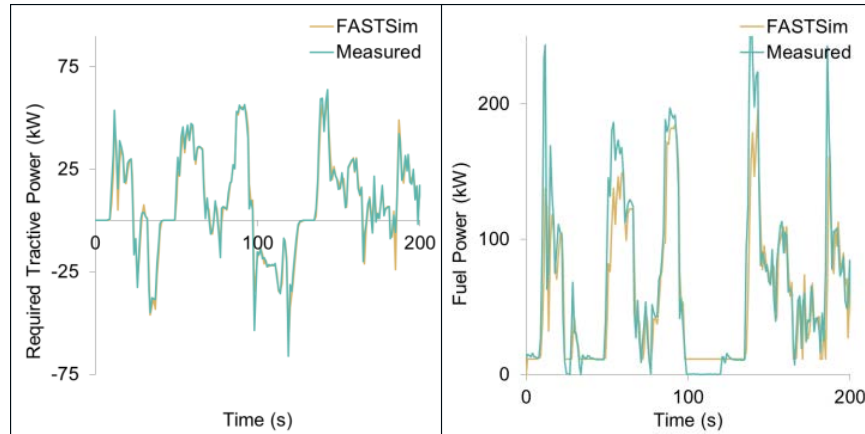


Figure 25. Time series validation: 2012 Ford Fusion, US06

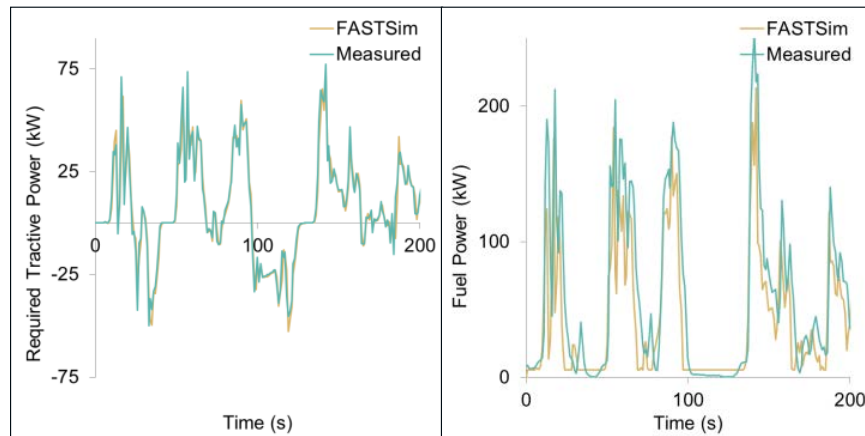


Figure 26. Time series validation: 2014 Chevrolet Cruze, US06

HEV and PHEV results are shown in Figure 27 (Toyota Prius), Figure 28 (Toyota Prius Plug-in), and Figure 29 (Chevrolet Volt), which also include battery power results. FASTSim's time series matches for these advanced vehicles are generally good. Finally, strong FASTSim fits for EVs are shown in Figure 30 (Nissan Leaf) and Figure 31 (Volkswagen e-Golf).

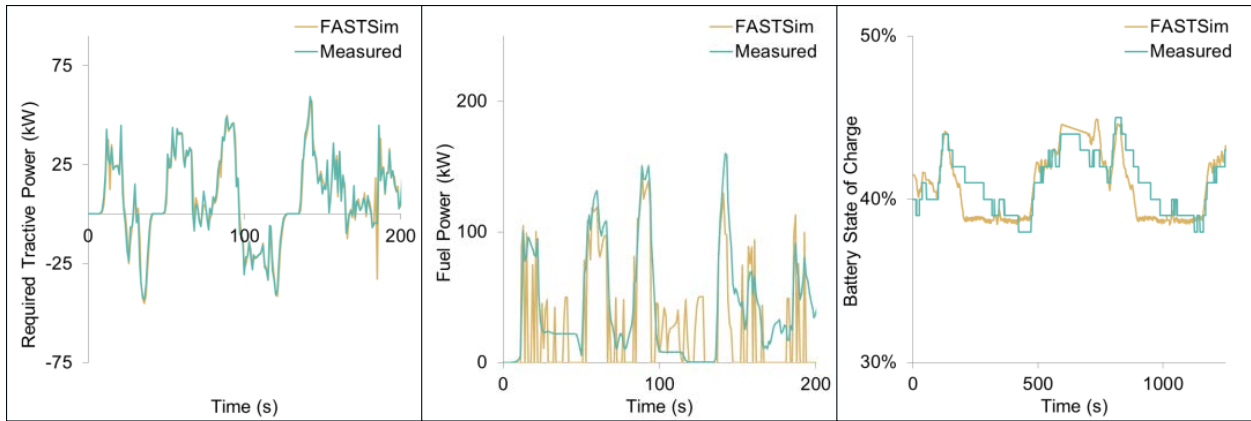


Figure 27. Time series validation: 2010 Toyota Prius, US06

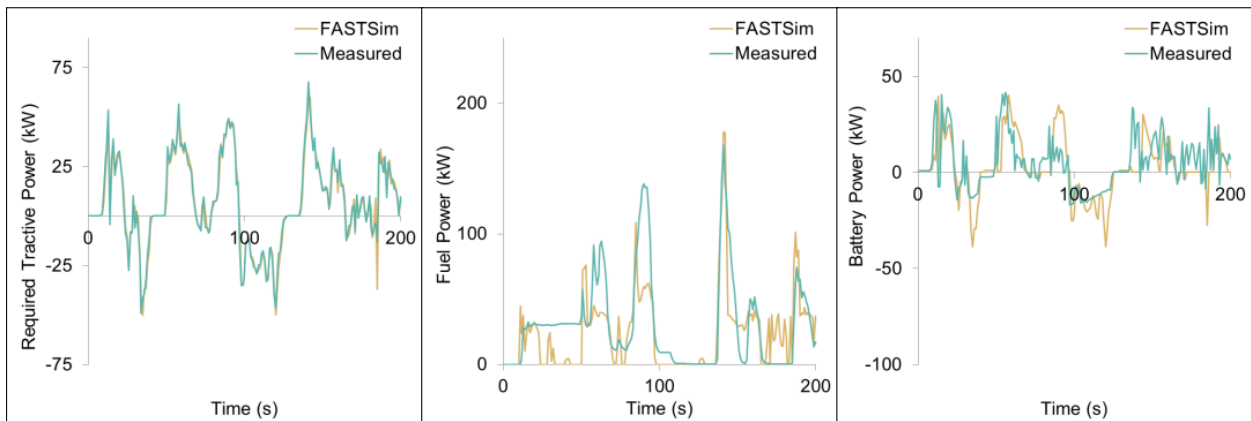


Figure 28. Time series validation: 2013 Toyota Prius Plug-in, US06

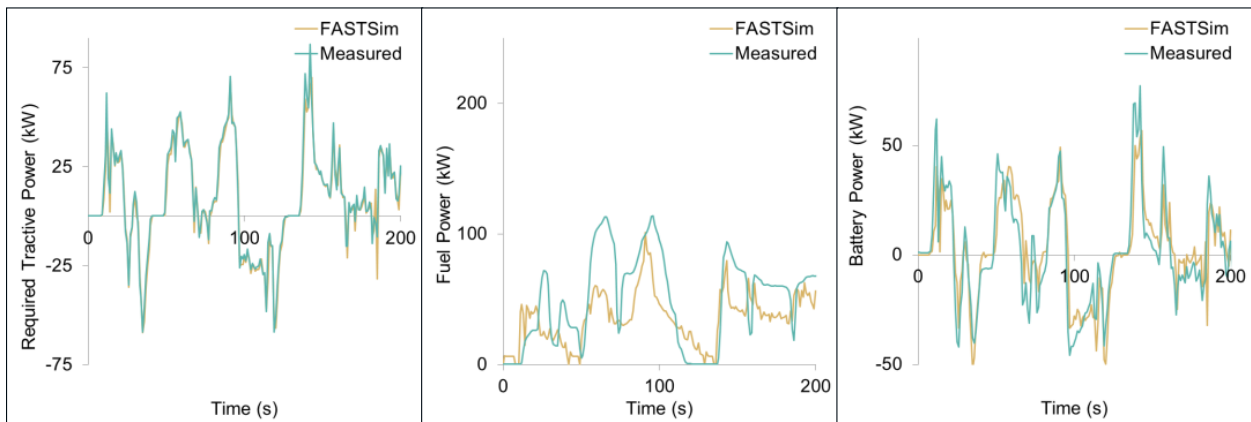


Figure 29. Time series validation: 2012 Chevrolet Volt, US06

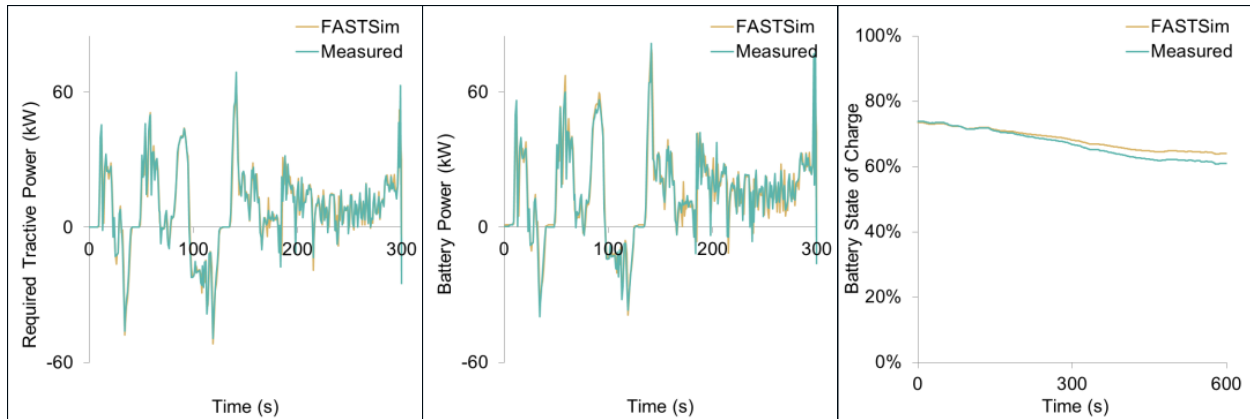


Figure 30. Time series validation: 2013 Nissan Leaf, US06

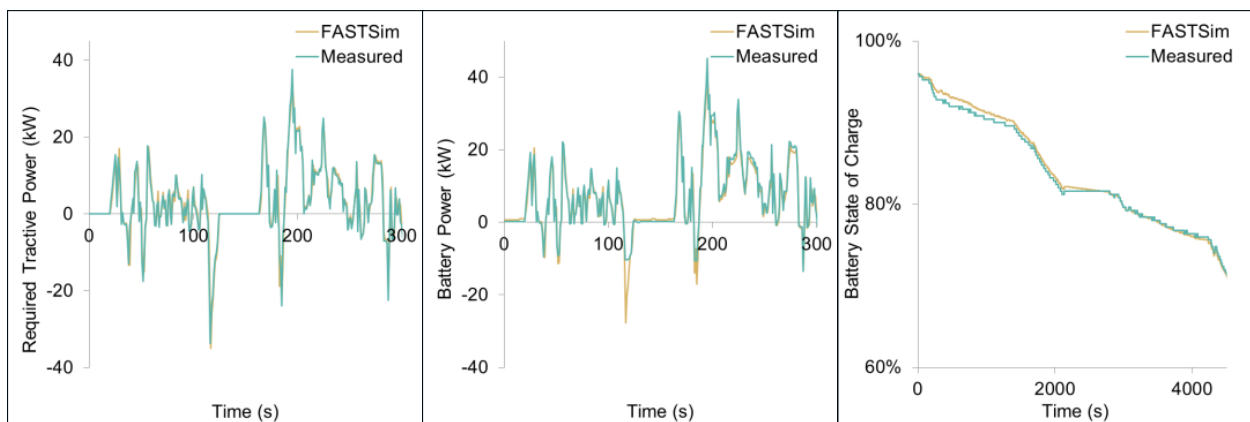


Figure 31. Time series validation: 2015 Volkswagen e-Golf, US06

4.2 Fuel Economy and Performance Validation

For fuel economy validation, the base FASTSim modeling in this section calibrates vehicle aerodynamic drag, rolling resistance, and test mass to EPA-reported values. FASTSim composite fuel economy results (derived from UDDS + HWFET drive cycle simulations, followed by application of the EPA’s real-world adjustment equations for 2-cycle testing) are compared with the actual EPA window sticker data for the corresponding vehicles.

For performance validation, FASTSim-simulated acceleration is compared with acceleration data from the website Zeroto60Times (Zeroto60Times 2018). This website aims to compile credible 0-to-60-mph acceleration times and average the results.

Section 4.2.1 presents validation results on a subset of vehicles for which NREL has rigorously vetted input data (for all the standard FASTSim base inputs such as engine power, motor power, etc.). Section 4.2.2 presents the overall validation results on a larger set of vehicles for which the corresponding input data have been partially vetted. Appendix A shows the individual vehicle-by-vehicle validation results for the roughly 700 vehicles with partially vetted input data.

4.2.1 Validation Results for Vehicles with Vetted Inputs

Figure 32 shows the FASTSim base fuel economy validation for 11 conventional, hybrid, plug-in hybrid, and fuel cell vehicles with NREL-vetted input data, and Figure 33 shows the electricity consumption validation for five EVs with NREL-vetted input data. Even for the FASTSim base modeling with generalized component and powertrain representations across this wide variety of simulated vehicles, the modeled energy efficiency is typically within 10% of the measured/rated value, and often within 5%. The largest disparities tend to be for vehicles with very high fuel economy, where the actual energy consumption differences end up being quite small due to the high efficiency of such vehicles.

Figure 34 shows the FASTSim acceleration validation for these vehicles. Similarly, the modeled and actual results are very close, with the FASTSim base modeled acceleration values for this broad assortment of vehicles typically within 10% of the measured values, and often within 5%. While not the focus of this report, FASTSim’s estimated manufacturer’s suggested retail price has additionally shown strong validation against actual pricing data for a variety of vehicles. FASTSim’s abilities to accurately estimate vehicle fuel economy, acceleration performance, and price are leveraged in its integration with the Automotive Deployment Options Projection Tool (ADOPT), which NREL uses for vehicle choice modeling (Brooker 2015-0974; NREL 2020).

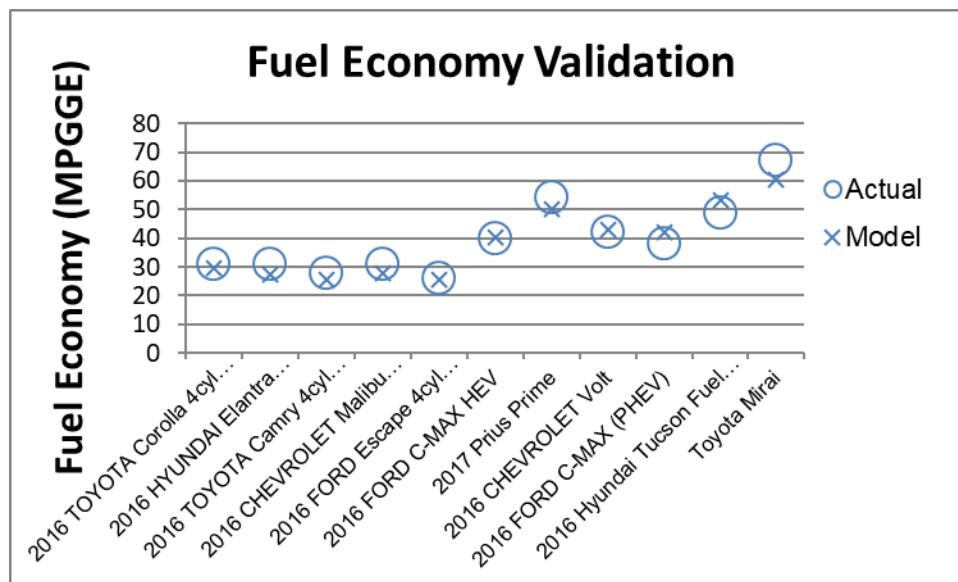


Figure 32. FASTSim base fuel economy validation versus EPA window sticker data for subset of vehicles with vetted inputs

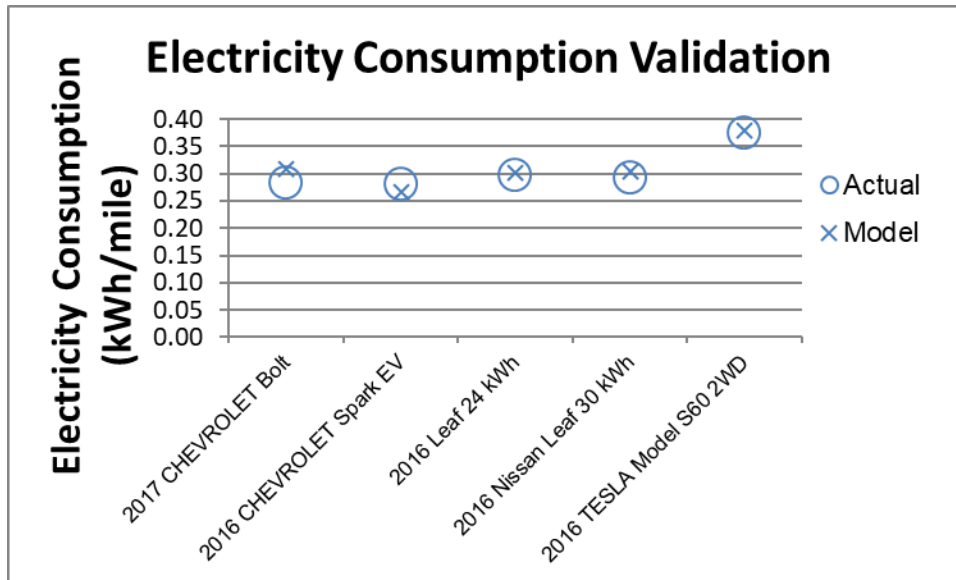


Figure 33. FASTSim base electricity consumption validation versus EPA window sticker data for subset of EVs with vetted inputs

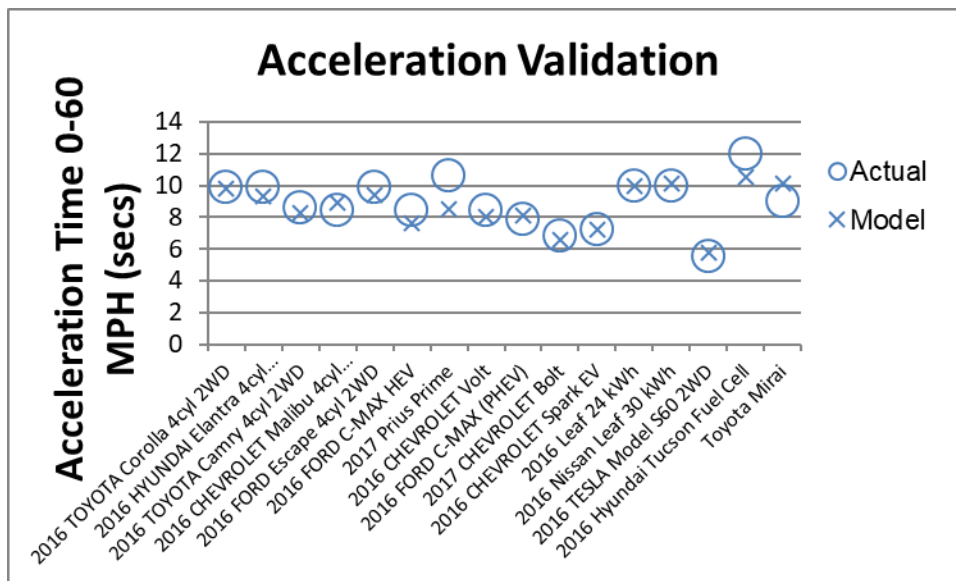


Figure 34. FASTSim base acceleration validation versus Zeroto60Times website data for subset of vehicles with vetted inputs

4.2.2 Large-Scale Validation Results for Vehicles with Partially Vetted Inputs

In its integration with ADOPT, FASTSim estimates fuel economy, acceleration performance and price for future vehicles that ADOPT anticipates will enter the market under different scenarios. The starting point for each future market evolution scenario is a set of roughly 700 existing vehicles. These existing vehicles are also represented by FASTSim models to provide the basis for future vehicle variations. As project resources permit, the input data for this large set of initial vehicles are vetted with respect to component sizes along with factors such as the presence of

turbocharging (affects efficiency and acceleration), two-wheel versus four-wheel drive (affects efficiency and acceleration), and front-wheel versus rear-wheel drive (center of gravity affects acceleration). Simulation results compared with measured/rated values for these vehicles are therefore subject to any data quality issues that have not been caught through the partial vetting. The summarized results shown here along with the individual vehicle results shown in Appendix A are nevertheless similar to those presented for the vetted vehicles discussed in Section 4.2.1.

For example, Figure 35 shows for a sample of partially vetted conventional gasoline vehicles that the modeled and measured values are again quite close for both fuel economy and acceleration performance. Figure 36 shows percent fuel consumption error histograms on both a per-vehicle and a per-sales basis for the full set of existing conventional vehicles with partially vetted inputs used in ADOPT. The results again show FASTSim base typically modeling fuel consumption within 10% accuracy, and often within 5%. Note for the plots throughout this section that the acronym CD indicates “charge depleting” results where the battery in a PHEV or EV is depleted over the evaluated test cycles, as opposed to charge sustaining (CS) test results, where there is no net change to battery state of charge over the test cycles.

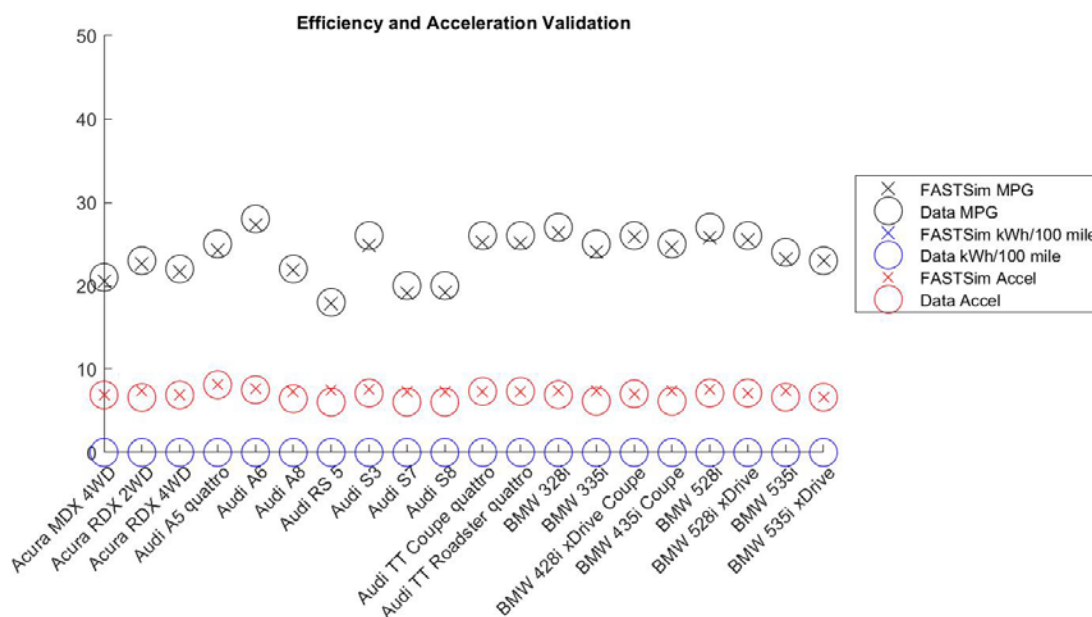


Figure 35. Example of FASTSim base fuel economy (versus EPA window sticker data) and acceleration (versus Zeroto60Times website data) validation for conventional gasoline vehicles with partially vetted inputs⁴

⁴ Electricity consumption for these conventional vehicles is zero. Electricity consumption points are plotted here merely for consistency with other similar figures.

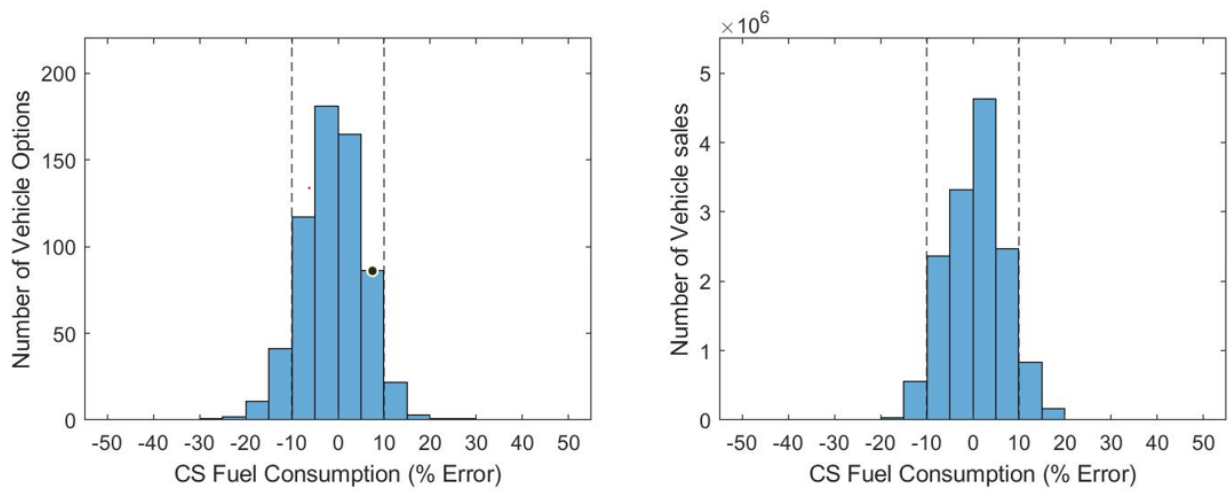


Figure 36. Histograms of error (difference between FASTSim base modeled and measured fuel consumption) for partially vetted conventional gasoline vehicles

Figure 37 shows the fuel economy and acceleration validation results for HEVs that sold more than 10,000 vehicles in 2015. Figure 38 shows the fuel consumption percent error histograms for these vehicles on both a per-vehicle and a per-sales basis. Similarly, Figure 39 shows the electricity consumption and acceleration validation results for EVs that sold more than 1,000 vehicles in 2015, and Figure 40 shows the corresponding electricity consumption percent error histograms on both a per-vehicle and a per-sales basis. As with the conventional vehicles, the validation for these advanced technology vehicles shows FASTSim base typically estimating energy consumption within a 10% accuracy level, and often within 5%.

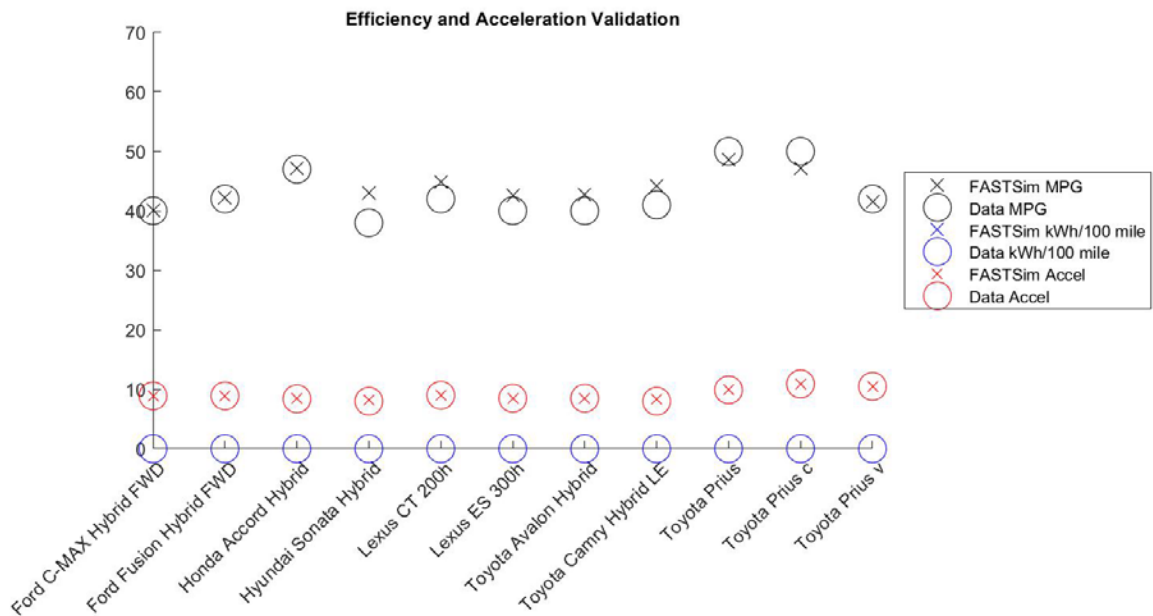


Figure 37. FASTSim base fuel economy (versus EPA window sticker data) and acceleration (versus Zeroto60Times website data) validation for HEVs (with 2015 sales of more 10,000 vehicles) with partially vetted inputs

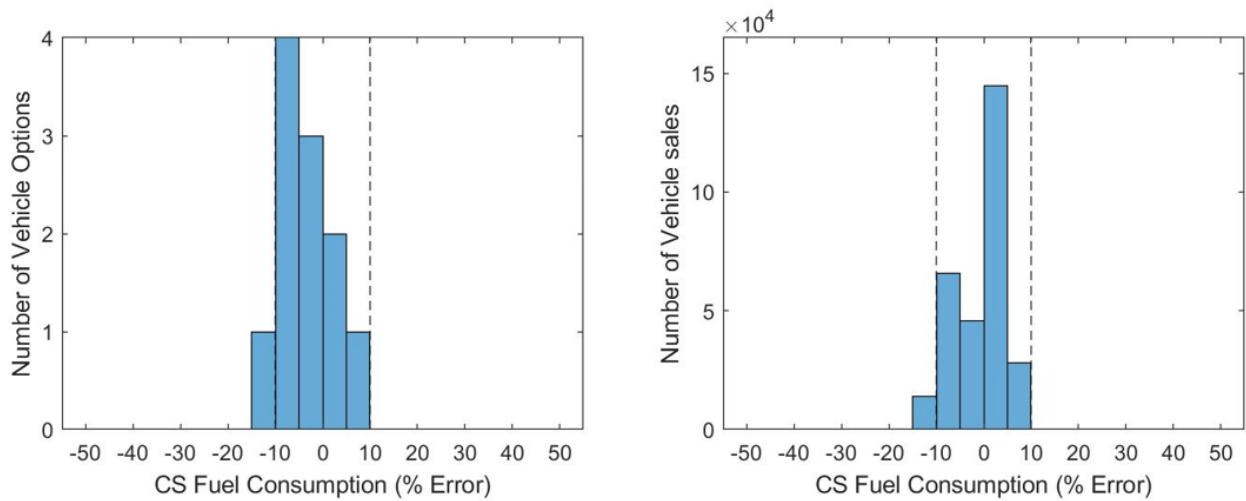


Figure 38. Histograms of fuel consumption percent error (difference between FASTSim base modeled and measured results) for partially vetted HEVs

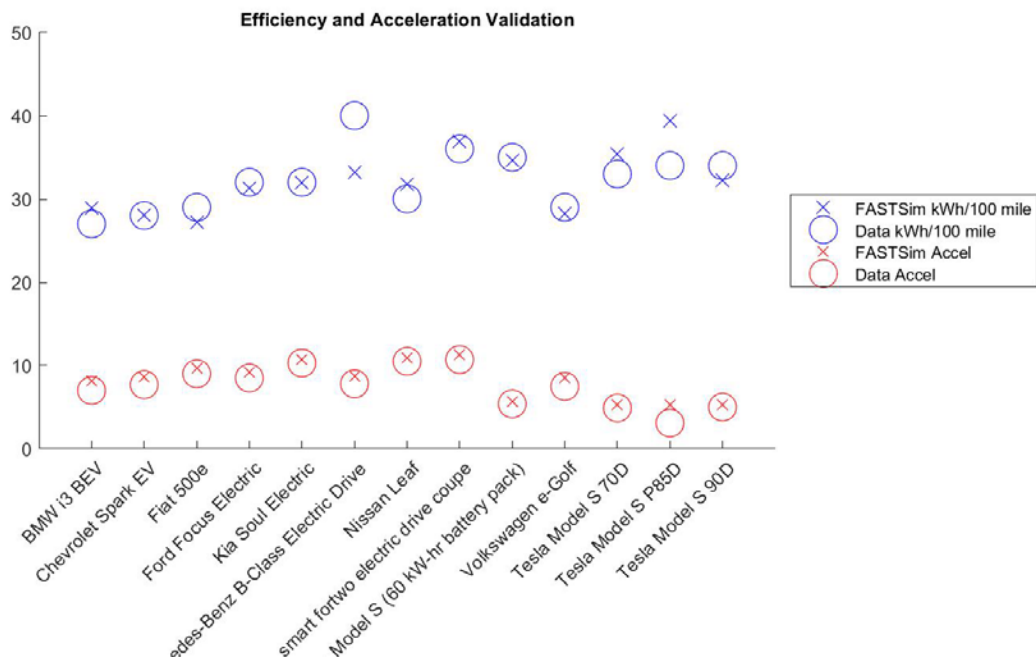


Figure 39. FASTSim base electricity consumption (versus EPA window sticker data) and acceleration (versus Zeroto60Times website data) validation for EVs (with 2015 sales of more 1,000 vehicles) with partially vetted inputs

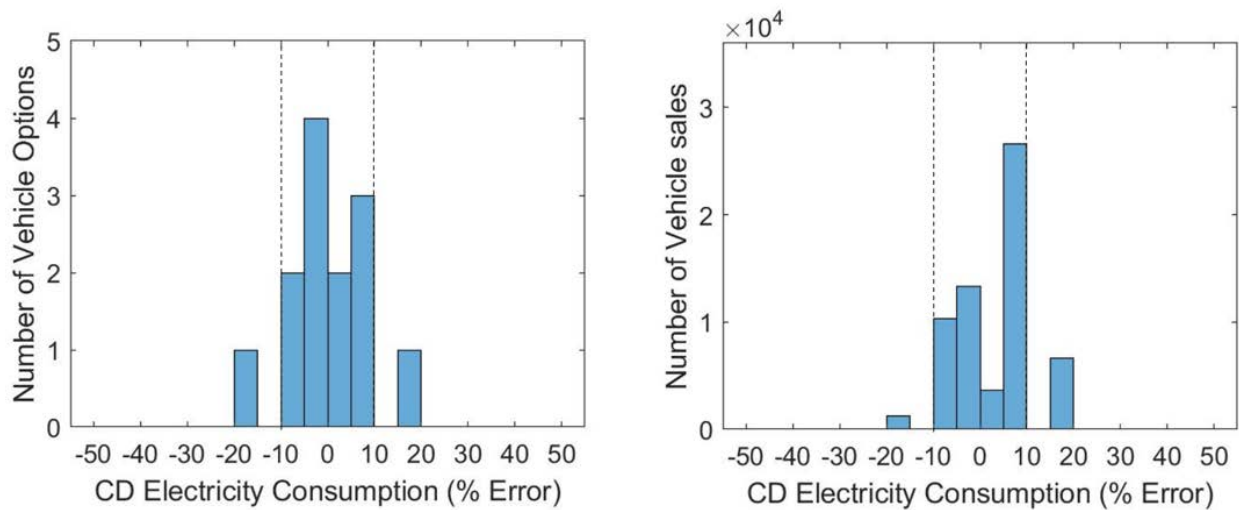


Figure 40. Histograms of electricity consumption percent error (difference between FASTSim base modeled and measured results) for partially vetted EVs

5 On-Road/Real-World Validation

The previous two sections focus on component- and vehicle-level modeling and validation within FASTSim’s base option. This section explores the more detailed end of the FASTSim continuum—the customized option with extensions (see Table 1). Specifically, it summarizes the calibration of FASTSim to an individual vehicle using chassis dynamometer data over standard drive cycles, followed by validation of the model against data collected during on-road operation of the vehicle. See Wood, Gonder, and Jehlik (2017) for additional details. Note that the component adjustments to the engine map in response to the number of gears are not included in this section, as the engine map was instead calibrated directly against dynamometer data. As such, any real-world impacts from the transmission are inherent in the validation data. The generalized transmission adjustments previously discussed are used when exhaustive dynamometer data are not available (as is often the case).

First, chassis dynamometer data were collected from a four-cylinder, six-speed 2011 Ford Fusion, which is representative of a typical midsize vehicle, at ANL’s test facility. Instrumentation of the vehicle included more than 27 channels of thermal data (Figure 41). The vehicle was exercised over a matrix of 16 dynamometer tests characterized by different drive cycles, initial thermal conditions, and ambient temperatures (Table 4).

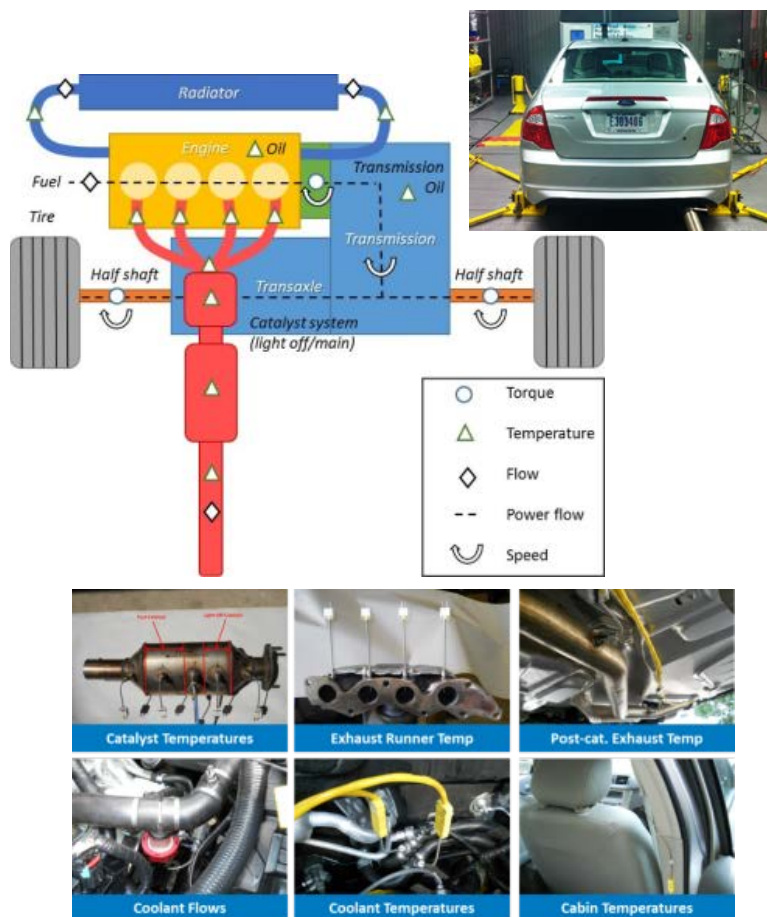


Figure 41. Instrumentation of Ford Fusion test vehicle

Photo credit: Forrest Jehlik, ANL

Table 4. Matrix of Dynamometer Tests

Variable	Values
Drive cycle	UDDS × 2, US06 × 2
Start condition	Hot start, cold start
Test cell temperature	-17°C, -7°C, +20°C, +35°C

The dynamometer data were then used to calibrate a customized FASTSim model of the Ford Fusion. This calibration included estimation of engine oil viscosity and fuel enrichment using lumped thermal models for engine oil/coolant and exhaust catalyst as well as modeling of mechanical losses relative to power and thermal state. The resulting model calculates fuel consumption to within 5.2% of measured data under all 16 test conditions, with a 2.4% root-mean-square error (RMSE). These differences are within the range of cycle-to-cycle dynamometer test uncertainty (Figure 42). For model validation, EPA 5-cycle testing was conducted, including the Federal Test Procedure (FTP), HWFET, US06, SC03, and Cold FTP. The modeled fuel economy was within 3.0% of the measured data. To capture the impacts of cabin AC use, a simplified cabin model was calibrated to test data over the SC03 cycle, which showed 19.6 mpg with the AC on and 26.0 mpg with the AC off.

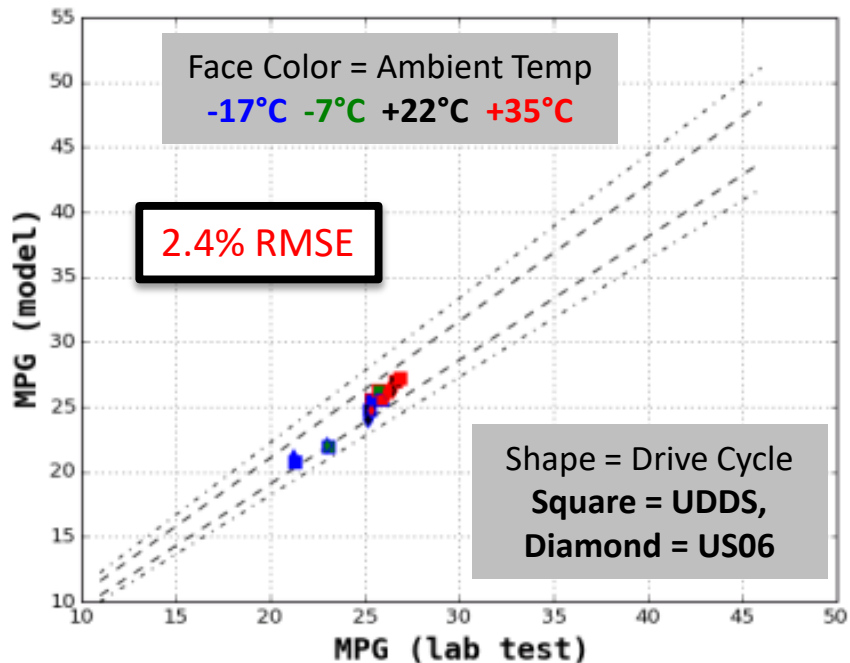


Figure 42. Calibration of FASTSim-modeled Ford Fusion fuel economy to dynamometer data

Next, NREL and ANL performed on-road testing of the Ford Fusion, retaining most of the instrumentation from the dynamometer testing but with some reconfiguration for mobile data collection. Important new elements included a Global Positioning System device for measuring vehicle position and a highly accurate inline fuel flow meter. The Global Positioning System device also enabled calculation of elevation via cross-referencing latitude/longitude data with a third-party elevation map and NREL-developed filtering routines. Overall, most of the instrumentation was customized for the testing, with less reliance on controller area network data.

The instrumented vehicle was driven in a mix of various conditions known to impact fuel economy (Table 5).

Table 5. On-Road Testing Characteristics

Data-collection period	August–September 2015
Trip count	85
Total distance	2,843 miles
Trip average speeds	15–75 mph
Trip types	36 “highway” (≥ 40 mph avg. speed), 49 “city” (< 40 mph)
Initial oil temps	20°C–100°C (68°F–212°F) 32 “hot” start ($\geq 80^\circ\text{C}$), 53 “cold” start ($< 80^\circ\text{C}$) trips
Ambient temps	17°C–38°C (63°F–100°F)
AC status	31 trips with AC on, 54 trips with AC off
Elevation range	535–11,100 ft
Trips with elevation change of $\pm 3,000$ ft	6

Figure 43 shows the validation of the customized FASTSim model against the on-road data. The shape and colors of the symbols signify various conditions as noted in the legend. Wind was not directly accounted for during the testing, but weather data suggested that winds of 5–10 mph were typical; thus, the figure includes error bars representing fuel economy impacts from 5-mph head/tail winds. Overall, the modeled and measured results match well, with an RMSE of 5.6%, showing that FASTSim trained on a limited set of dynamometer cycles can perform well over a broad range of real-world conditions (over which trip-level fuel economy varies by over $\pm 50\%$ from the average for the vehicle).

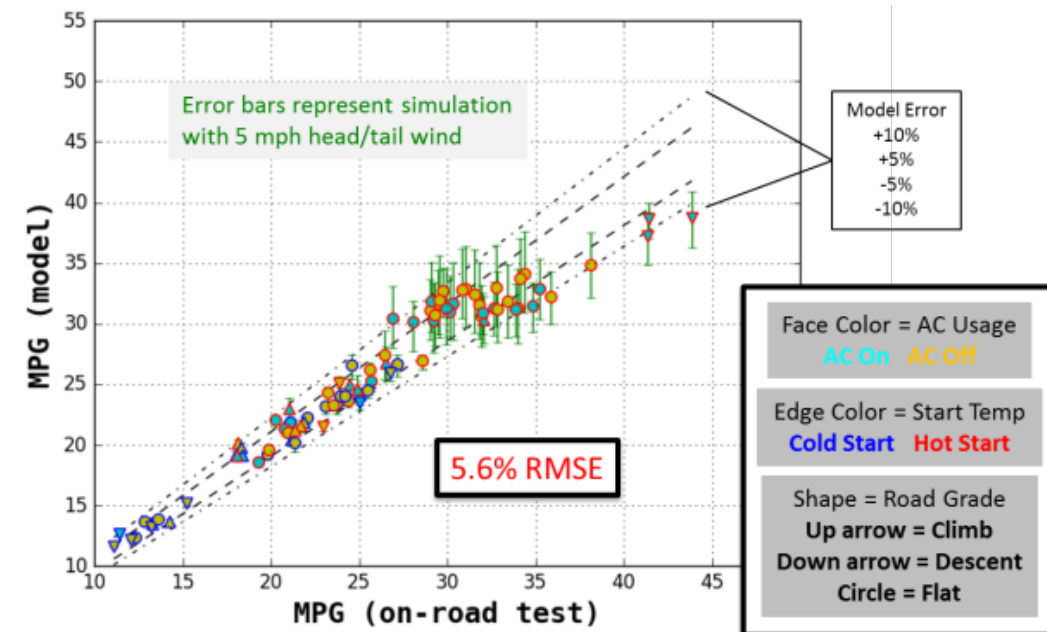


Figure 43. Validation of FASTSim-modeled versus measured fuel economy over on-road driving

Finally, Figure 44 breaks out the effects on the fit between FASTSim modeled and measured results due to the incorporation of various vehicle and environmental conditions. The baseline model produces considerably more variation, with an RMSE of 16.8%.⁵ The largest improvements come from considering the thermal sensitivity of vehicle components and estimating road grade. Adjusting for air density improves the fit further, and accounting for cabin AC load results in the final model with a 5.6% RMSE. Clearly, effects not captured on a dynamometer are important for estimating real-world fuel economy. Further enhancements may include investigation of wheel set thermal sensitivities and the significance of wind on aerodynamic loads.

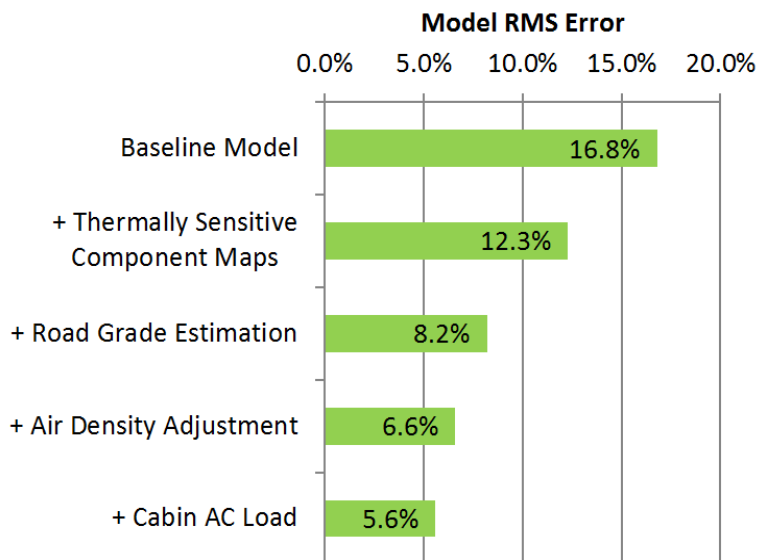


Figure 44. Effects on RMSE of incorporating various vehicle and environmental conditions into the FASTSim model

⁵ The baseline includes Ford Fusion-specific engine mapping but assumes hot starts for each trip.

6 FASTSim Applications and Publications

FASTSim has been leveraged in a wide range of studies and to support hundreds of research publications. Many of these are from NREL, but the list also includes contributions from DOE, other national laboratories, automakers, the California Air Resources Board, Google, and American and foreign universities and research centers. This section highlights a handful of example research papers and applications. Appendix B, together with the FASTSim website (NREL 2021a), provides a more exhaustive list of known FASTSim publications.

Google Maps Eco-Friendly Routing

Author/sponsor: Google/NREL

Application: New Google Maps feature

Year Launched: 2021

Summary: Leveraging both FASTSim and NREL’s Route Energy Prediction Model (RouteE) (NREL 2021b), NREL partnered with Google to develop more eco-friendly routing in Google Maps. After launching of the updated routing algorithm in the United States, Google Maps began defaulting to the route with the lowest carbon footprint when it has approximately the same estimated time of arrival as the fastest route. In cases where the eco-friendlier route could increase travel time, Google Maps shows users the relative CO₂ impact between routes, allowing them to make an informed choice about which route to take. Google plans to continue working with NREL, FASTSim, and RouteE to expand the feature to Europe and beyond in 2022 (Dicker 2021).

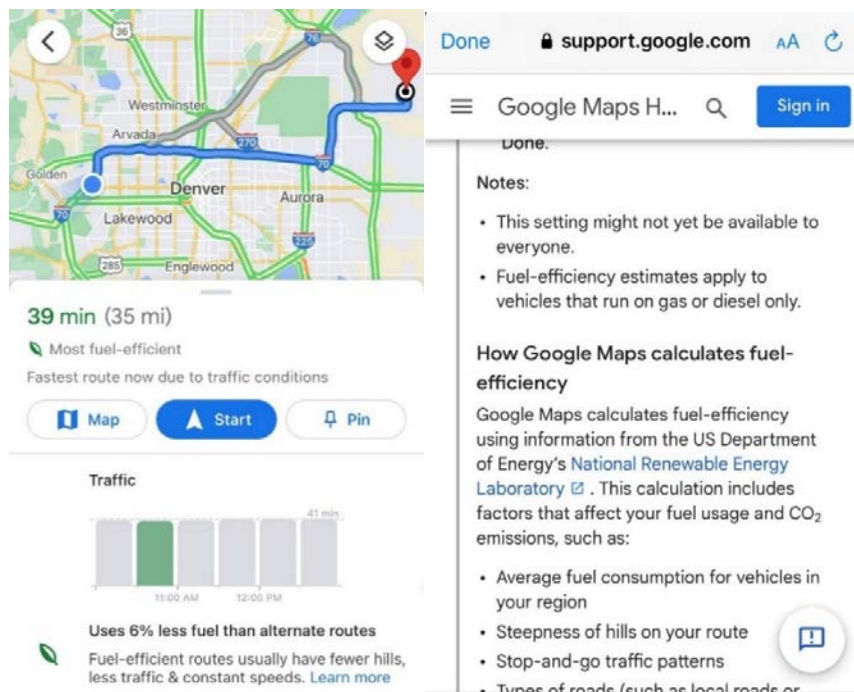


Figure 45. Fuel-efficient routing options in Google Maps

In-Route Inductive Versus Stationary Conductive Charging for Shared Automated Electric Vehicles: A University Shuttle Service

Author/sponsor: NREL

Publication: *Applied Energy*

Publication year: 2021

Summary: This study presents a planning optimization analysis for fixed-route automated shuttles supported by in-route inductive charging technology. A techno-economic feasibility of inductive charging was assessed in comparison with stationary charging, including Level 2 alternating current chargers and direct current fast chargers. The outcomes show that the proper design of quasi-dynamic inductive chargers at designated stops allows shared automated electric vehicles to realize unlimited driving range and be cost-competitive to direct current fast charger technology.

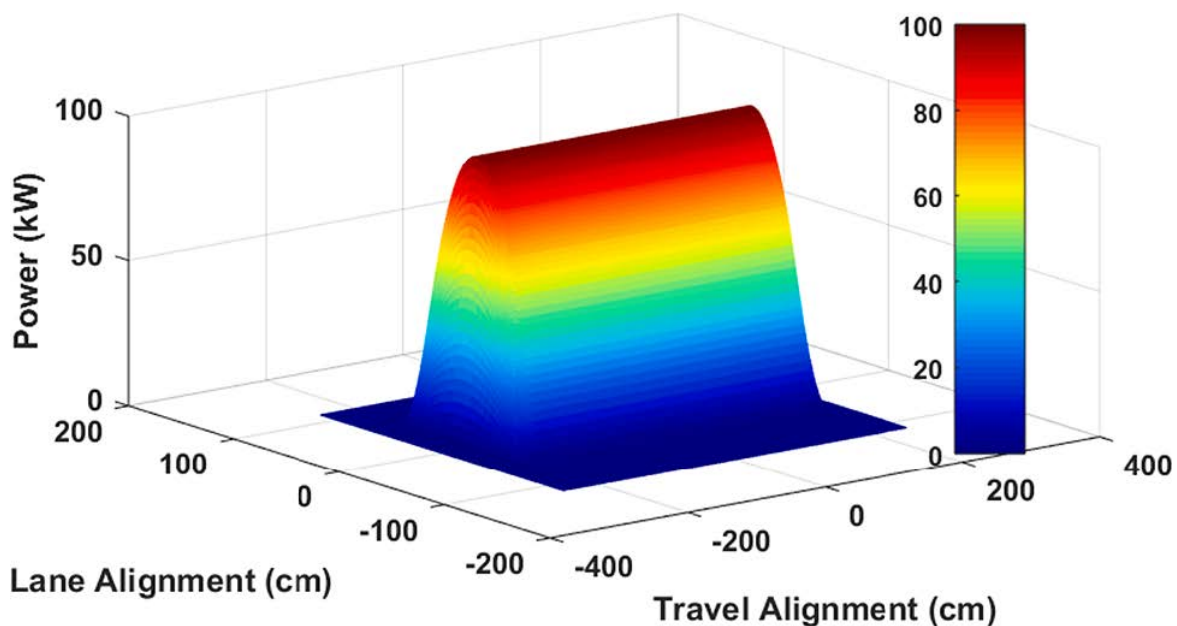


Figure 46. Power transfer profile for a 100-kW, 5-m inductive transmitter, considering vehicle's position in both travel and lane directions

Real-World Evaluation of National Energy Efficiency Potential of Cold Storage Evaporator Technology in the Context of Engine Start-Stop Systems

Author/sponsor: NREL, ANL, Toyota, Denso International America/Toyota

Publication: *SAE Technical Paper 2020-01-1252*

Publication year: 2020

Summary: Evaluated the national effects of a two-phase cold storage evaporator on climate control fuel use. The cold storage technology maintains the thermal state of air-conditioning evaporators to enable longer and more frequent engine-off operation in vehicles equipped with start-stop functionality. Test

results from ANL were analyzed and provided to NREL, where a simulation framework built with FASTSim and other models was calibrated to the test data. The vehicle model was then exercised over a large set of real-world drive cycle and ambient condition data to estimate national-level fuel economy benefits. This publication was referenced in Toyota’s EPA credit application.

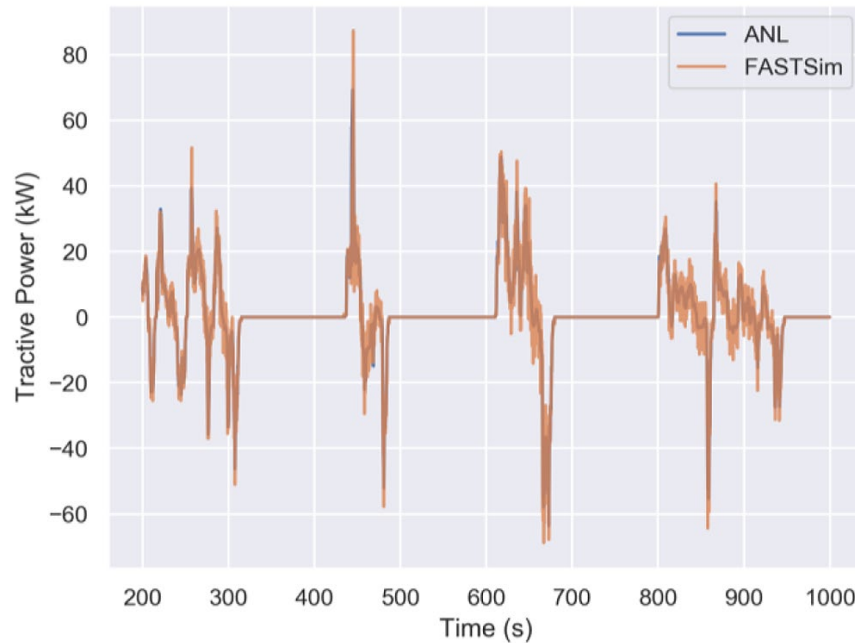


Figure 47. Comparison of tested and modeled tractive power for the 2018 Toyota Highlander from an example test cycle

Estimating Region-Specific Fuel Economy in the United States from Real-World Driving Cycles

Author/sponsor: NREL, Hyundai America Technical Center (HATCI)

Publication: *Transportation Research Part D: Transport and Environment*

Publication year: 2020

Summary: Developed method for estimating region-specific, real-world, light-duty vehicle fuel economy in the United States that is unique in both the size and representativeness of real-world driving that was considered, and for its ability to model regional variations in driving patterns. By simulating driving over the six representative driving cycles with FASTSim and applying the appropriate regional weighting factors, the authors found that regional fuel economy varies by more than 11% (inner 95th percent range) due to differences in driving patterns alone. Rural areas consistently have better fuel economies than urban areas. Urban areas experience much greater variation, ranging from a 1% improvement to more than 10% worse than the national average.

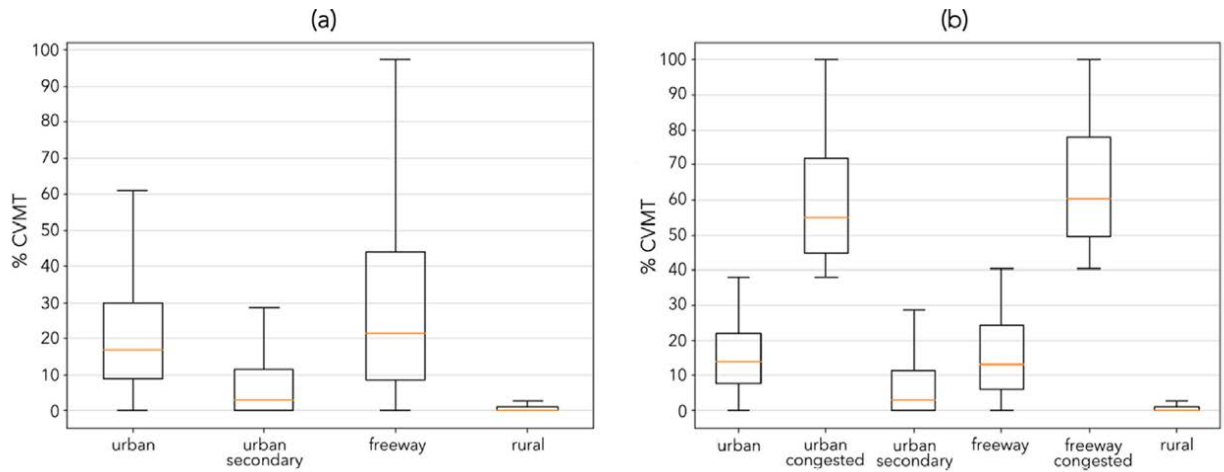


Figure 48. Percentage of congested vehicle miles traveled (CVMT) for trips within each of the four road type clusters (a) before and (b) after partitioning by congestion

An Approach for Characterizing Scenarios of Interest in Parameterized Pareto Plots: Application to Competitiveness Assessment of Light-Duty Plug-in Vehicles

Author/sponsor: Toyota Motors North America R&D

Publication: The World Congress of Structural and Multidisciplinary Optimization

Publication year: 2019

Summary: The authors developed an evolutionary algorithm for exploring Pareto trade-offs among cost and greenhouse gas emissions with varied battery cost, fuel cost, electricity cost, and charging behavior for various electrified powertrain types modeled in FASTSim.

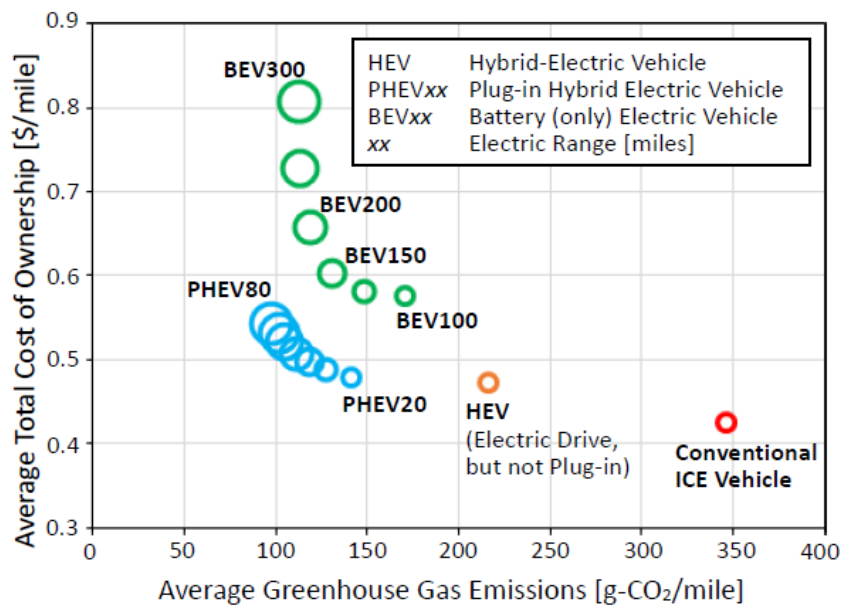


Figure 49. Pareto plot of average total cost of ownership and greenhouse gas emissions for BEV, PHEV, HEV, and conventional powertrain types and EV-mode ranges for applicable powertrain types. Circle area is indicative of battery size, where applicable.

Aerodynamic Drag Reduction Technologies Testing of Heavy-Duty Vocational Vehicles and a Dry Van Trailer

Author/sponsor: NREL, California Air Resources Board

Publication: NREL technical report

Publication year: 2016

Summary: On-road testing of commercial vehicles equipped with aerodynamic devices was used to calibrate FASTSim models, which were simulated over real-world drive cycles. This study complements EPA work on greenhouse gas regulations for commercial vehicles.

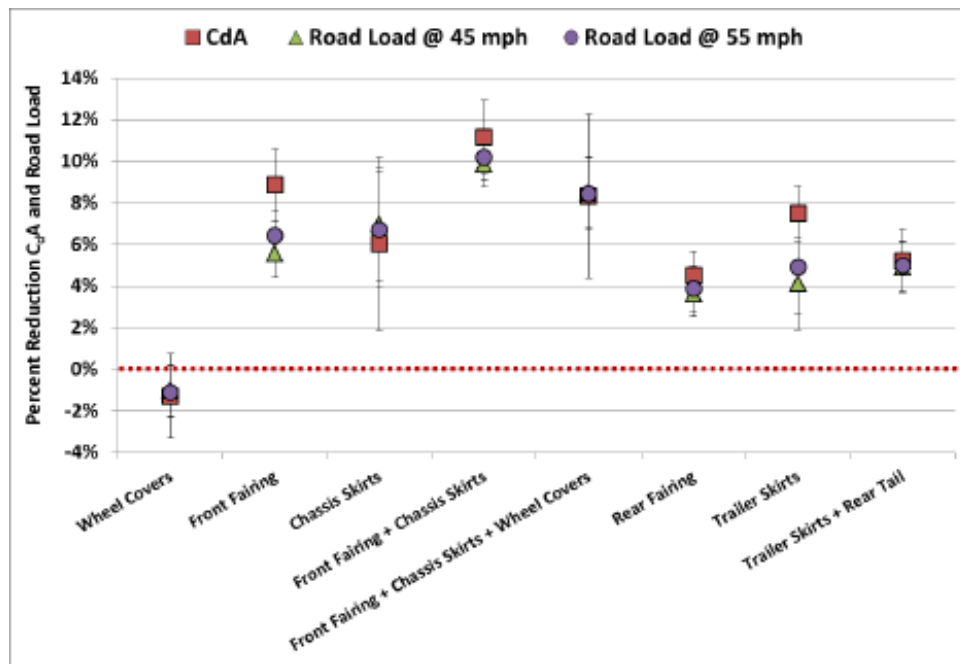


Figure 50. Observed change in coefficient of drag × frontal area (CdA) and road load without wind correction

Updating United States Advanced Battery Consortium and Department of Energy Battery Technology Targets for Battery Electric Vehicles

Author/sponsor: NREL, Ford, Chrysler, DOE

Publication: *Journal of Power Sources*

Publication year: 2014

Summary: The United States Advanced Battery Consortium updated EV technology targets with the support of NREL modeling, including FASTSim. The result was an aggressive target, implying that (as of 2012) batteries needed considerable advancement to make EVs competitive.

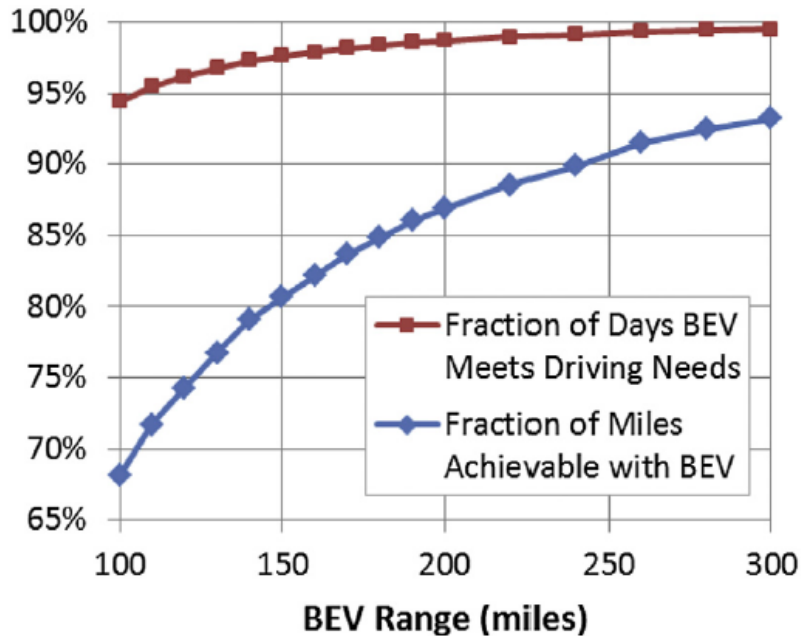


Figure 51. Day- and mile-based fleet utility factors for battery electric vehicles as a function of range based upon 2009 National Household Travel Survey data

A Cluster Analysis Study of Opportune Adoption of Electric Drive Vehicles for Better Greenhouse Gas Reduction

Author/sponsor: Toyota

Publication: ASME Design Automation Conference

Publication year: 2016

Summary: FASTSim was used to model real-world fuel economy from California Global Positioning System driving traces. The results suggest that the benefits of advanced technology vehicles are maximized when applied to specific driving patterns.

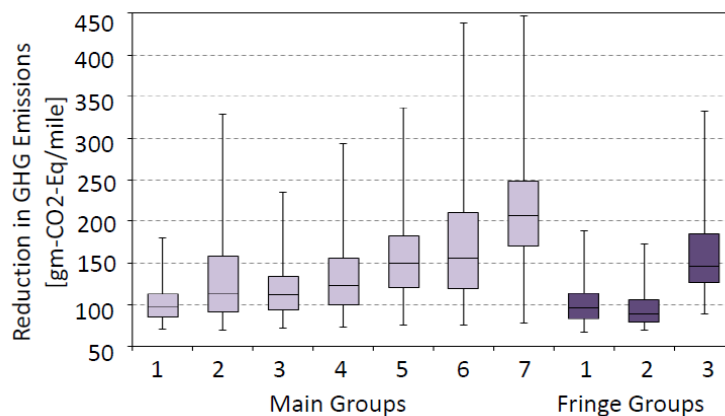


Figure 52. Box plots for reduction in greenhouse gases when switching a conventional vehicle with its equivalent hybrid electric vehicle in different vehicle groups

The Importance of Grid Integration for Achievable Greenhouse Gas Emissions Reductions from Alternative Vehicle Technologies

Author/sponsor: University of California, Irvine

Publication: *Energy*

Publication year: 2015

Summary: FASTSim was used within a larger framework to investigate California’s Executive Order S-21-09 goal of achieving an 80% greenhouse gas reduction in light of EV interactions with the electric grid.

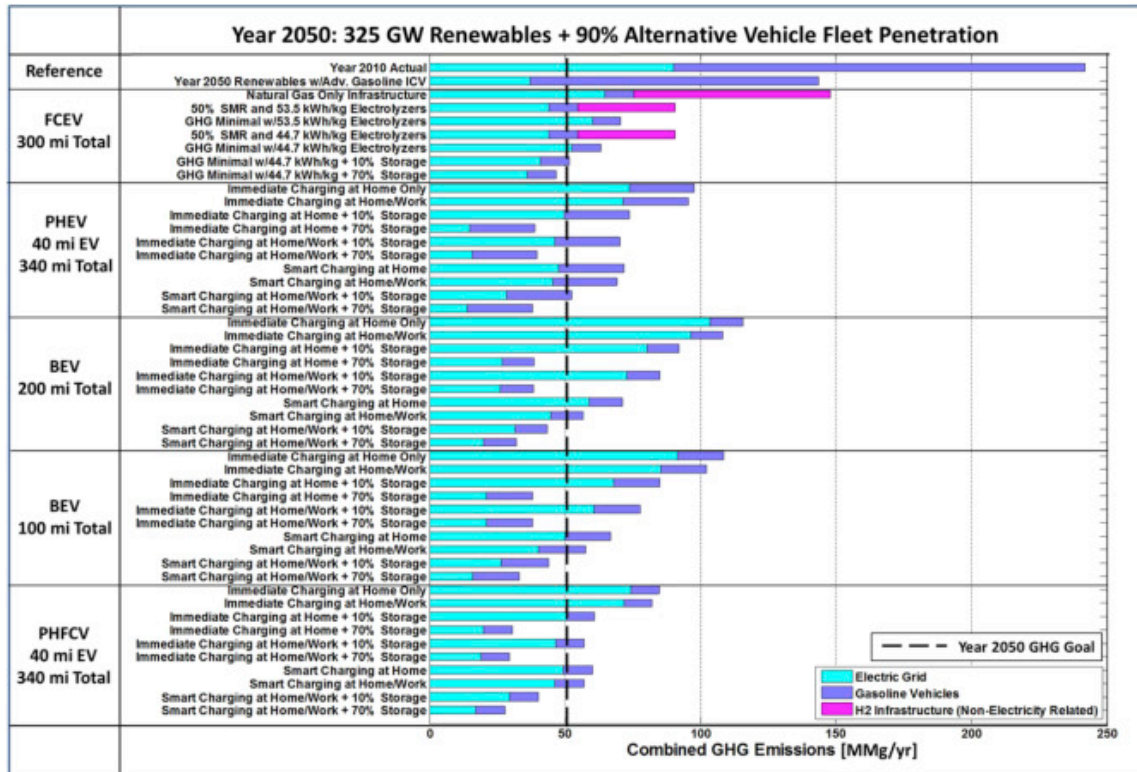


Figure 53. Combined greenhouse gas emissions at 325-GW renewable capacity

Accounting for the Variation of Driver Aggression in the Simulation of Conventional and Advanced Vehicles

Author/sponsor: NREL

Publication: SAE International technical paper

Publication year: 2013

Summary: FASTSim was used to simulate the effect of driver aggression on fuel economy for various powertrain types over a range of real-world drive data sets.

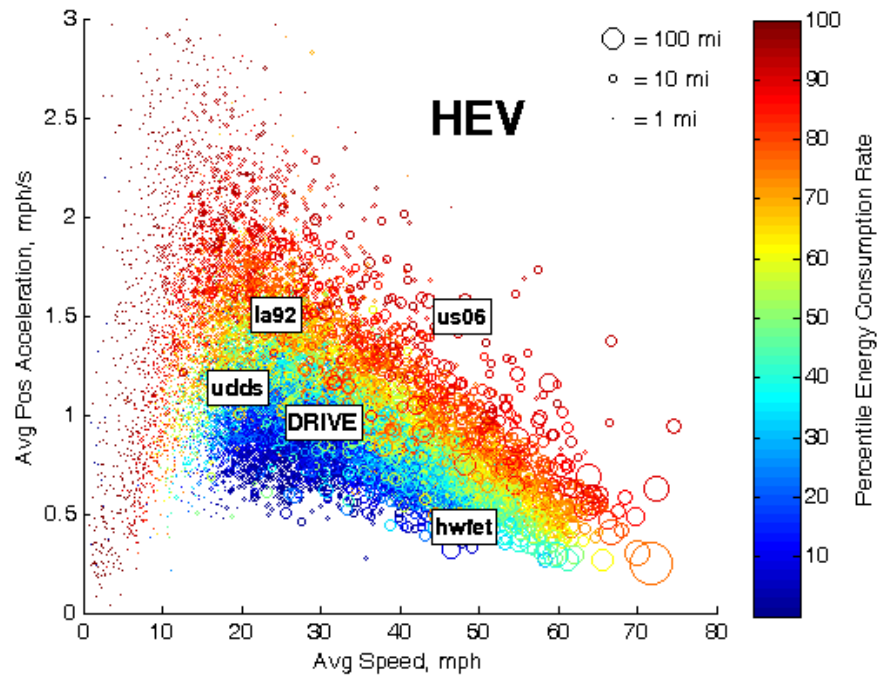


Figure 54. Effect of driver aggressiveness (trip-averaged forward acceleration and speed) and trip distance on fuel economy for HEV powertrain

7 Summary

The primary advantage of FASTSim is its useful balance of modeling accuracy and complexity. It captures the most important factors influencing vehicle fuel economy and performance using simplified efficiency maps, 1-second time steps, and low data requirements for standard calibration. Little effort is required to set up and run numerous simulations.

At the same time, FASTSim is well validated. Its simplest modeling option with generic component maps provides good large-scale agreement. As has been demonstrated in this report, such FASTSim base modeling results for fuel economy, electricity consumption and acceleration are typically within 10% of the measured or rated value for a given vehicle, and often within 5%. Vehicle price estimation from FASTSim base has also been shown to validate reasonably well. In addition, complexity can be added to FASTSim to accurately capture a range of real-world considerations such as road grade, AC use, component thermal sensitivity, and air density as validated via detailed on-road testing.

FASTSim is also widely referenced. Of the numerous studies that use FASTSim, many are from NREL, but additional users include DOE, other national laboratories, automakers, the California Air Resources Board, Google, and American and foreign universities and research centers.

Finally, public sponsorship and open-source code add transparency and credibility to FASTSim, making it well suited for analyses that must be shared and understood among multiple stakeholders such as automakers and regulatory agencies. In this capacity, it can be a powerful tool for building large-scale future scenarios of the type that might support public interest discussions related to vehicle fuel economy and design.

References

- Argonne National Laboratory (ANL). 2021. "Downloadable Dynamometer Database." Accessed April 5, 2021. <https://www.anl.gov/es/downloadable-dynamometer-database>.
- Blank, J. and K. Deb. 2020. "Pymoo: Multi-Objective Optimization in Python." *IEEE Access* 8: 89497–89509. <https://doi.org/10.1109/ACCESS.2020.2990567>.
- Brooker, A., J. Gonder, L. Wang, E. Wood, S. Lopp, and L. Ramroth. 2015. "FASTSim: A Model to Estimate Vehicle Efficiency, Cost and Performance." SAE Technical Paper 2015-01-0973. doi:10.4271/2015-01-0973. <http://www.nrel.gov/docs/fy15osti/63623.pdf>.
- Brooker, A., J. Gonder, S. Lopp, and J. Ward. 2015 "ADOPT: A Historically Validated Light Duty Vehicle Consumer Choice Model," SAE Technical Paper 2015-01-0974. doi:10.4271/2015-01-0974. <https://www.nrel.gov/docs/fy15osti/63608.pdf>.
- Dicker, Russell. 2021. "3 new ways to navigate more sustainably with Maps." *The Keyword*, October 6, 2021. <https://www.blog.google/products/maps/3-new-ways-navigate-more-sustainably-maps/>.
- Incropera, Frank P. and David P. DeWitt. 2002. *Fundamentals of Heat and Mass Transfer*. New York: J. Wiley.
- Jehlik, F., N. Chevers, M. Moniot, Y. Song, H. Hirabayashi, M. Nomura, and E. Wood. 2018. "Determining Off-cycle Fuel Economy Benefits of 2-Layer HVAC Technology." SAE Technical Paper 2018-01-1368. doi:10.4271/2018-01-1368.
- Jehlik, F., S. Iliev, E. Wood, and J. Gonder. 2017. "Investigation of Transmission Warming Technologies at Various Ambient Conditions." SAE Technical Paper 2017-01-0157. doi:10.4271/2017-01-0157.
- Mahmud, K. and G. Town. 2016. "A Review of Computer Tools for Modeling Electric Vehicle Energy Requirements and Their Impact on Power Distribution Networks." *Applied Energy* 172: 337–359. <http://dx.doi.org/10.1016/j.apenergy.2016.03.100>.
- National Renewable Energy Laboratory (NREL). 2017. "Transportation Secure Data Center (TSDC)." Accessed February 23, 2017. <https://www.nrel.gov/tsdc>.
- National Renewable Energy Laboratory (NREL). 2020. "ADOPT: Automotive Deployment Options Projection Tool." Accessed December 1, 2020. <https://www.nrel.gov/adopt>.
- National Renewable Energy Laboratory (NREL). 2021a. "FASTSim: Future Automotive Systems Technology Simulator." Accessed September 22, 2021. <https://www.nrel.gov/fastsim>.
- National Renewable Energy Laboratory (NREL). 2021b. "RouteE: Route Energy Prediction Model." Accessed October 25, 2021. <https://www.nrel.gov/transportation/route-energy-prediction-model.html>.

Simmons, R.A., G.M. Shaver, W.E. Tyner, and S.V. Garimella. 2015. “A benefit-cost assessment of new vehicle technologies and fuel economy in the U.S. market.” *Applied Energy* 157: 940–952. <https://doi.org/10.1016/j.apenergy.2015.01.068>.

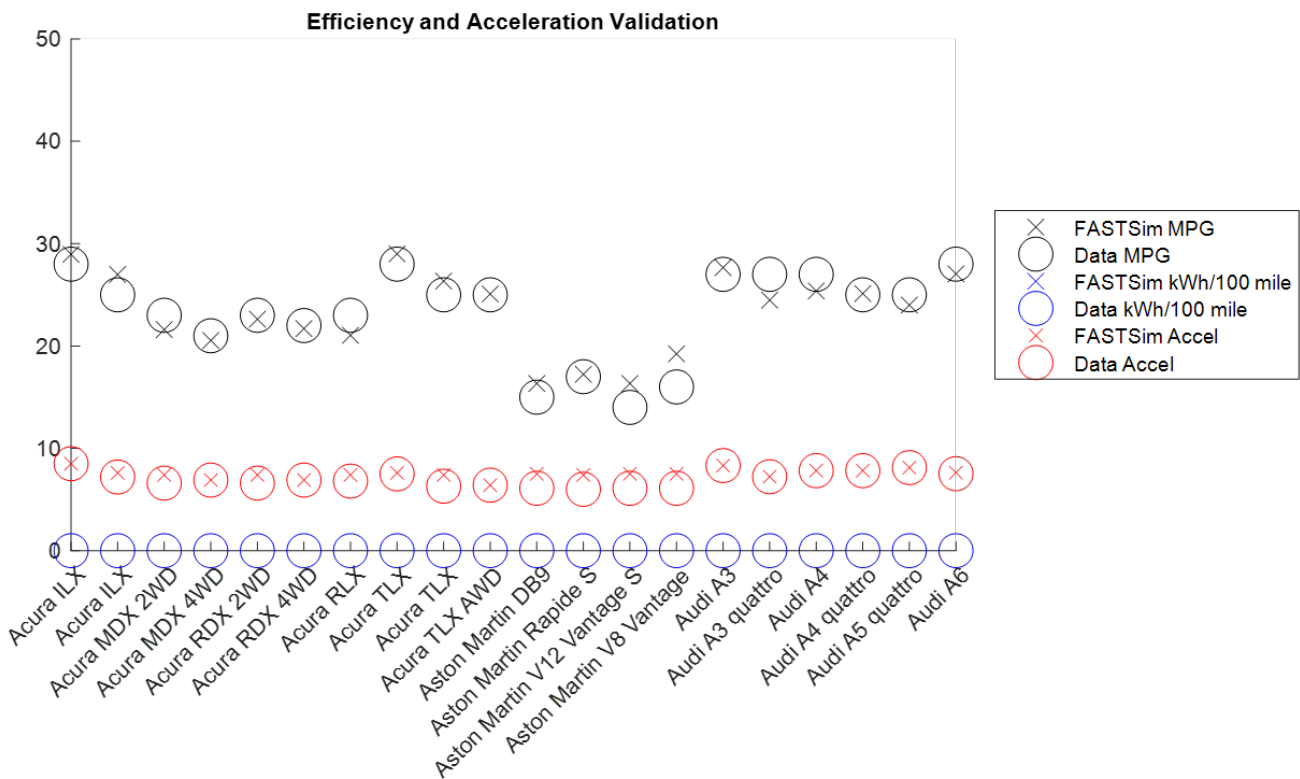
U.S. Environmental Protection Agency (EPA). 2020. *The 2019 EPA Automotive Trends Report: Greenhouse Gas Emissions, Fuel Economy, and Technology since 1975*. Washington, D.C.: EPA. EPA-420-R-20-006.

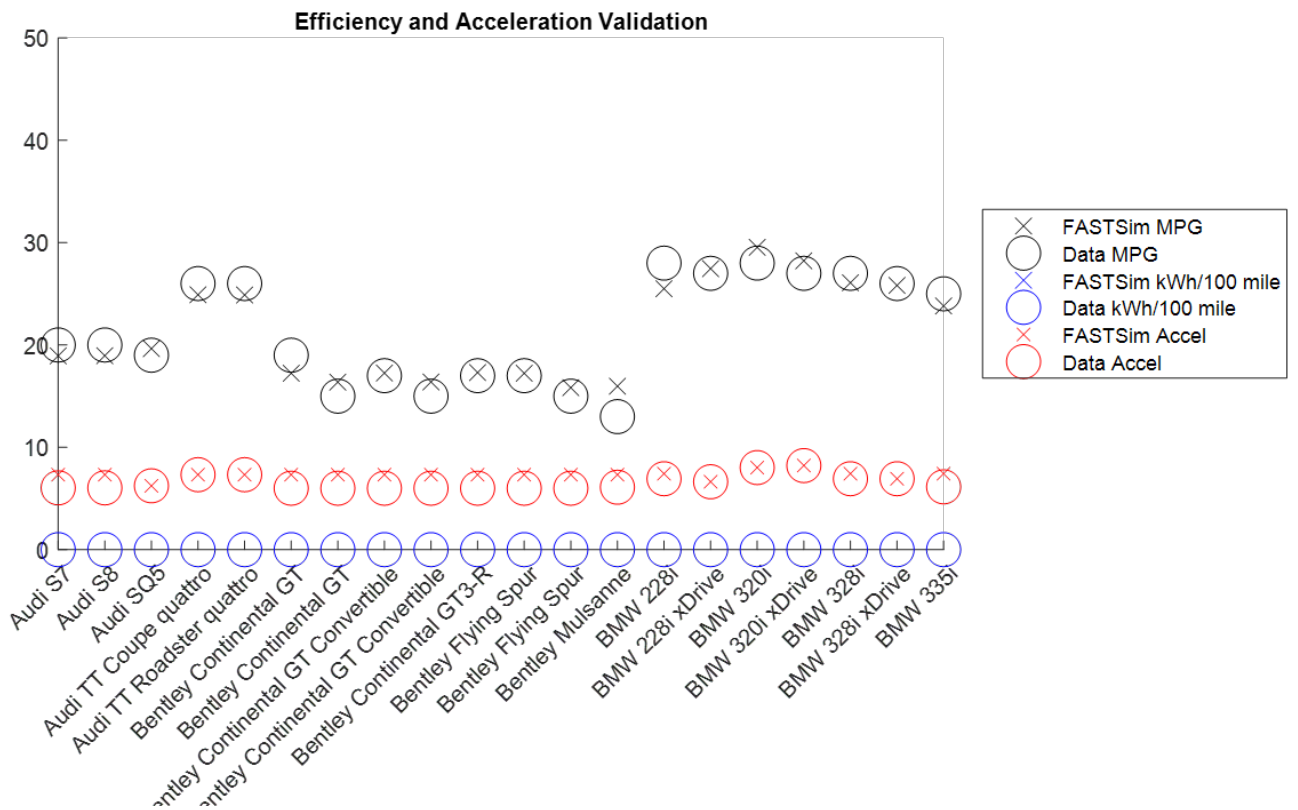
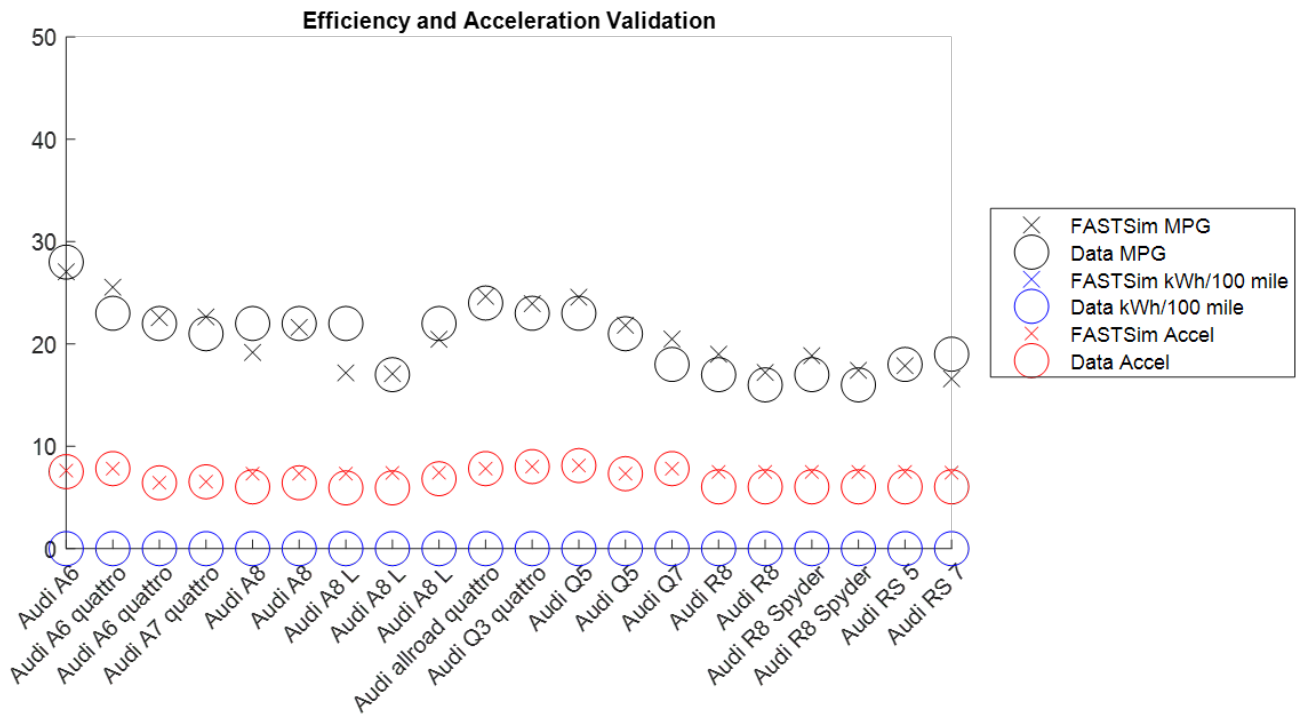
Wood, E., J. Gonder, and F. Jehlik. 2017. *On-Road Validation of a Simplified Model for Estimating Real-World Fuel Economy*. Golden, CO: National Renewable Energy Laboratory. NREL/CP-5400-67682. <http://www.nrel.gov/docs/fy17osti/67682.pdf>.

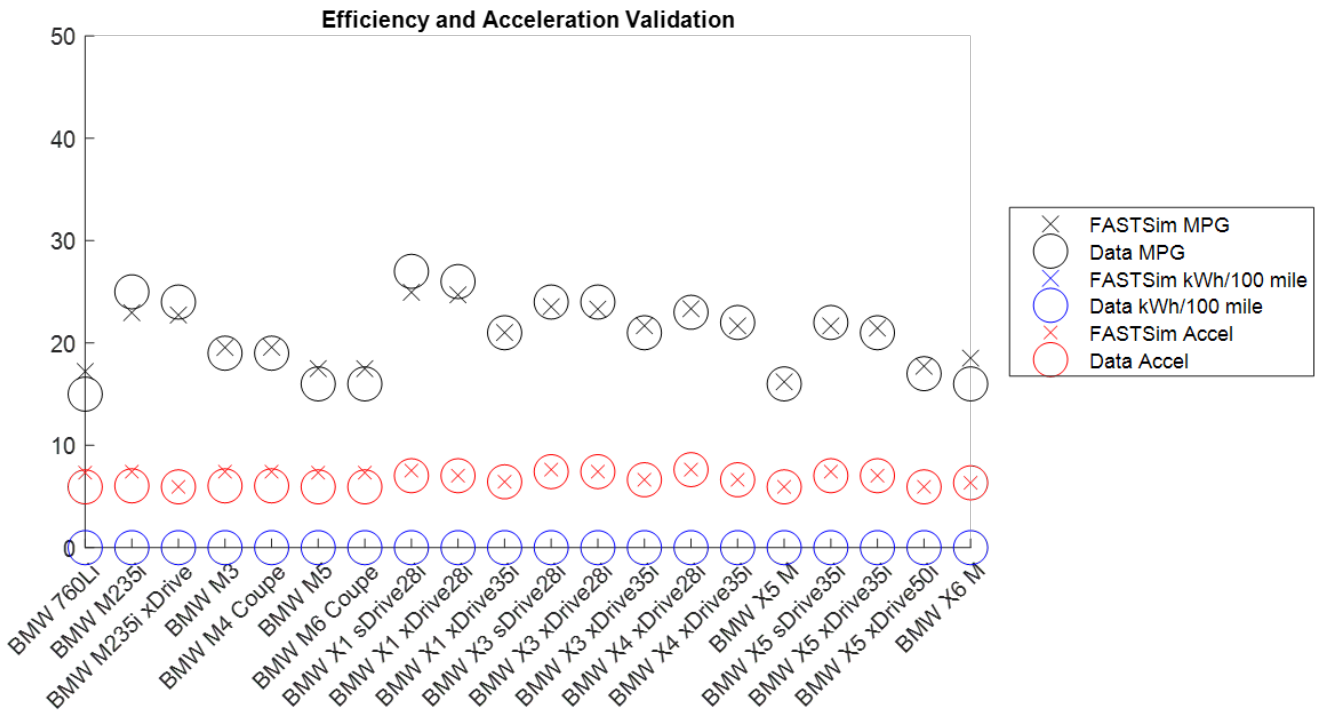
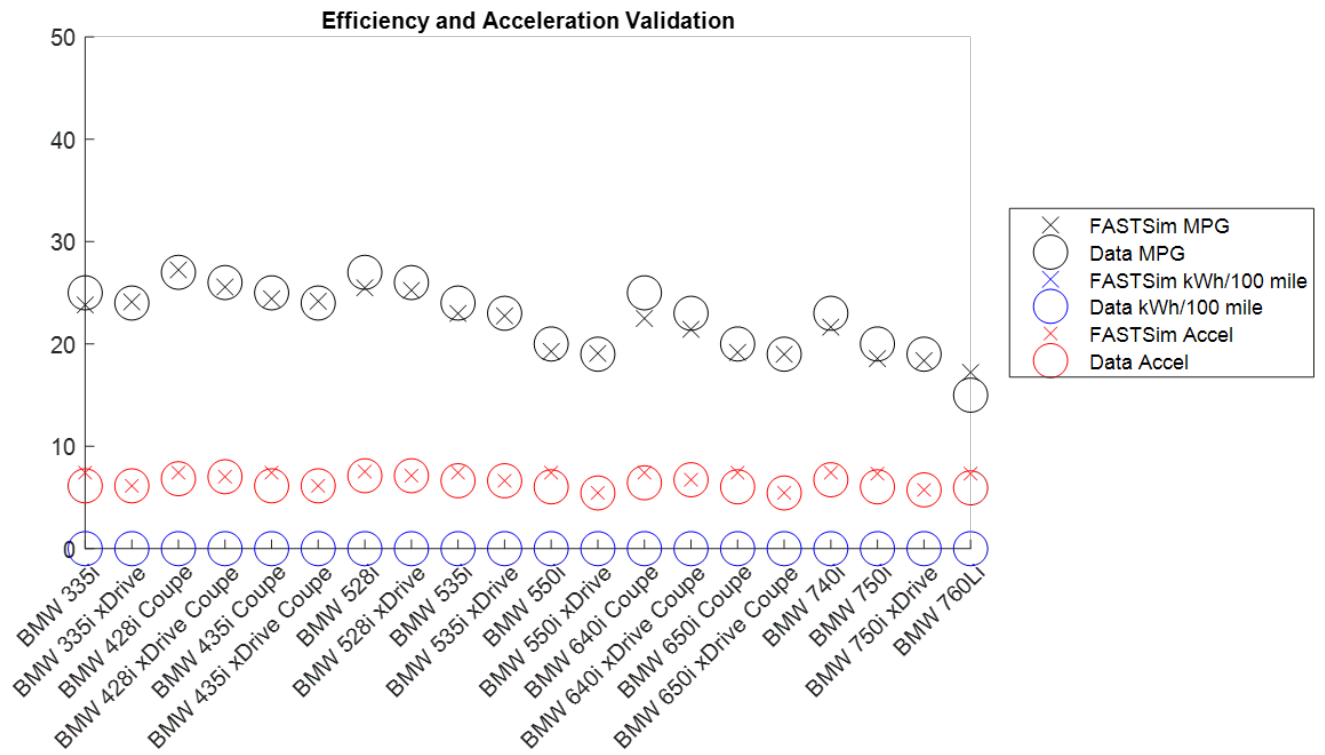
Zeroto60Times. 2018. “0-60 Times: Find 0 to 60 & Quarter Mile Time Car Specs.” <http://www.zeroto60times.com>.

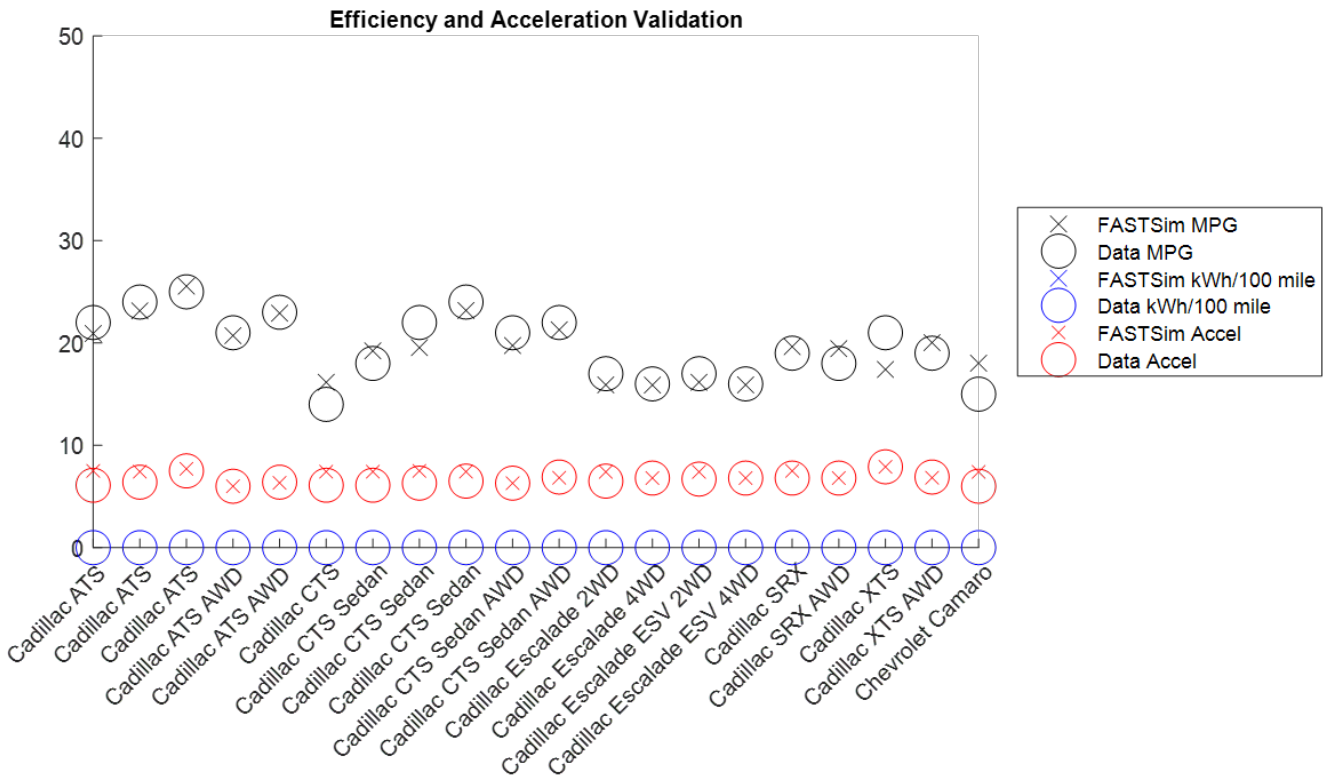
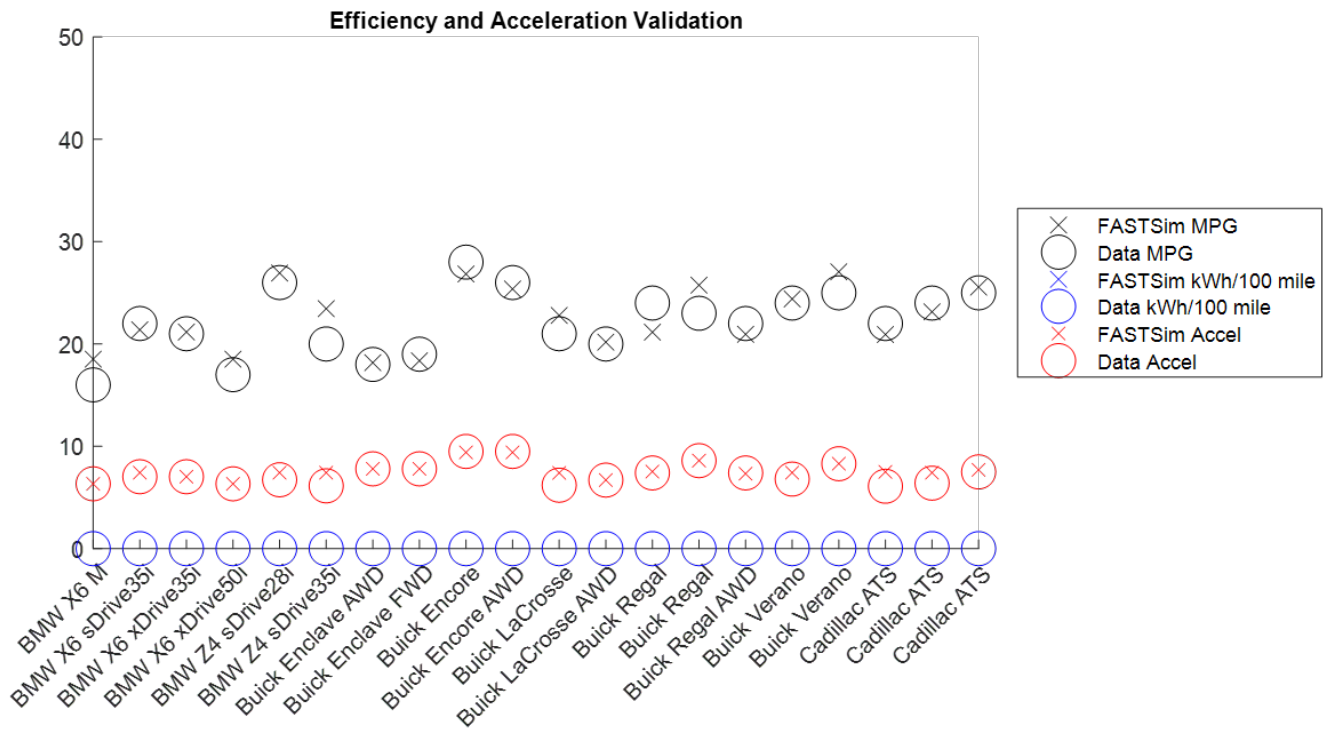
Appendix A: Partially Vetted Vehicle Validation Results

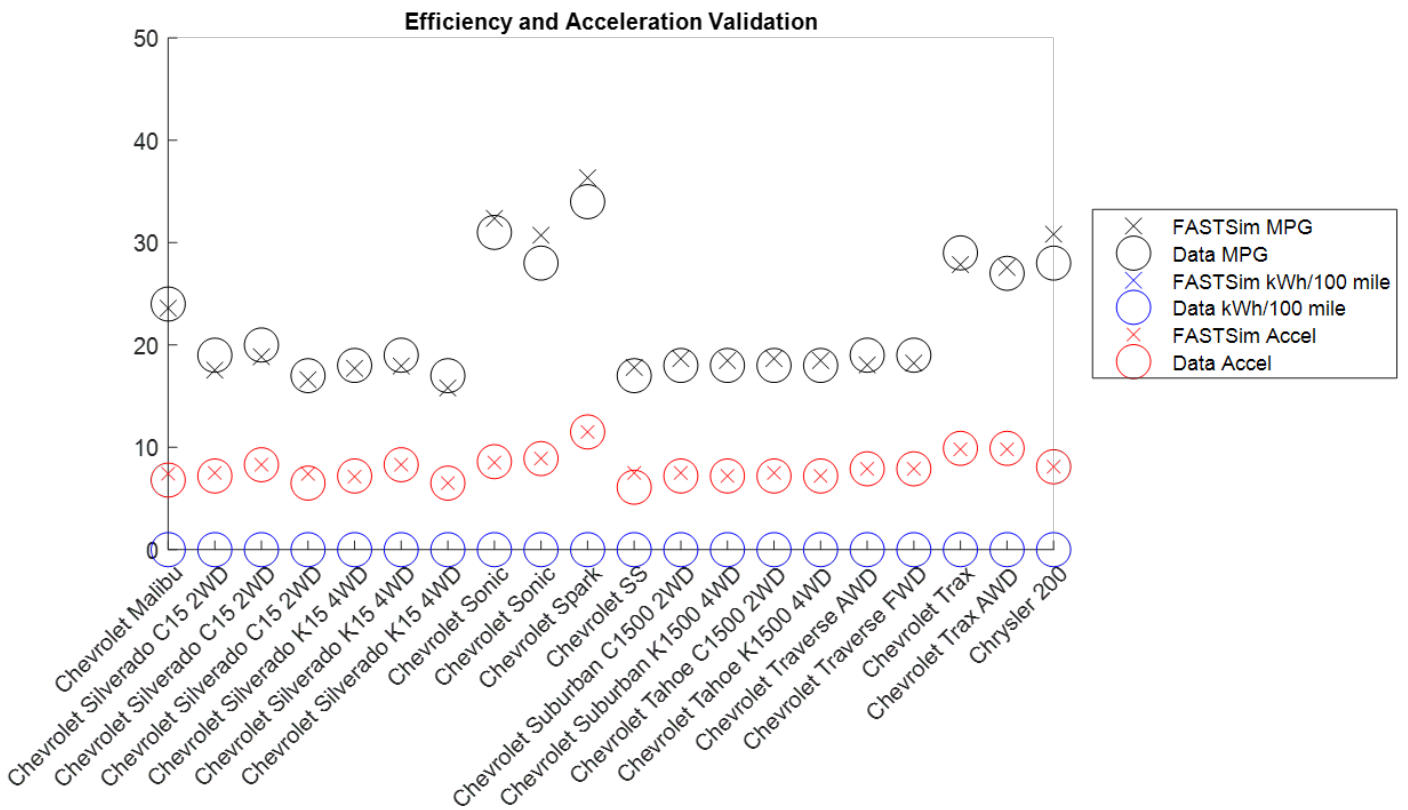
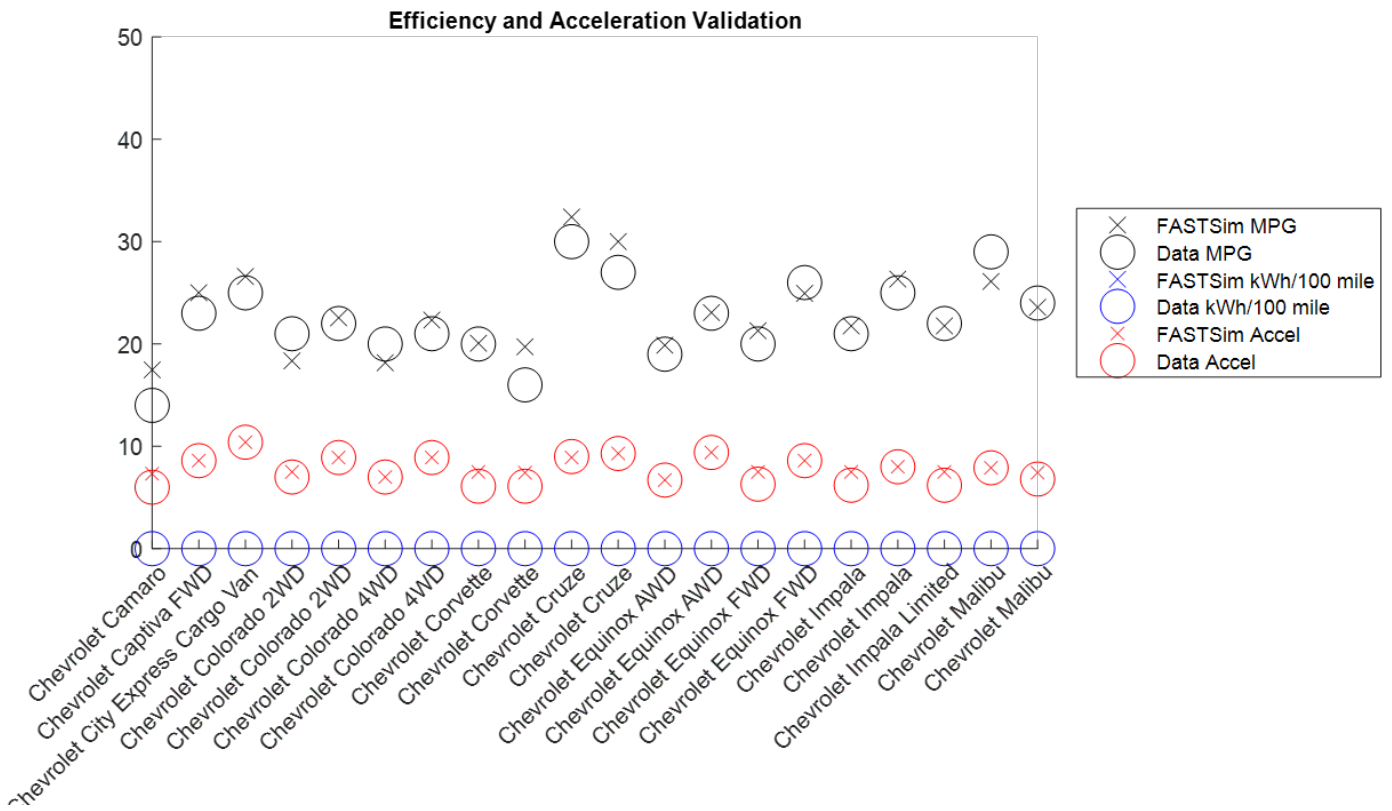
As described in Section 4.2.2, NREL includes information for more than 700 existing vehicles in its vehicle choice model, the Automotive Deployment Options Projection Tool (ADOPT), which integrates with FASTSim to simulate the fuel economy, acceleration performance, and price for this initialization set of vehicles. As project resources permit, the input data for this set of vehicles are vetted with respect to component sizes along with factors such as the presence of turbocharging (affects efficiency and acceleration), two-wheel versus four-wheel drive (affects efficiency and acceleration), and front-wheel versus rear-wheel drive (center of gravity affects acceleration). The simulated results compared with measured/rated values for these vehicles are therefore subject to any data quality issues that have not been caught through the partial vetting. The summarized results shown in Section 4.2.2 along with the individual vehicle results shown here are nevertheless similar to those presented for the vetted vehicles discussed in Section 4.2.1—with FASTSim base typically modeling within 10% accuracy, and often within 5%. Note in the following figures that duplicated vehicle labels represent the same vehicle with different options (e.g., four-cylinder versus six-cylinder engine).

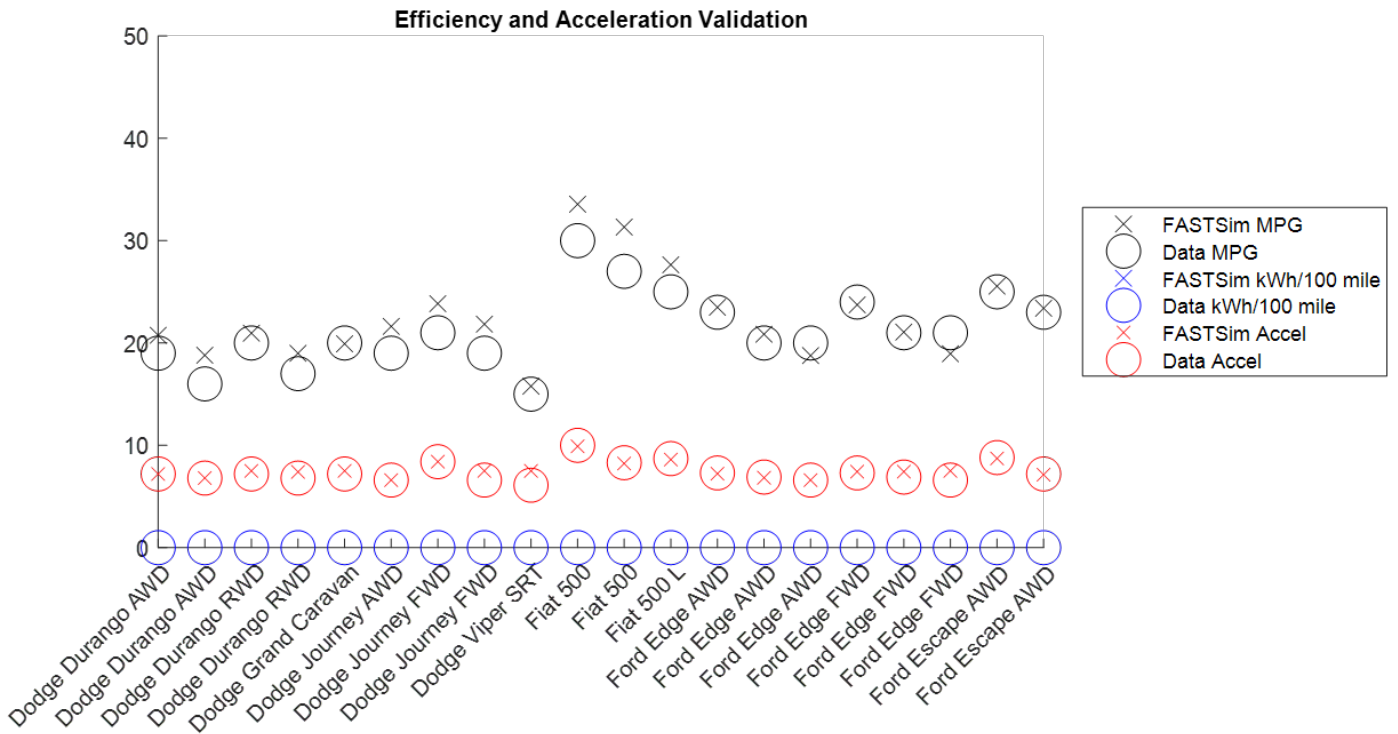
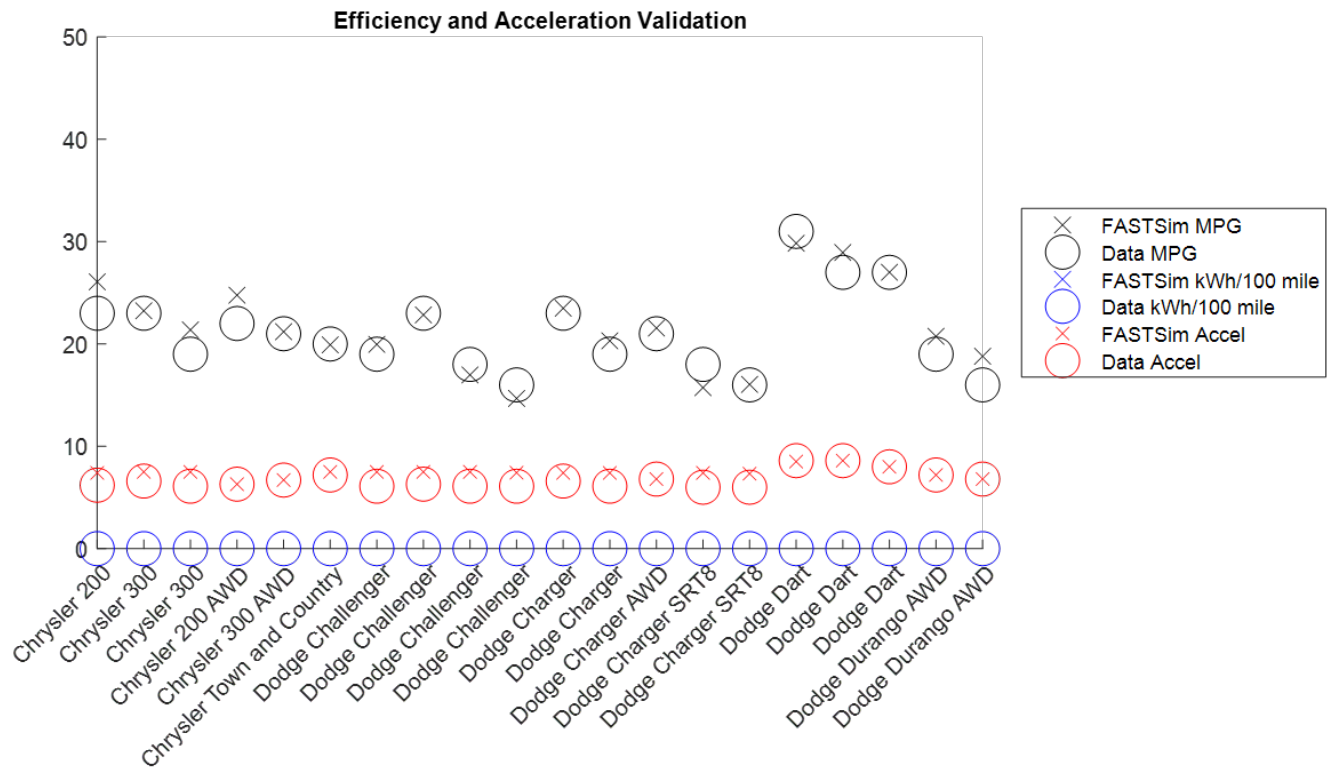


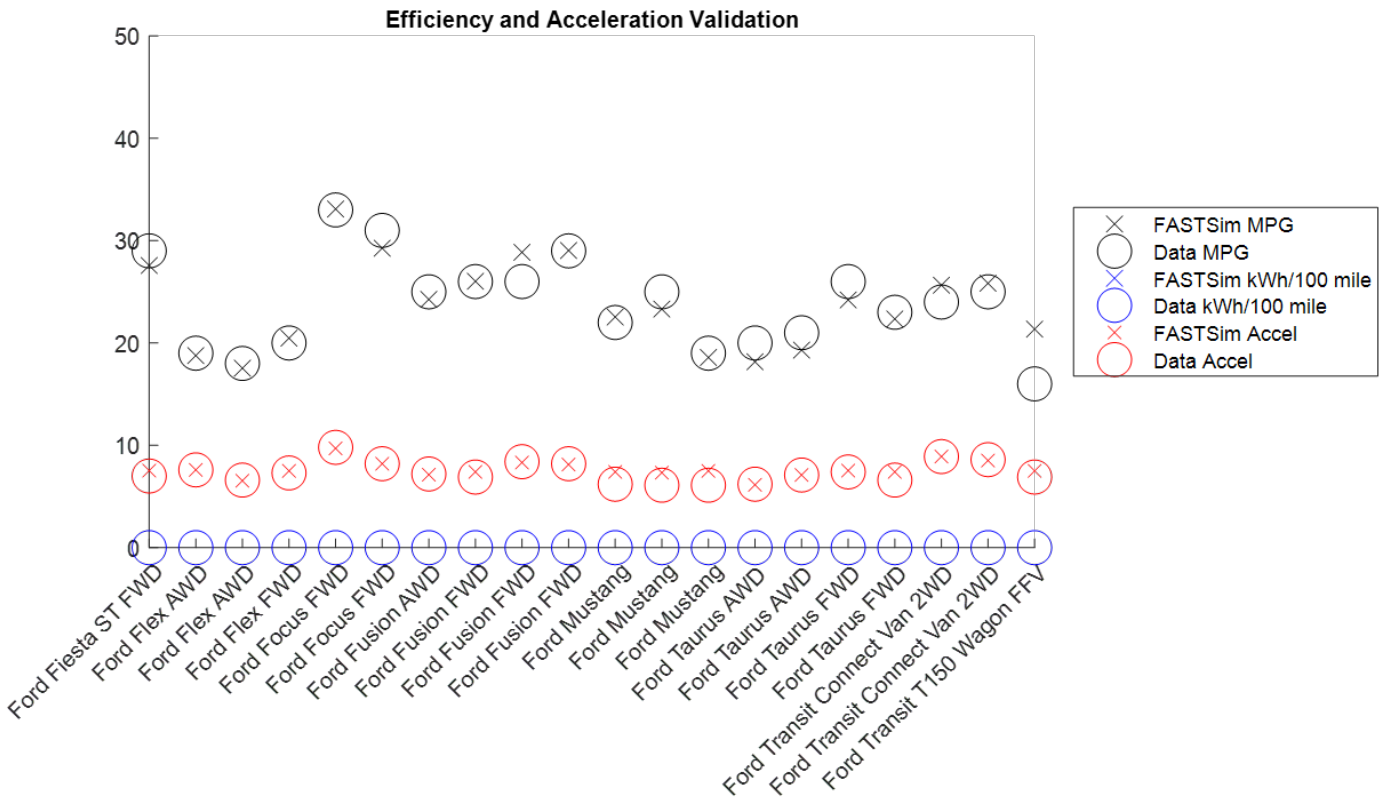
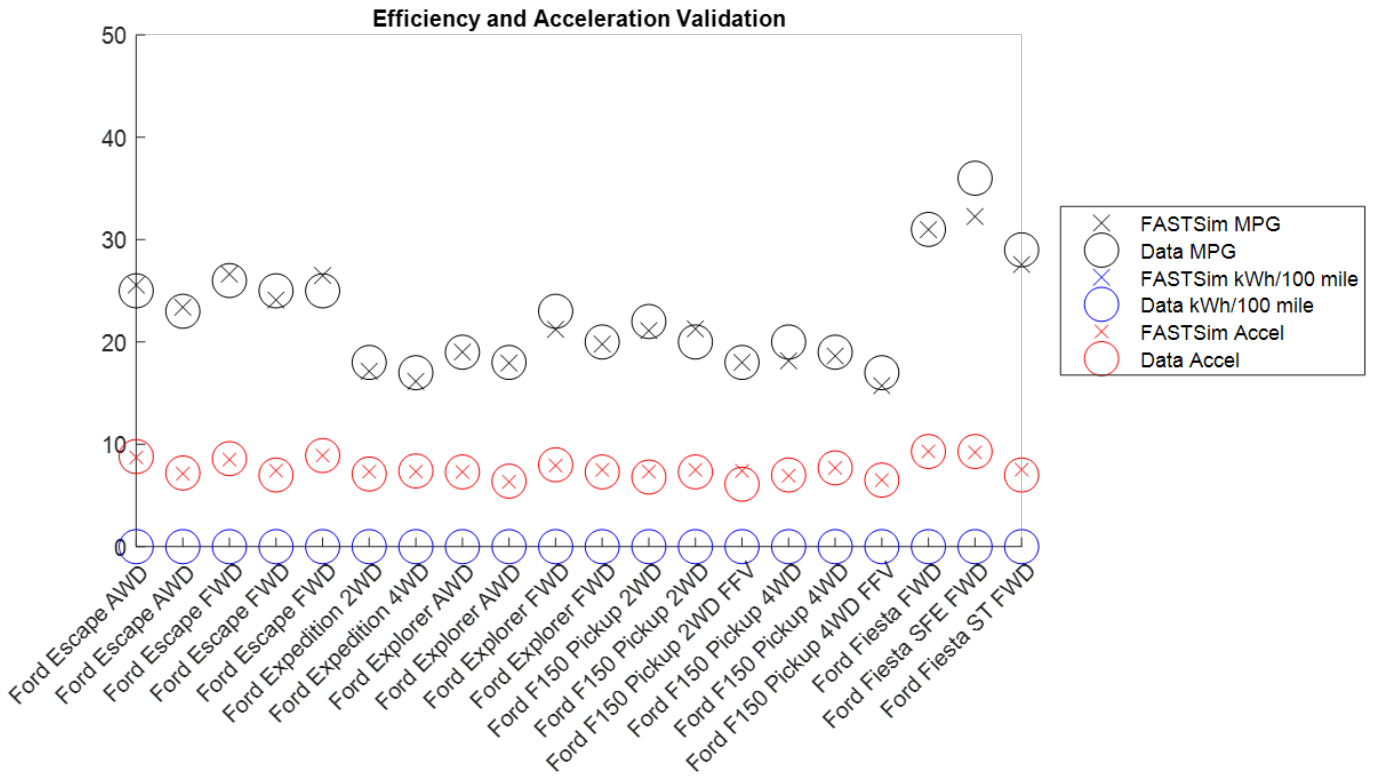




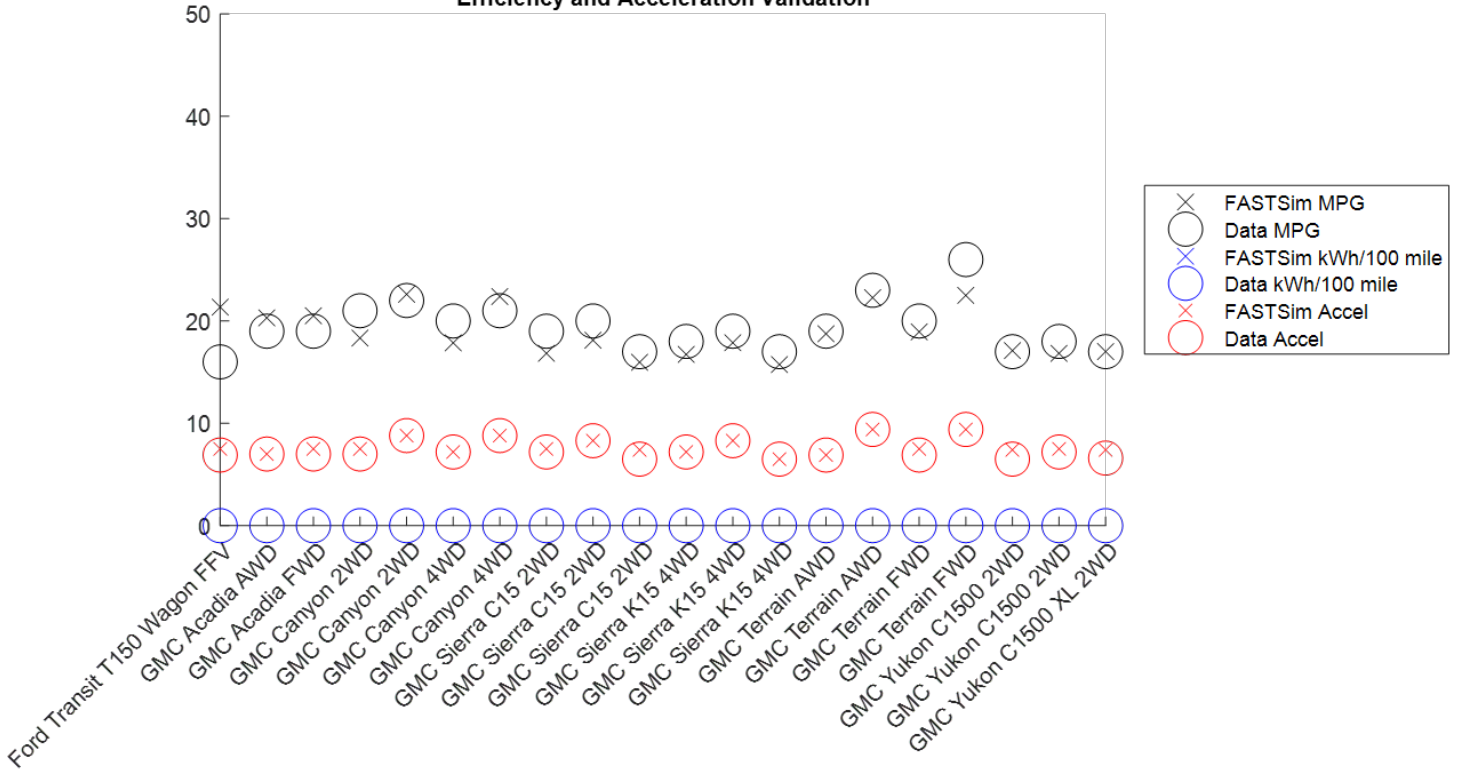




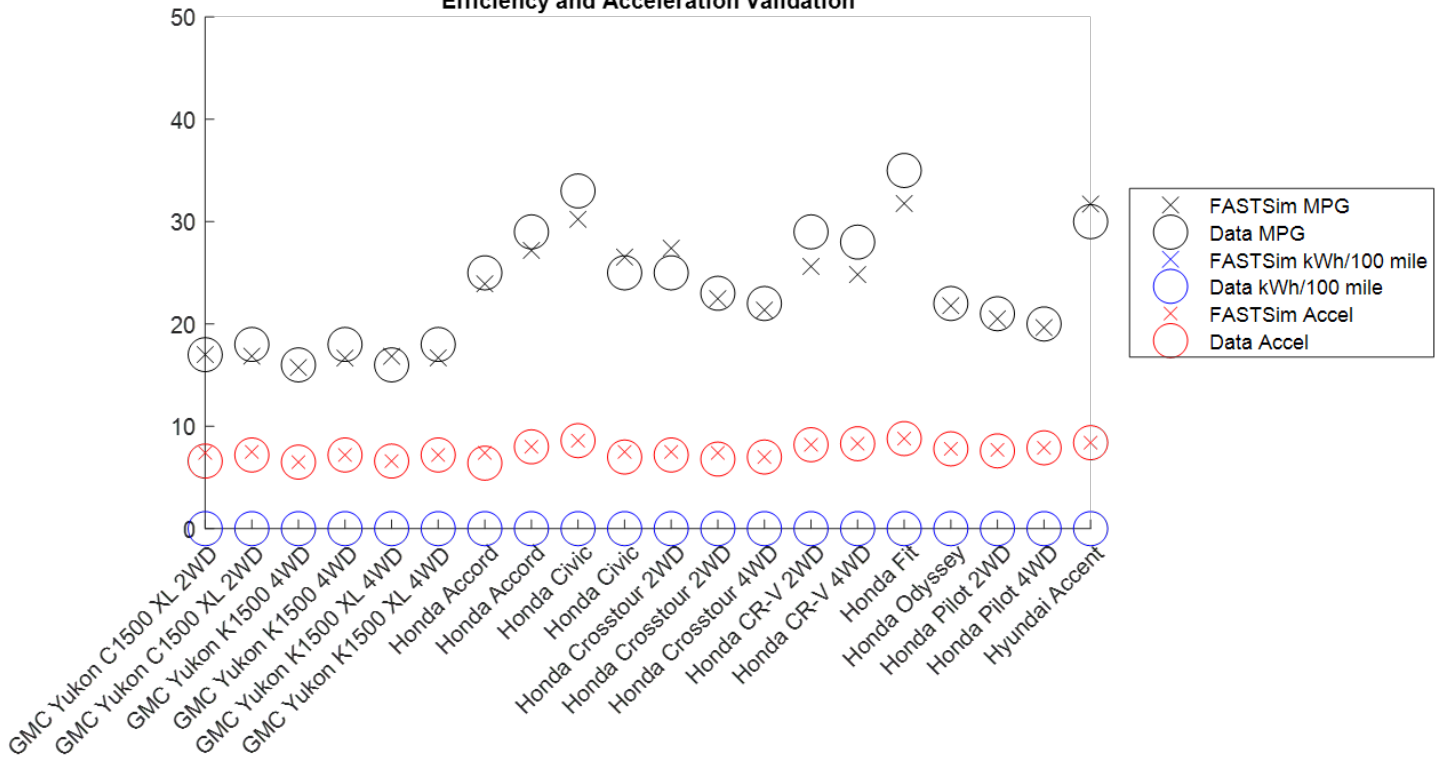


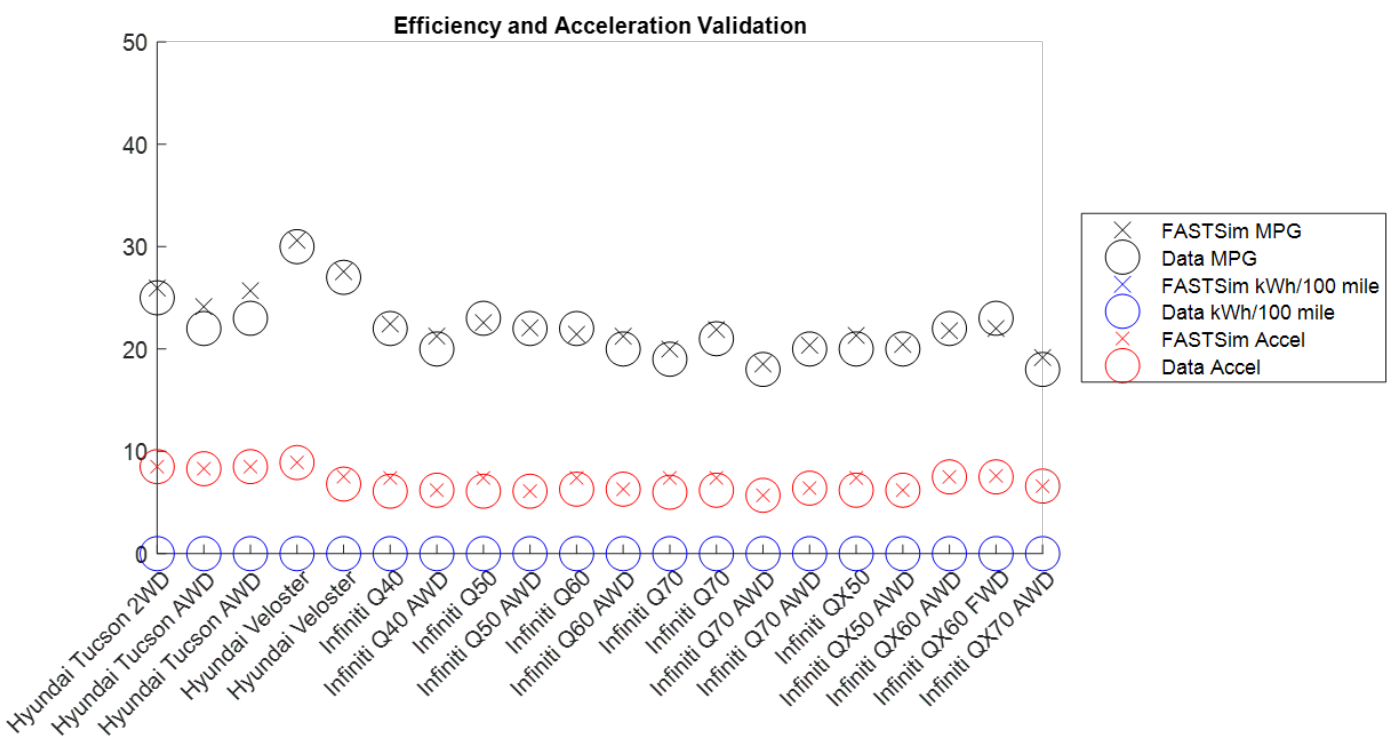
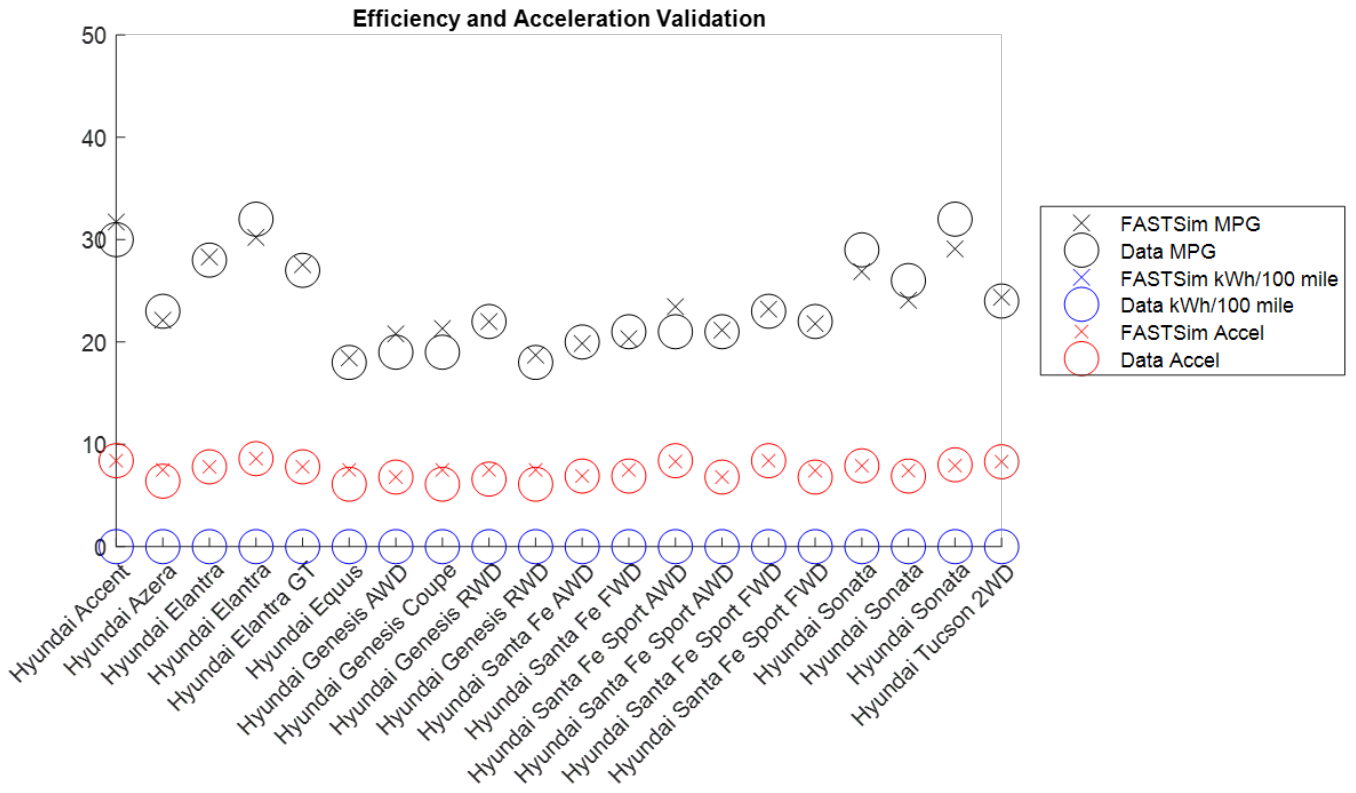


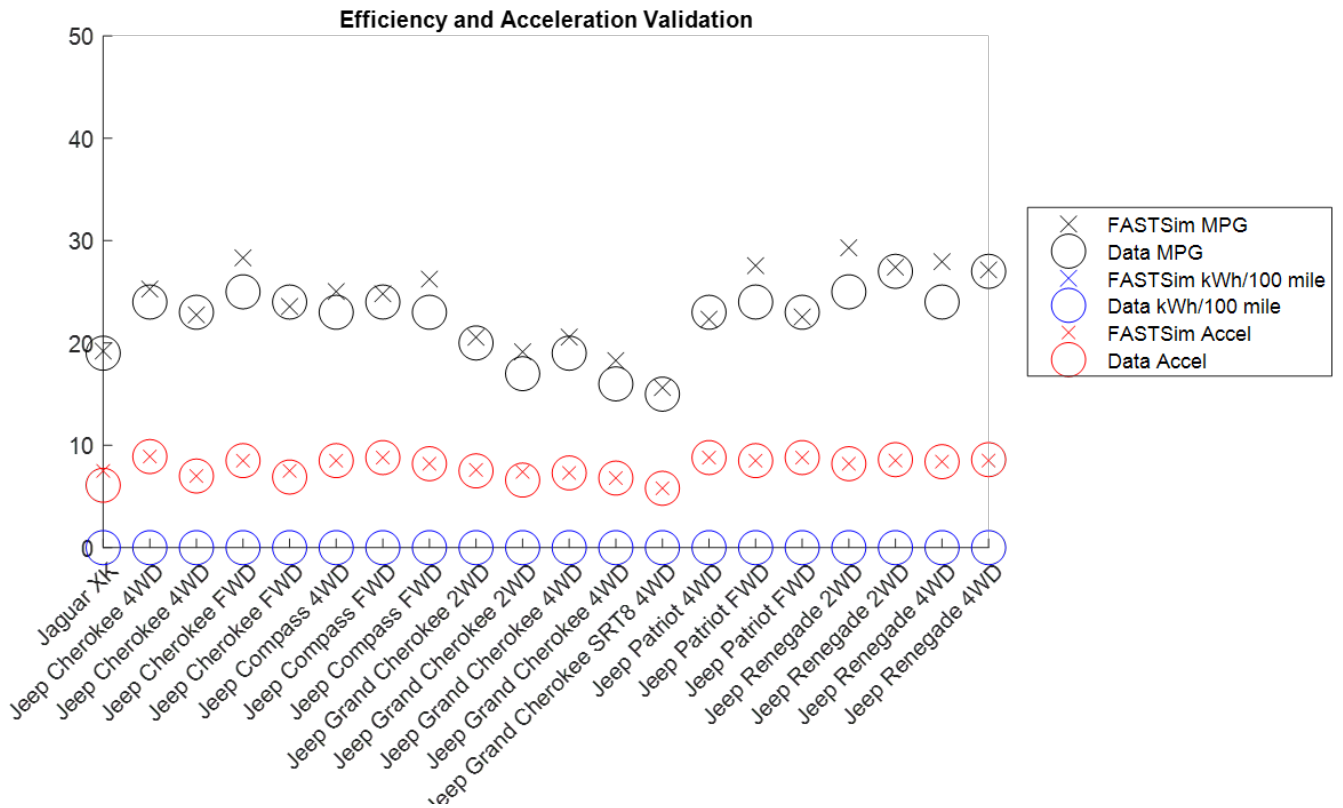
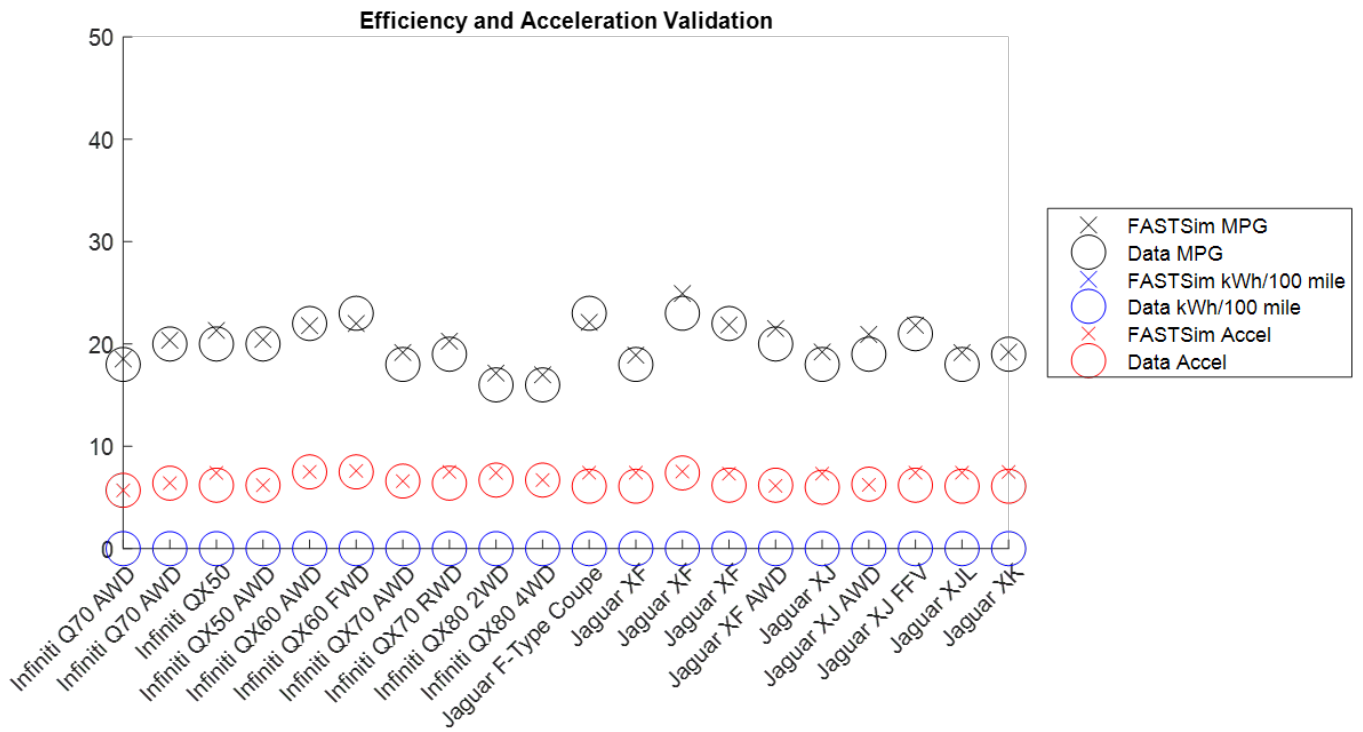
Efficiency and Acceleration Validation

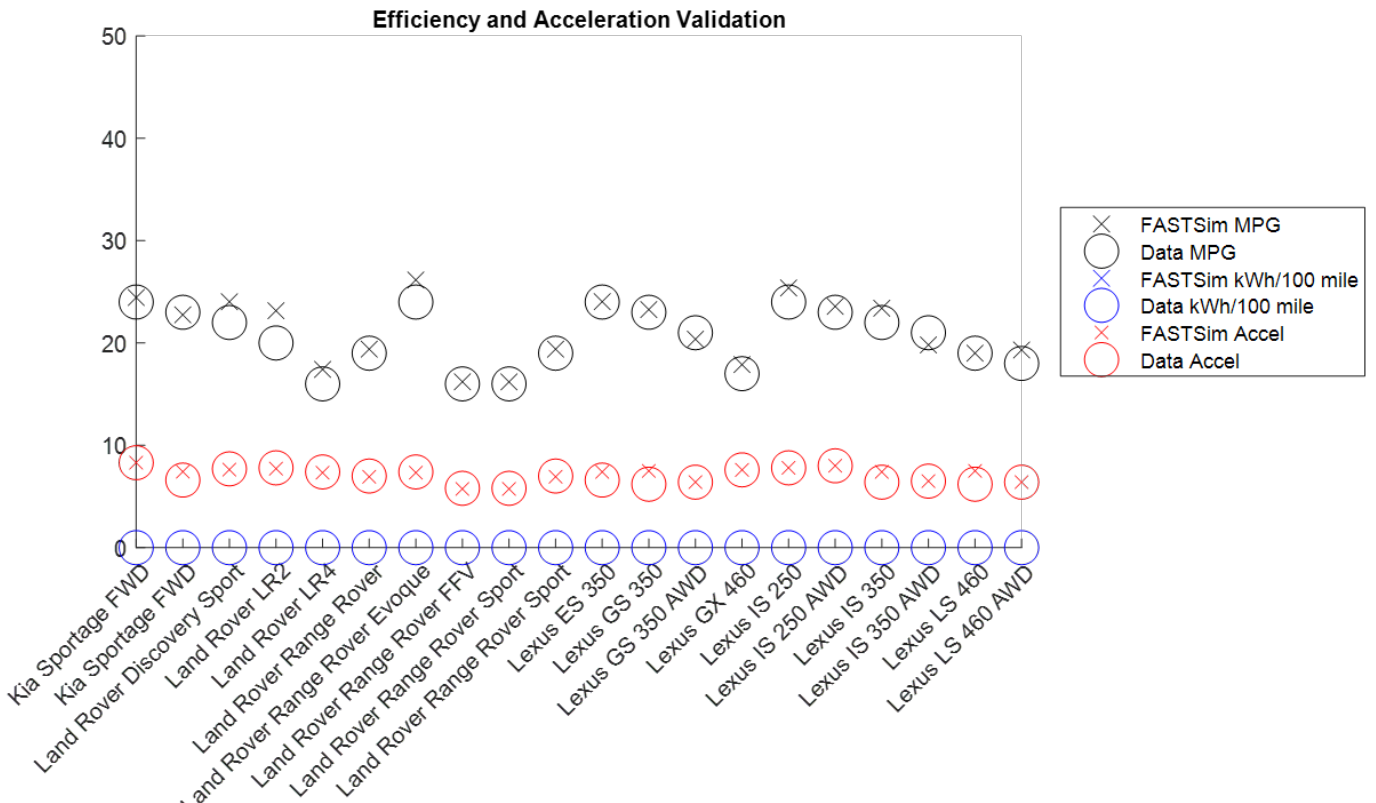
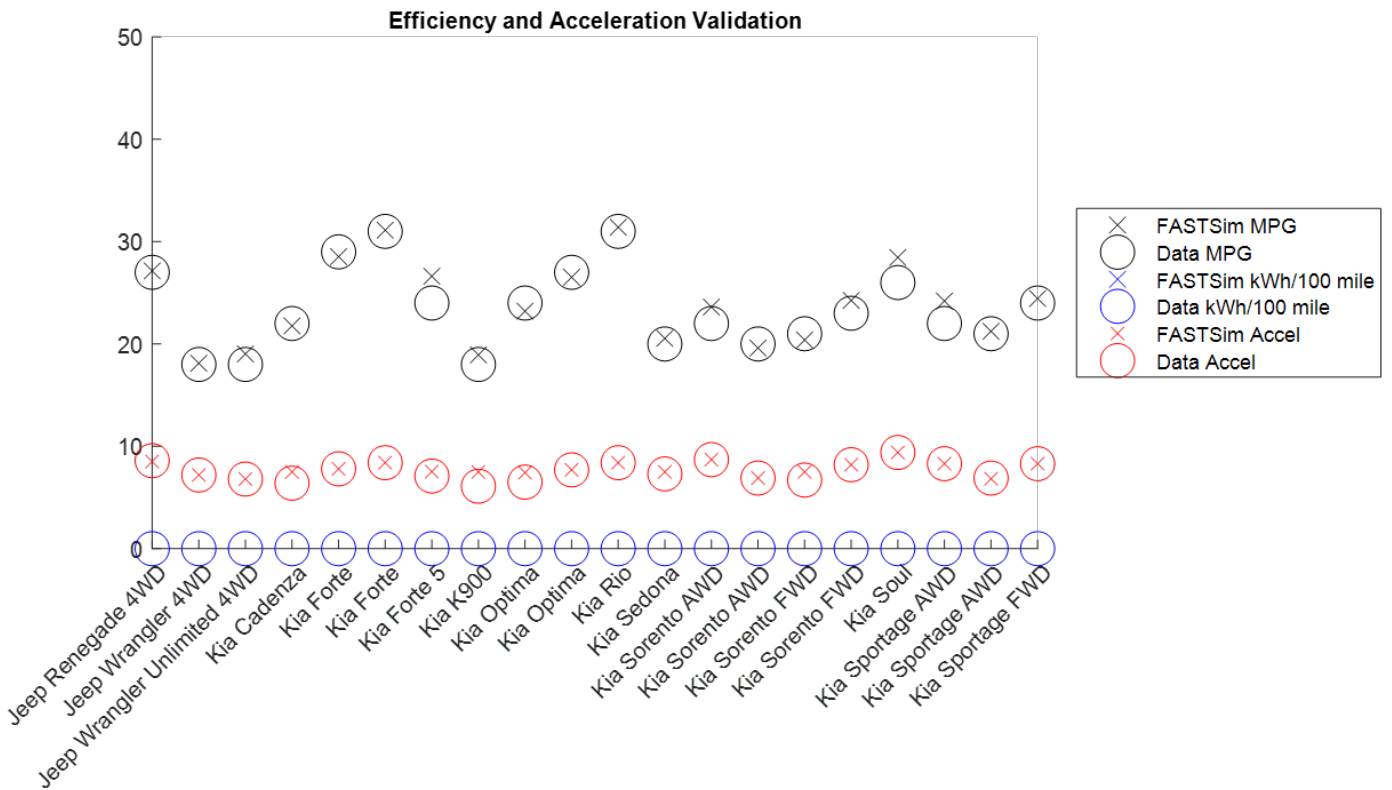


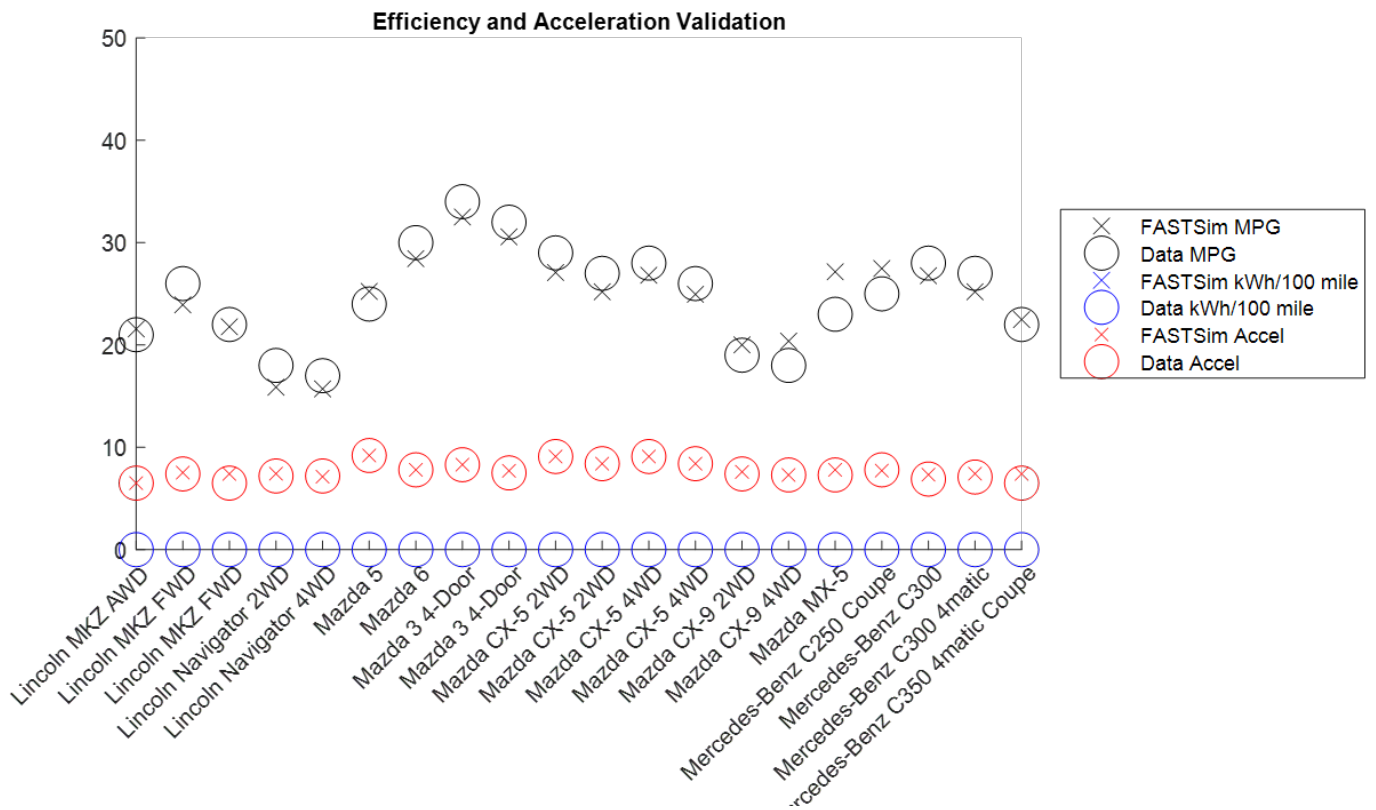
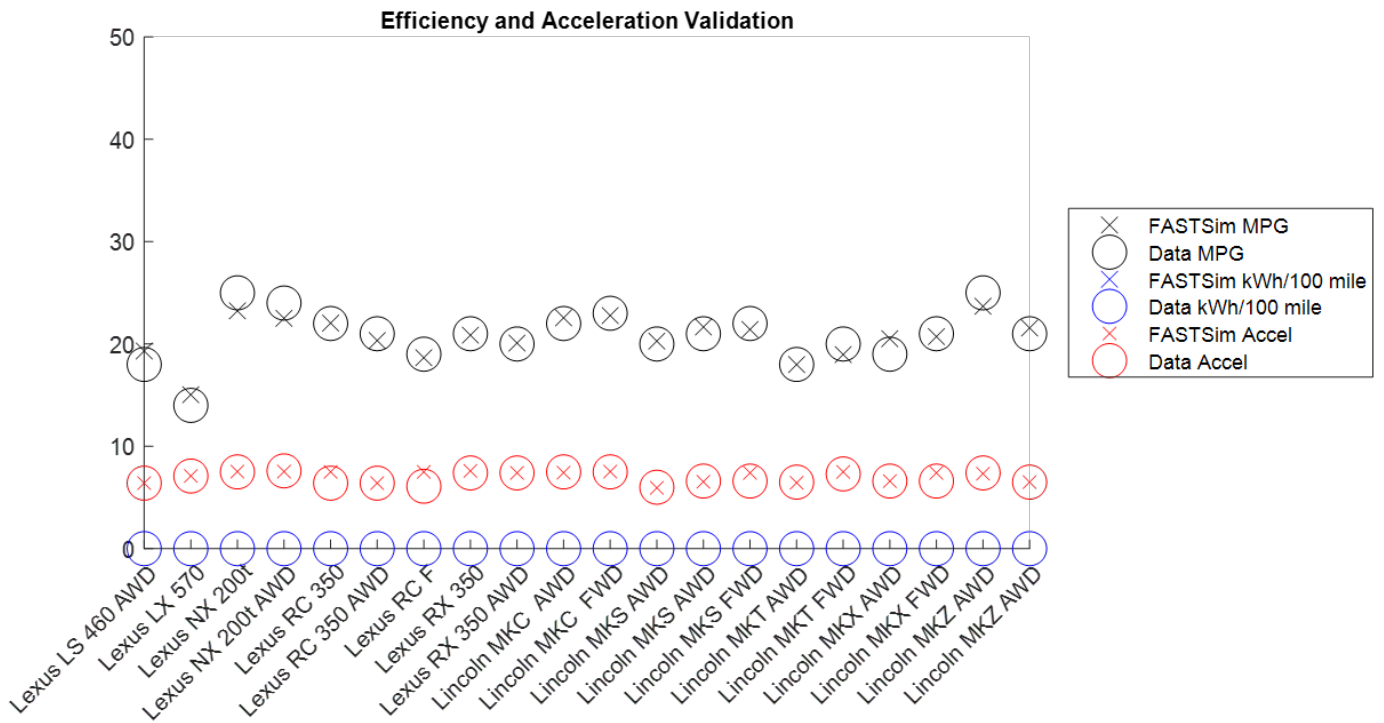
Efficiency and Acceleration Validation

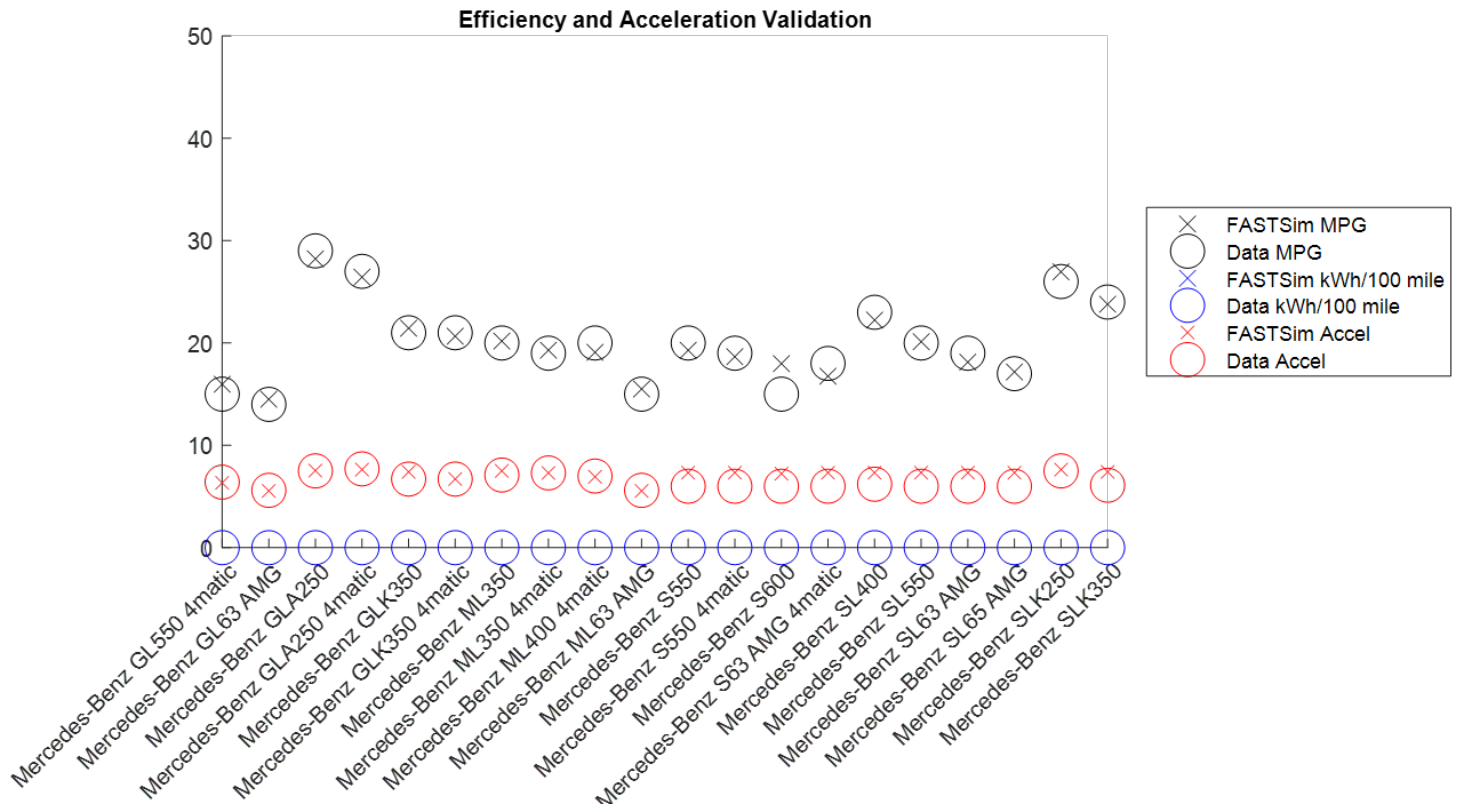
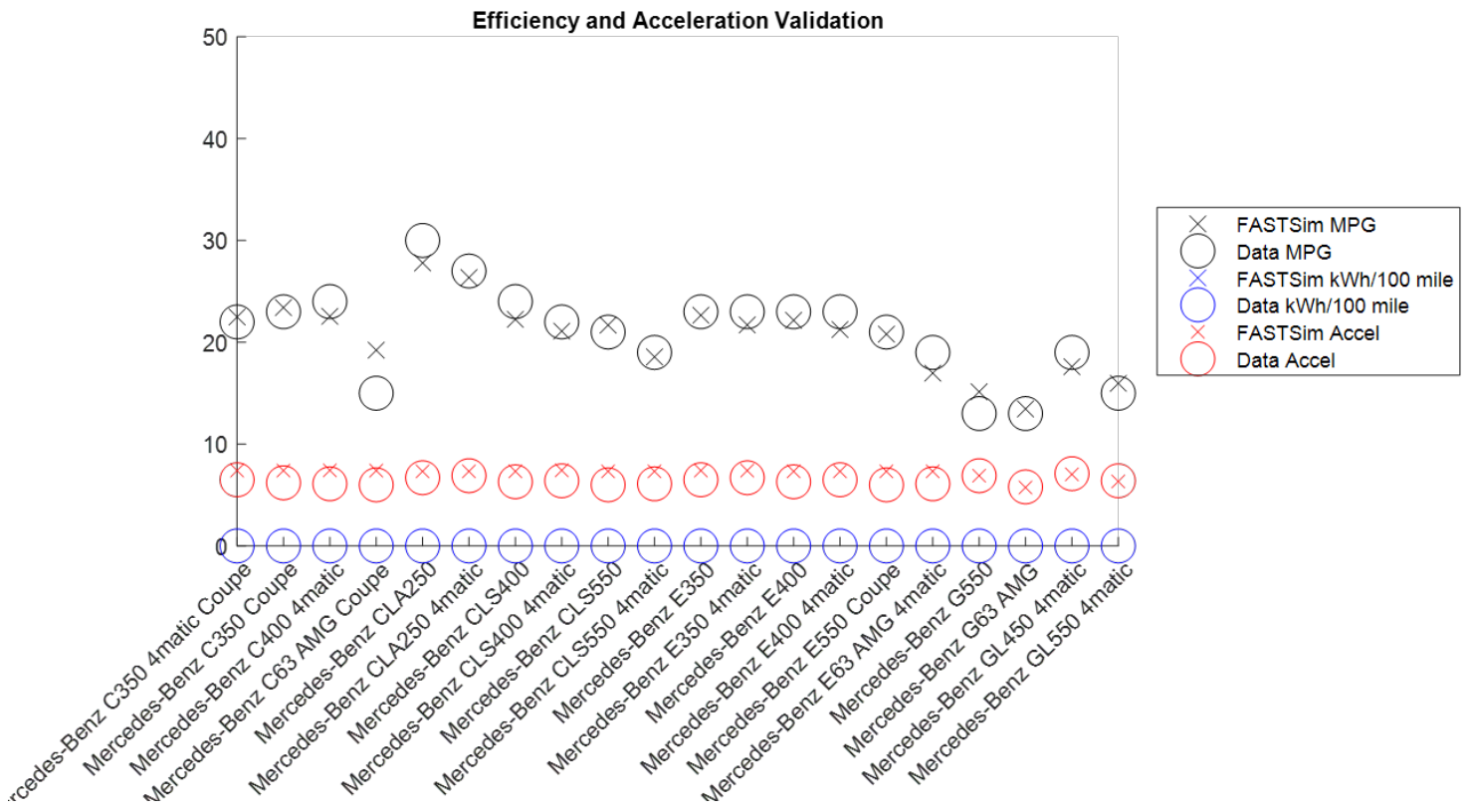


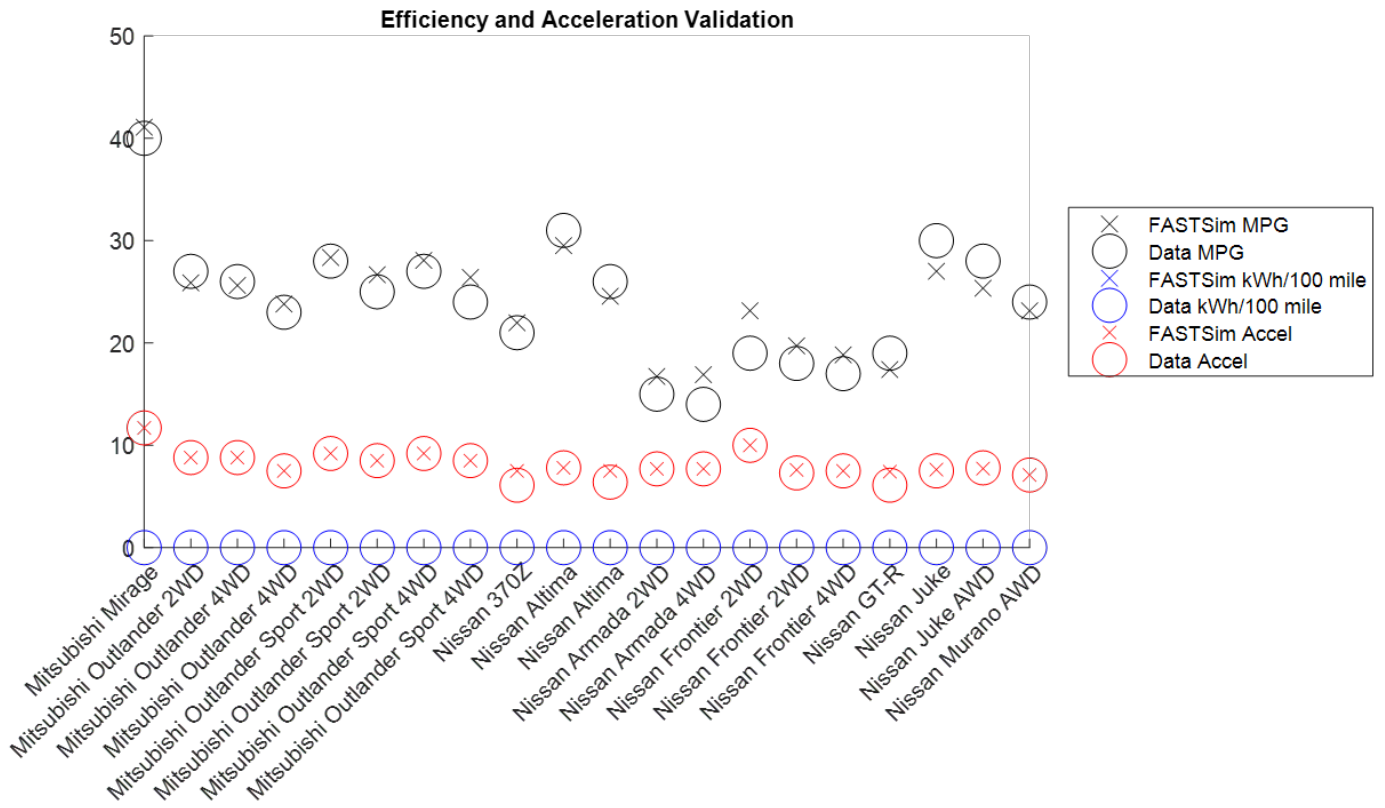
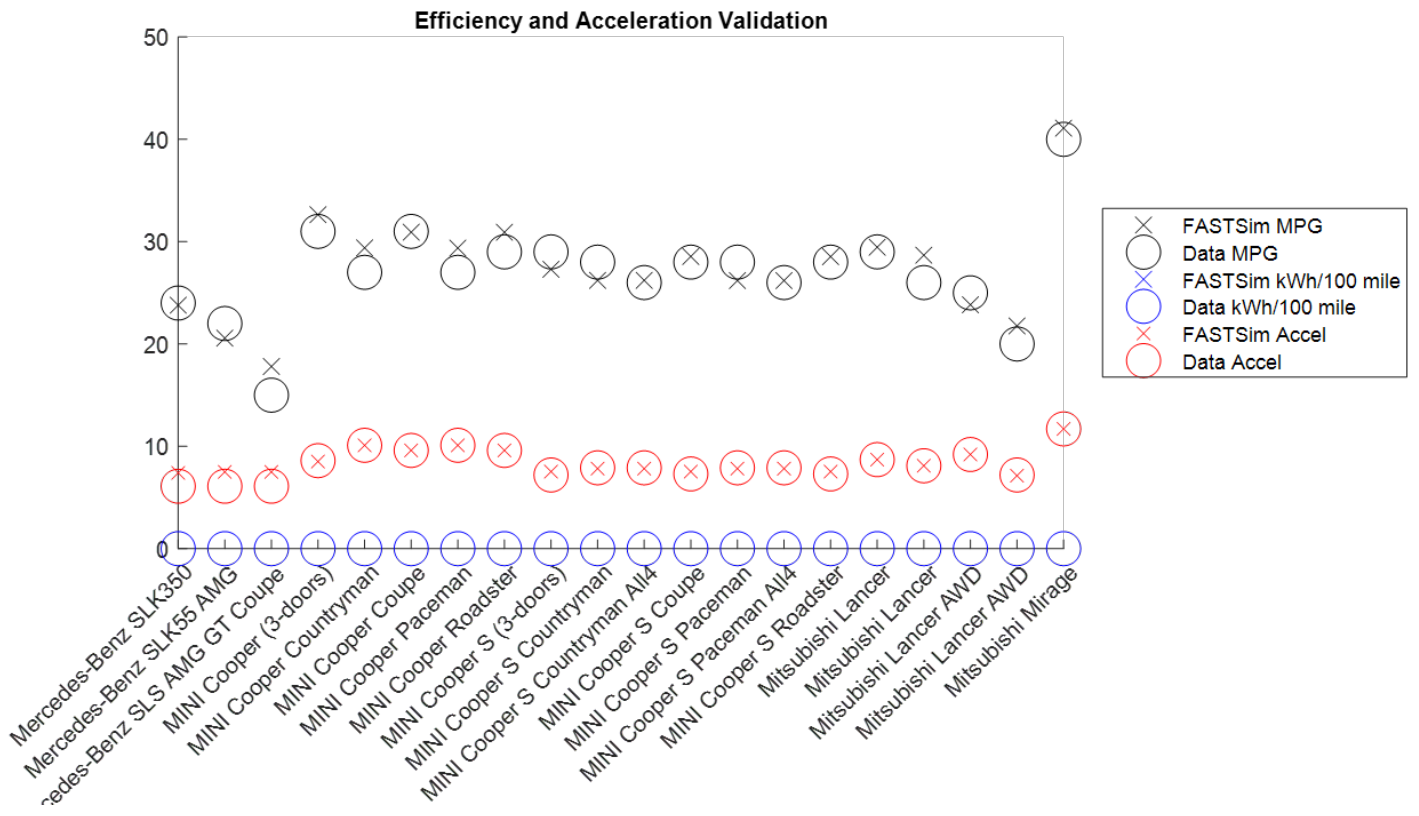


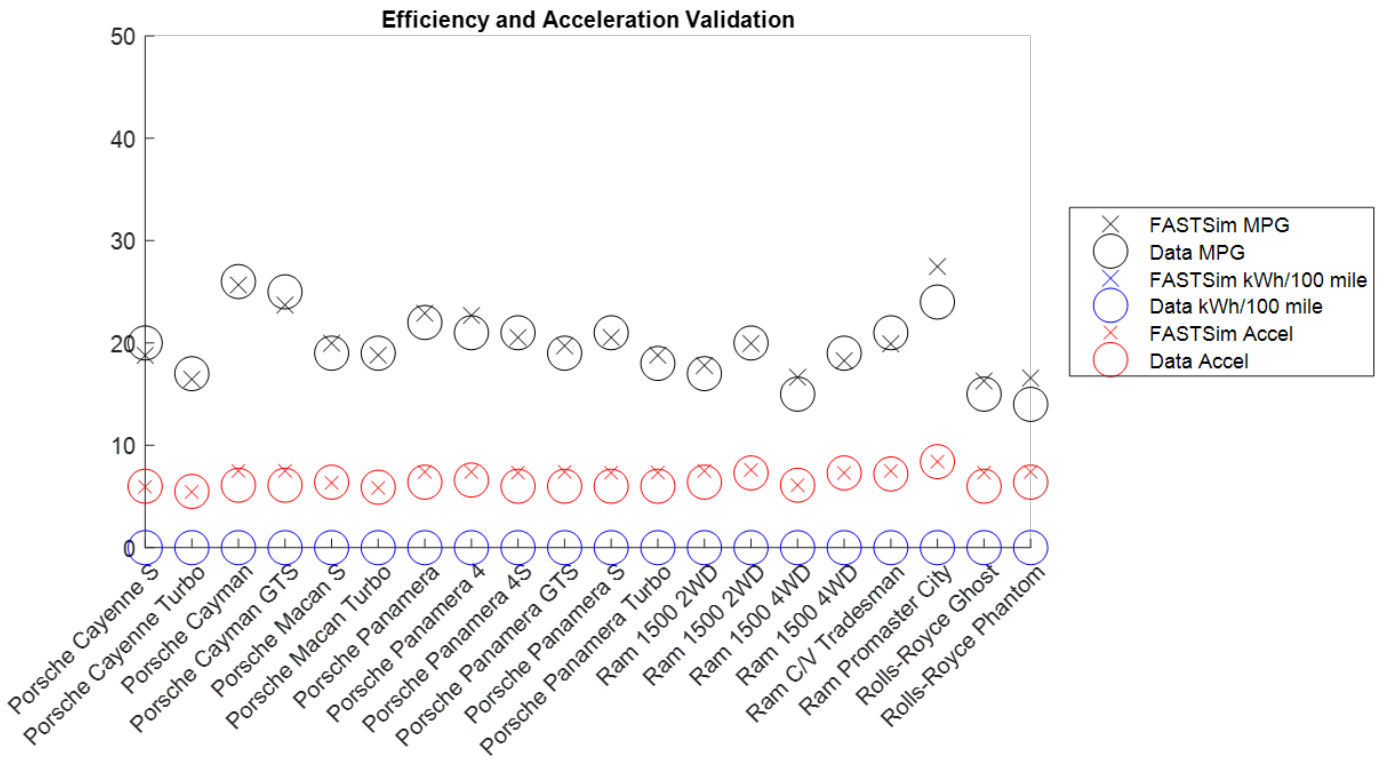
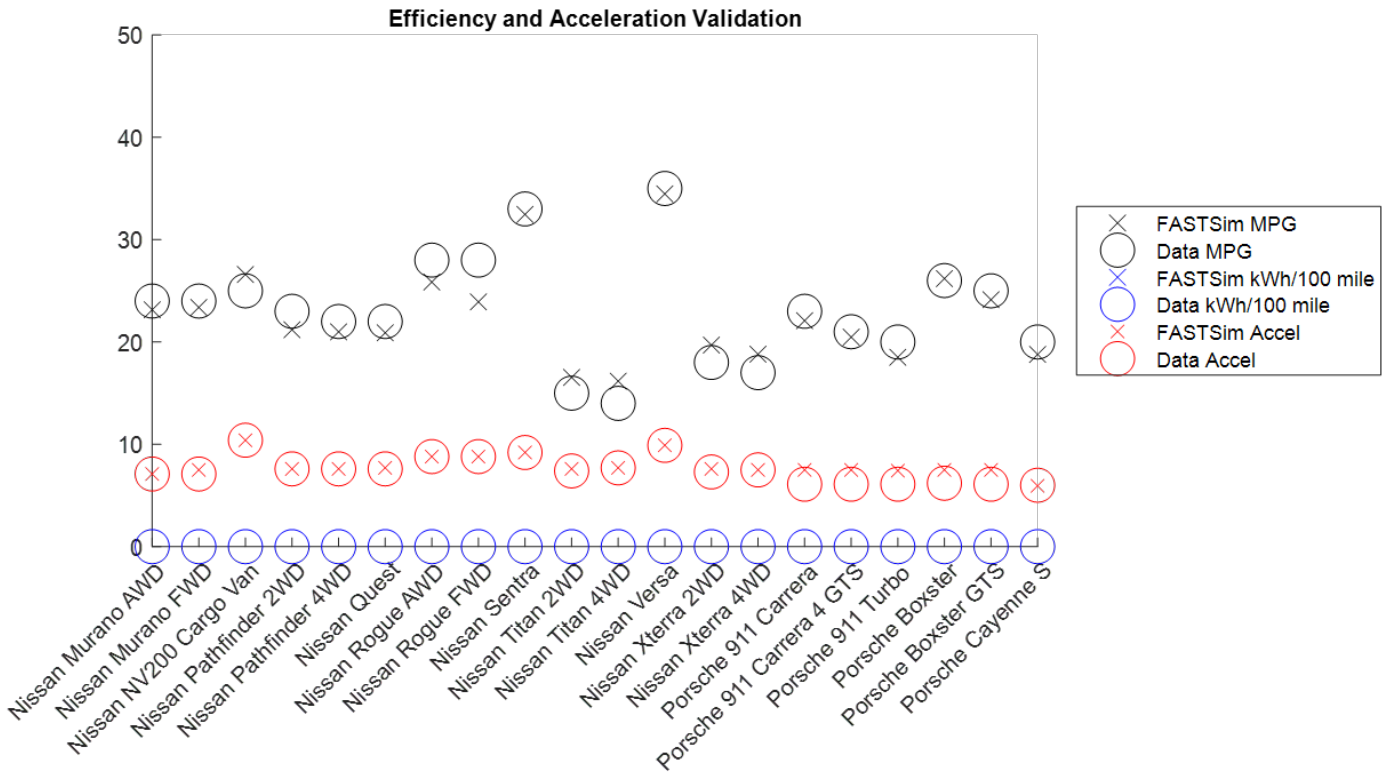


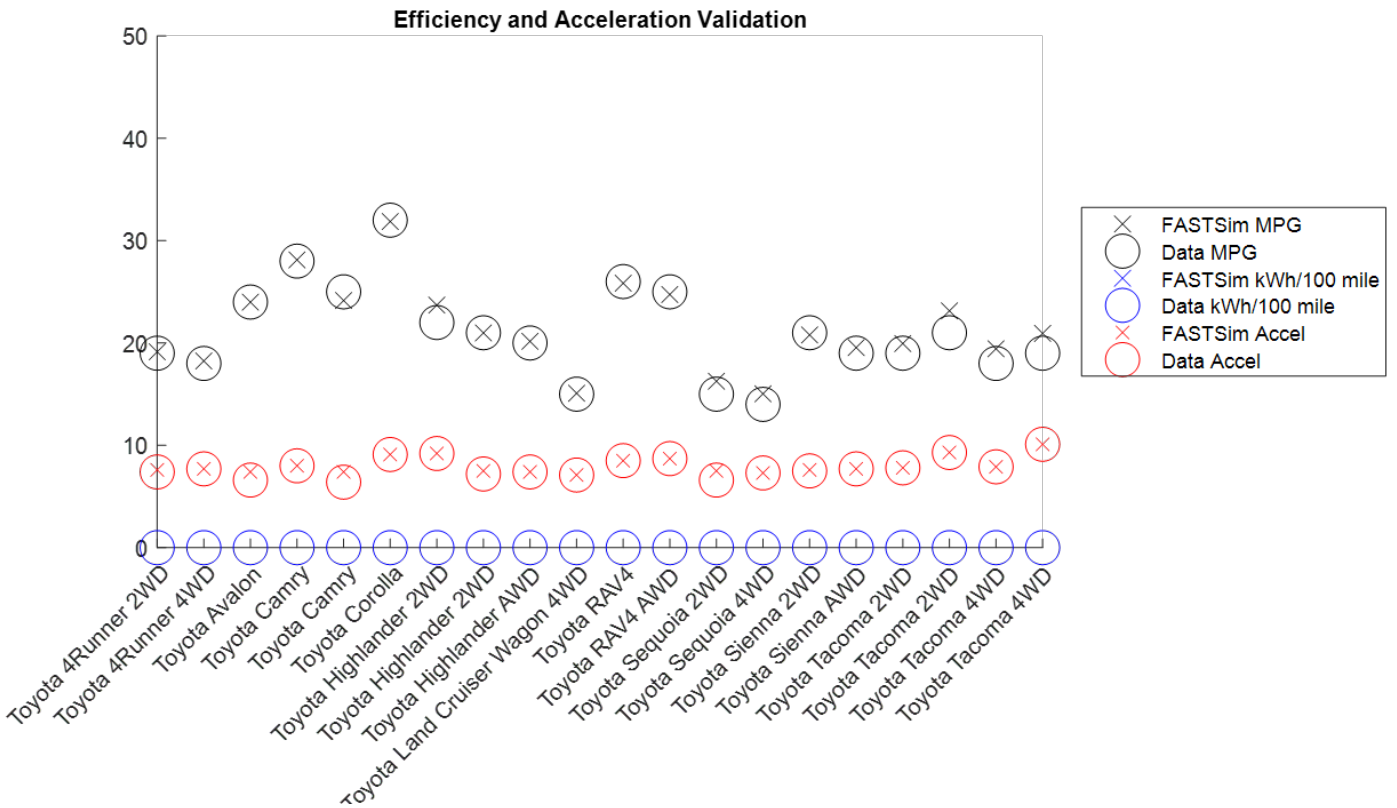
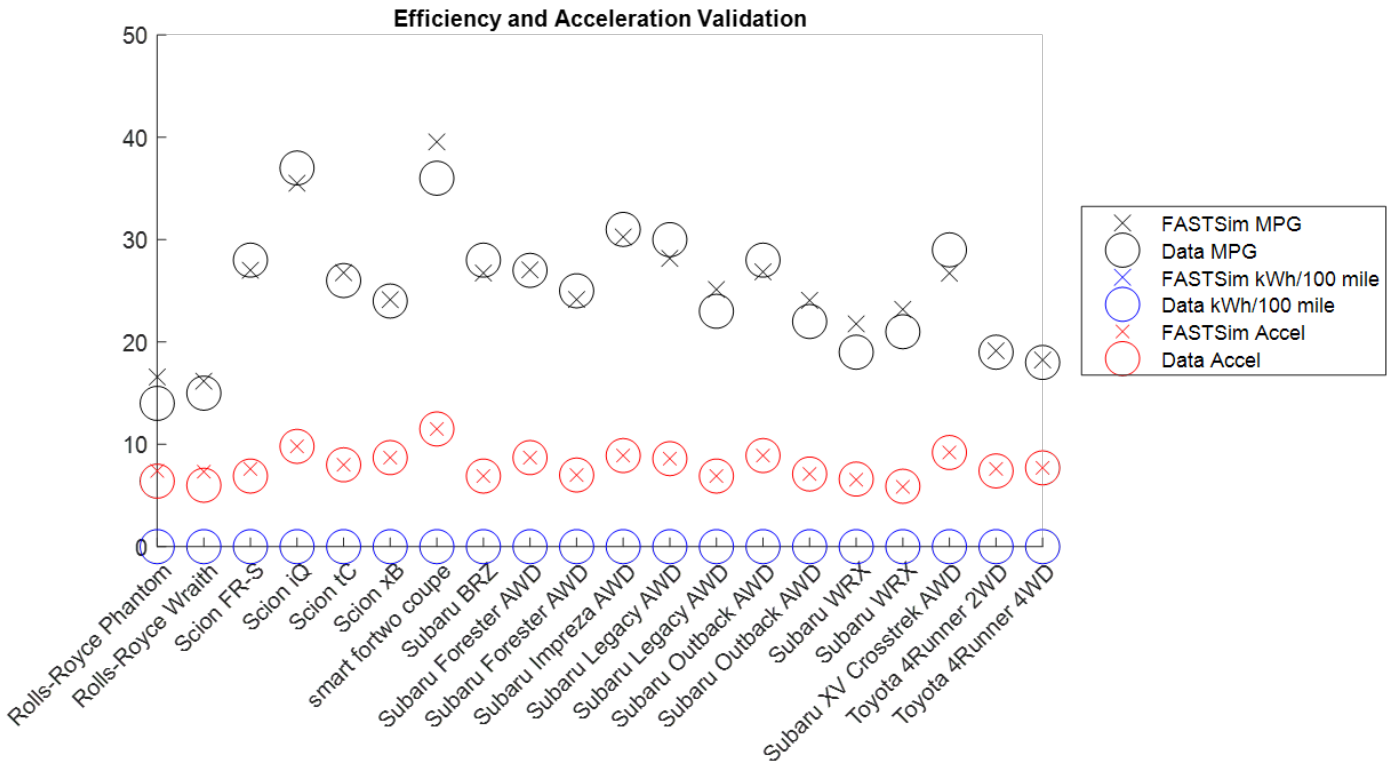


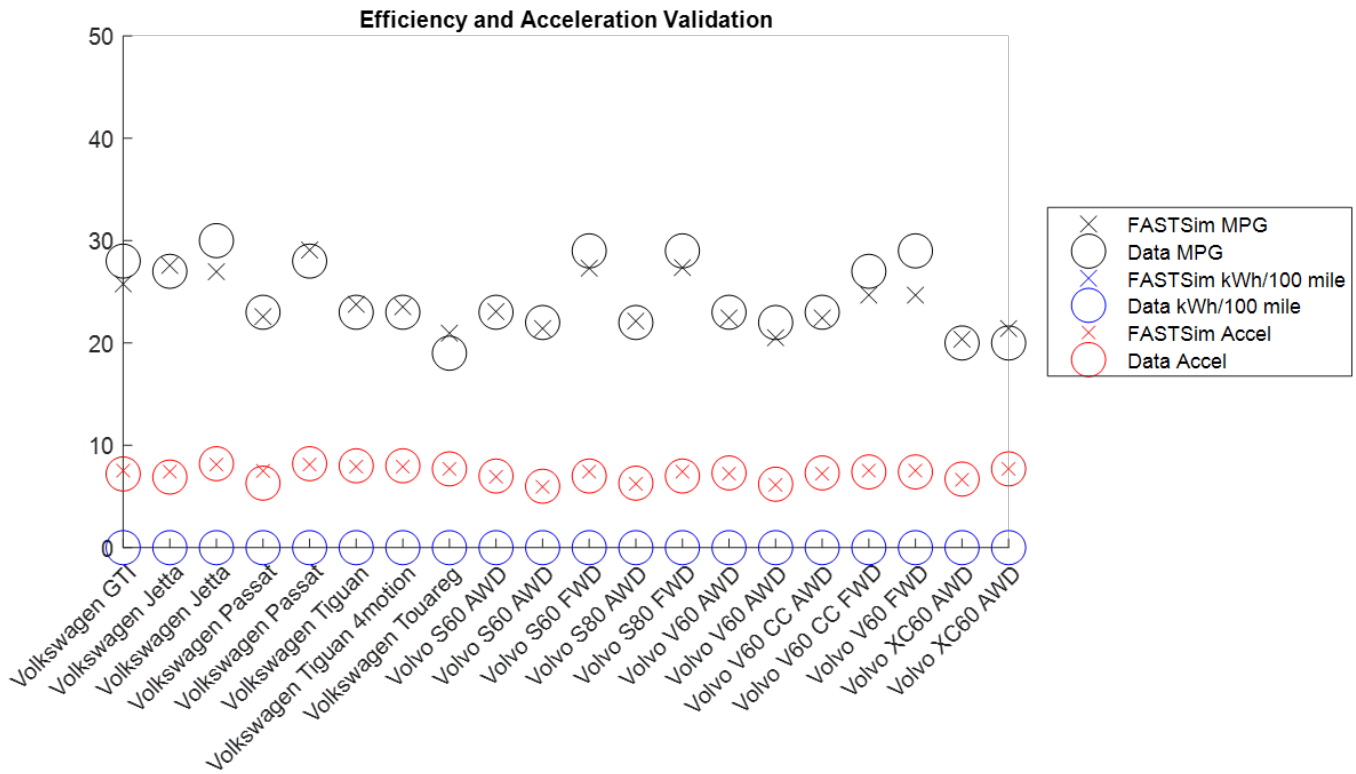
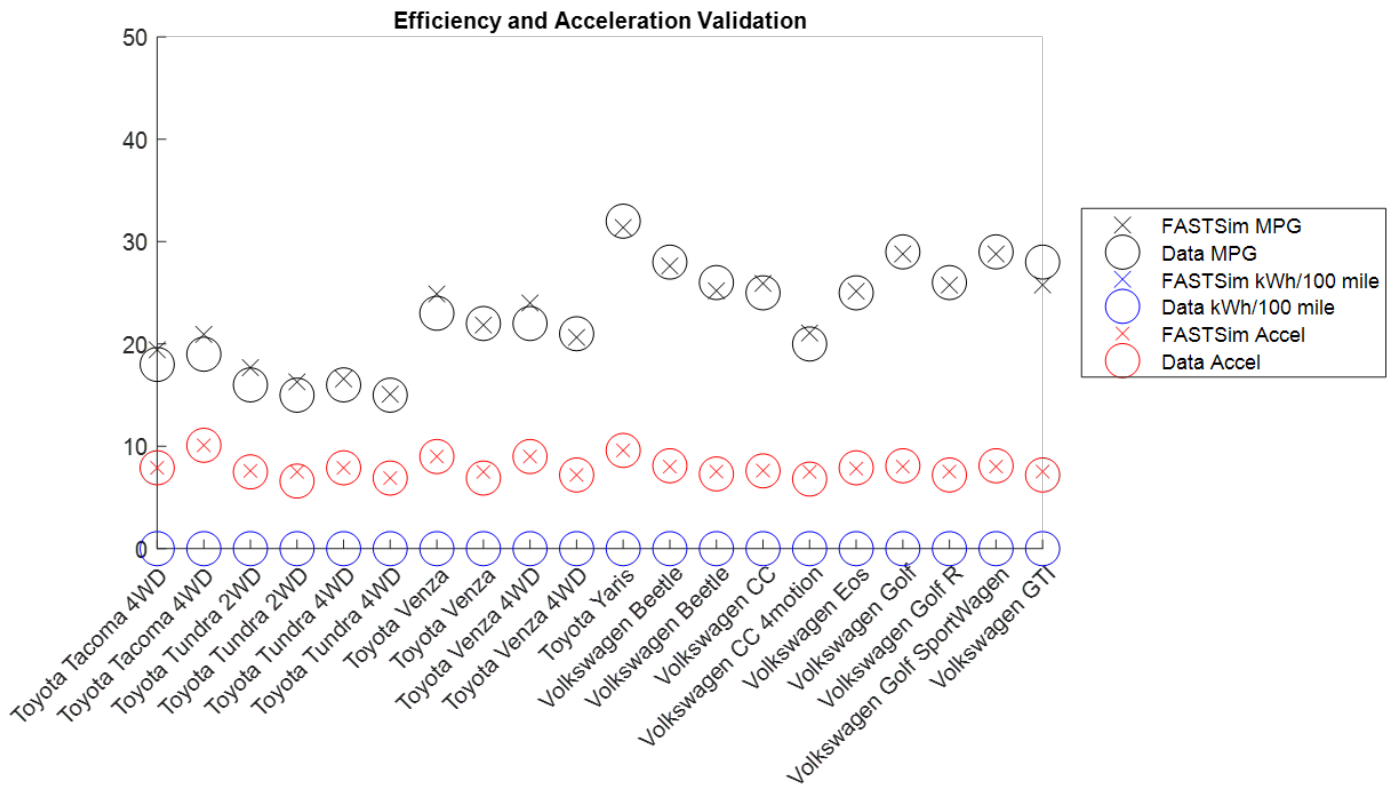


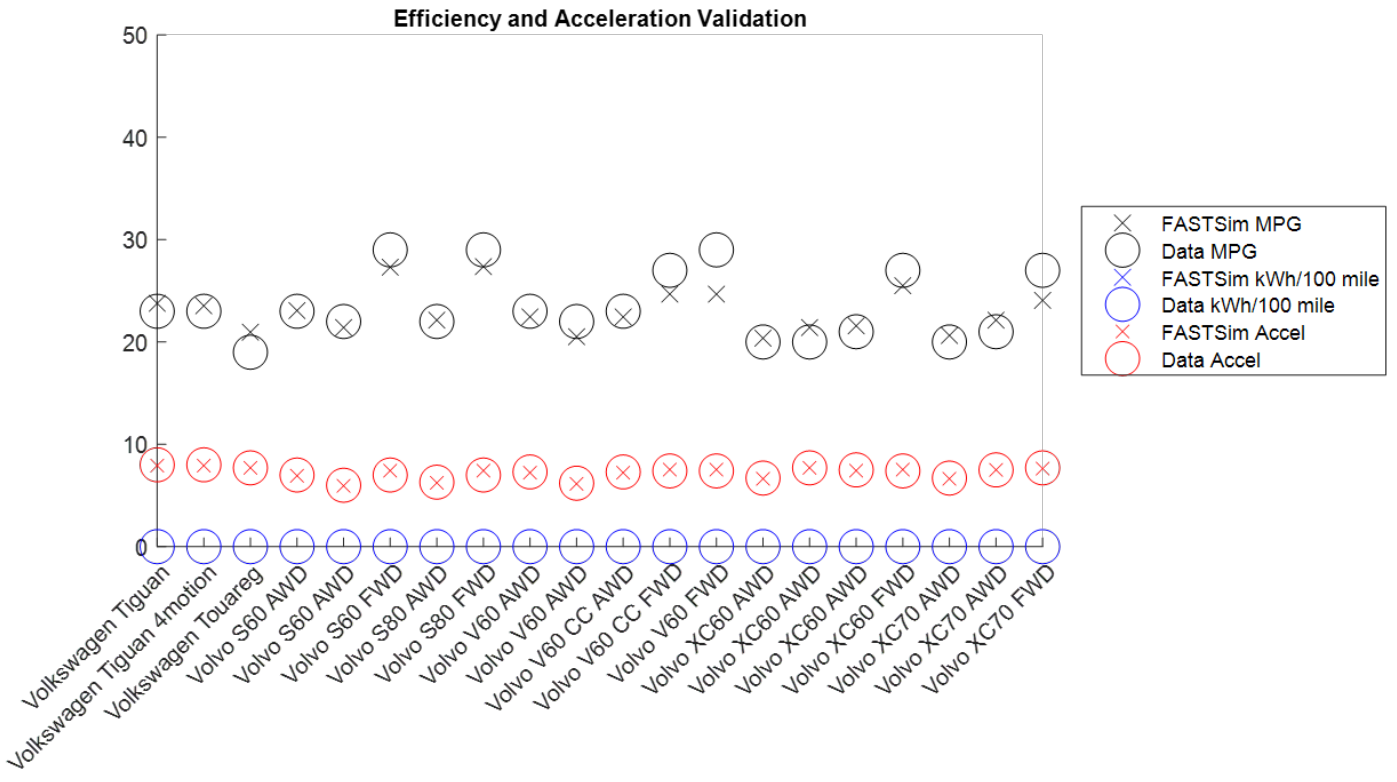












Appendix B: Studies Using FASTSim

The publications area of the FASTSim website at <https://www.nrel.gov/transportation/fastsim-publications.html> continues to be updated as new publications are identified, but the below table lists those FASTSim-supported publications that were identified as of the beginning of 2021.

Title	Authors	Year	Publication
In-Route Inductive Versus Stationary Conductive Charging for Shared Automated Electric Vehicles: A University Shuttle Service	Ahmed A. S. Mohamed, Eric Wood, and Andrew Meintz	2021	<i>Applied Energy</i>
An Optimization-Based Planning Tool for On-Demand Mobility Service Operations	H. M. Abdul Aziz, Venu Garikapati, Tony K. Rodriguez, Lei Zhu, Bingrong Sun, Stanley E. Young, and Yuche Chen	2020	<i>International Journal of Sustainable Transportation</i>
Comparison of Electric Bus Power Consumption Modelling and Simulation Using Basic Power Model, ADVISOR and FASTSim	Chai Wayne Ng and Laonual Yossapong	2020	2nd International Conference on Smart Power and Internet Energy Systems
Route-Sensitive Fuel Consumption Models for Heavy-Duty Vehicles	Alexander Schoen, Andy Byerly, Euzeli Cipriano dos Santos, and Zina Ben-Miled	2020	<i>SAE International Journal of Commercial Vehicles</i>
Scenarios for Transitioning Cars from ICEV to BEVs and PHEVs Using Household Level GPS Travel Data	Wei Ji and Gil Tal	2020	<i>Transportation Research Part D: Transport and Environment</i>
Range Cost-Effectiveness of Plug-in Electric Vehicle for Heterogeneous Consumers: An Expanded Total Ownership Cost Approach	Xu Hao, Zhenhong Lin, Hewu Wang, Shiqi Ou, and Minggao Ouyang	2020	<i>Applied Energy</i>
Automotive Lightweight Design: Simulation Modeling of Mass-Related Consumption for Electric Vehicles	Francesco Del Pero, Lorenzo Berzi, Andrea Antonacci, and Massimo Delogu	2020	<i>Machines</i>
The Impact of Socio-Demographic Characteristics and Driving Behaviors on Fuel Efficiency	He Zhang, Jian Sun, and Ye Tian	2020	<i>Transportation Research Part D: Transport and Environment</i>

Title	Authors	Year	Publication
Estimating Region-Specific Fuel Economy in the United States from Real-World Driving Cycles	Brennan Borlaug, Jacob Holden, Eric Wood, Byungho Lee, Justin Fink, Scott Agnew, and Jason Lustbader	2020	<i>Transportation Research Part D: Transport and Environment</i>
Technical Evaluation of Battery Electric Bus Potential in Mexico City and Leon, Mexico	Kamyria Coney, Karlynn Cory, and Alexandra Aznar	2020	NREL and USAID
Hybrid Electric Drivetrain Testing and Design; Cooperative Research and Development Final Report	Jonathan Burton and Riley Abel	2020	NREL Technical Report
Convolutional Neural Network-Bagged Decision Tree: A Hybrid Approach to Reduce Electric Vehicle's Driver's Range Anxiety by Estimating Energy Consumption in Real Time	Shatrughan Modi, Jhilik Bhattacharya, and Prasenjit Basak	2020	ArXiv Preprint
Influences on Fuel Consumption: The Impact of Driver's Socio-Demographic Characteristics	He Zhang, Jian Sun, and Ye Tian	2020	20th COTA International Conference of Transportation Professionals
Techno-Economic Analysis of Implementing Hybrid Electric Utility Vehicles in Municipal Fleets	Will Northrop, Darrick Zarling, and Shawn Haag	2020	Minnesota Department of Transportation
Real-World Evaluation of National Energy Efficiency Potential of Cold Storage Evaporator Technology in the Context of Engine Start-Stop Systems	Jason Lustbader, Eric Wood, Michael O'Keefe, Nicholas Reinicke, Jeff Mosbacher, Forrest Jehlik, Alvaro Demingo, David Cosgrove, and Yuanpei Song	2020	WCX SAE World Congress Experience
Trends in Life Cycle Greenhouse Gas Emissions of Future Light Duty Electric Vehicles	Hanjiro Ambrose, Alissa Kendall, Mark Lozano, Sadanan Wachche, and Lew Fulton	2020	<i>Transportation Research Part D: Transport and Environment</i>
RouteE: A Vehicle Energy Consumption Prediction Engine	Jacob Holden, Nicholas Reinicke, and Jeff Cappellucci	2020	WCX SAE World Congress, SAE Technical Paper 2020-01-0939

Title	Authors	Year	Publication
Material Efficiency for Immediate Climate Change Mitigation of Passenger Vehicles	Paul Wolfram, Qingshi Tu, Niko Heeren, Stefan Pauliuk, and Edgar Hertwich	2020	<i>Journal of Industrial Ecology</i>
Documentation of Part IV of the RECC Model Framework: Open Dynamic Material Systems Model for the Resource Efficiency-Climate Change Nexus (ODYM-RECC), v2.2	Stefan Pauliuk	2020	Documentation for the UN IRP Assessment of Resource Efficiency and Climate Change Mitigation for G7, India, and China
Life Cycle Assessment of a Fuel Cell Electric Vehicle with an MS-100 System: A Comparison Between a Fuel Cell Electric Vehicle and a Battery Electric Vehicle	Sandra Franz and Anna Liljenroth	2020	Chalmers University of Technology
Techno-Economic Design of EV Powertrain Based on Customer Perspective	Dishanth Vishwanath and Malatesh Godi	2020	Chalmers University of Technology
Planning Optimization for Inductively Charged On-Demand Automated Electric Shuttles Project at Greenville, South Carolina	Ahmed Mohamed, Lei Zhu, Andrew Meintz, and Eric Wood	2019	<i>IEEE Transactions on Industry Applications</i>
Alternative Light- and Heavy-Duty Vehicle Fuel Pathway and Powertrain Optimization	Blake Lane	2019	University of California, Irvine, Mechanical and Aerospace Engineering
Core Modeling: Maintenance, Tools, Real-World Energy Impact Estimation, and Toyota Prius Prime Validation	Phillip Sharer and Aymeric Rousseau	2019	Energy Efficient Mobility Systems 2018 Annual Progress Report
Development of E-Help Manual Using Graphical User Interface (GUI) for Battery Management System (BMS) in Electric Vehicle	N.H. Mohd Amin, M.R. Ab Ghani, A. Jidin, S. Othman, and Z. Jano	2019	<i>Journal of Advanced Manufacturing Technology</i>
Emerging Modeling and Simulations	David Gohlke, Jarod Kelly, and Michael Wang	2019	Analysis, 2018 Annual Progress Report, Vehicle Technologies Office
Energy Analysis and Optimization of Multi-Modal Inter-City Freight Movement	Kevin Walkowicz, Yan Zhou, and Victor Walker	2019	Energy Efficient Mobility Systems 2018 Annual Progress Report

Title	Authors	Year	Publication
Estimation of Energy Consumption of Electric Vehicles Using Deep Convolutional Neural Network to Reduce Driver's Range Anxiety	Shatrughan Modi, Jhilik Bhattacharya, and Prasenjit Basak	2019	<i>ISA Transactions</i>
Impact of Time-Varying Passenger Loading on Conventional and Electrified Transit Bus Energy Consumption	Luying Liu, Andrew Kotz, Aditya Salapaka, Eric Miller, and William Northrop	2019	<i>Transportation Research Record: Journal of the Transportation Research Board</i>
Infrastructure Spatial Sensing at Intersections (LIDAR)	Lei Zhu, Stanley Young, and Erik Rask	2019	Energy Efficient Mobility Systems 2018 Annual Progress Report
Instantaneous Fuel Consumption Estimation Using Smartphones	Samuel Shaw, Yunfei Hou, Weida Zhong, Qingquan Sun, Tong Guan, and Lu Su	2019	IEEE 90th Vehicular Technology Conference
Jamaica Urban Transit Company Drive-Cycle Analysis	Mark Singer and Caley Johnson	2019	National Renewable Energy Laboratory
Light-Duty Hydrogen Infrastructure Analysis at NREL	Michael Penev, Chad Hunter, Brian Bush, Elizabeth Connelly, and Maggie Mann	2019	Green Transportation Summit
Modeling the Effect of Power Consumption in Automated Driving Systems on Vehicle Energy Efficiency for Real-World Driving in California	Karim Hamza, John Willard, Kang-Ching Chu, and Kenneth Laberteaux	2019	<i>Transportation Research Record: Journal of the Transportation Research Board</i>
Optimizing the Electric Range of Plug-in Vehicles via Fuel Economy Simulations of Real-World Driving in California	Kenneth Laberteaux, Karim Hamza, and John Willard	2019	<i>Transportation Research Part D: Transport and Environment</i>
Optimum Planning for Inductively Charged On-Demand Automated Electric Shuttles at Greenville, South Carolina	Ahmed Mohamed, Lei Zhu, Andrew Meintz, and Eric Wood	2019	IEEE Industry Applications Society Annual Meeting
Thermal System for Electric Vehicles with Coolant-Based Heat Pump	Sourav Chowdhury, Lindsey Leitzel, and Mark Zima	2019	<i>ATZ Worldwide</i>

Title	Authors	Year	Publication
A Pareto Trade-Off Analysis of Cost Versus Greenhouse Gas Emissions for a Model of a Mid-Sized Vehicle with Various Powertrains	K. Hamza, J. Willard, K. Chu, and K. Laberteaux	2018	ASME 2018 International Design Engineering Technical Conferences and Computers and Information in Engineering Conference
A Study on Opportune Reduction in Greenhouse Gas Emissions via Adoption of Electric Drive Vehicles in Light-Duty Vehicle Fleets	K. Laberteaux and K. Hamza	2018	<i>Transportation Research Part D: Transport and Environment</i>
A Study on Optimal Powertrain Sizing of Plugin Hybrid Vehicles for Minimizing Criteria Emissions Associated with Cold Starts	K. Hamza and K. Laberteaux	2018	SAE World Congress
Cooperative and Integrated Vehicle and Intersection Control for Energy Efficiency (CIVIC-E²)	Y. Hou, S. Seliman, E. Wang, J. Gonder, E. Wood, Q. He, A. Sadek, L. Su, and C. Qiao	2018	<i>IEEE Transactions on Intelligent Transportation Systems</i>
Decarbonisation of Urban Freight Transport Using Electric Vehicles and Opportunity Charging	T. Teoh, O. Kunze, C. Teo, and Y. Wong	2018	<i>Sustainability</i>
Determining Off-Cycle Fuel Economy Benefits of Two-Layer HVAC Technology	F. Jehlik, N. Chevers, M. Moniot, and Y. Song	2018	SAE International
Electric Drive Technologies Development	C. Zhu	2018	FY 2017 Annual Progress Report, Electric Drive Technologies Development, High-Efficiency High-Density GaN-Based 6.6 kW Bidirectional On-Board Charger for PEVs
EVLibSim: A Tool for the Simulation of Electric Vehicles' Charging Stations Using the EVLib Library	E. Rigas, S. Karapostolakis, N. Bassiliades, and S. Ramchurn	2018	<i>Simulation Modelling Practice and Theory</i>
Forecasting the Value of Battery Electric Vehicles Compared to Internal Combustion Engine Vehicles: The Influence of Driving Range and Battery Technology	J. Woo and C. Magee	2018	Massachusetts Institute of Technology

Title	Authors	Year	Publication
Future Automotive Systems Technology Simulator (FASTSim) Validation Report	J. Gonder, A. Brooker, E. Wood, and M. Moniot	2018	National Renewable Energy Laboratory
Impact of Battery Performance on Total Cost of Ownership for Electric Drive Vehicle	P. Prevedouros and L. Mitropoulos	2018	International Conference on Intelligent Transportation Systems
Increasing the Fuel Economy of Connected and Autonomous Lithium-Ion Electrified Vehicles	Z. Asher, D. Trinko, and T. Bradley	2018	<i>Behaviour of Lithium-Ion Batteries in Electric Vehicle</i>
Light-Duty Vehicle Attribute Projections (Years 2015–2030)	E. Kontou, M. Melaina, and A. Brooker	2018	California Energy Commission report prepared by the National Renewable Energy Laboratory
Microscopic Series Plug-in Hybrid Electric Vehicle Energy Consumption Model: Model Development and Validation	C. Fioria, K. Ahnb, and H. Rakhac	2018	<i>Transportation Research Part D: Transport and Environment</i>
Modeling and Simulation of Automated Mobility Districts	V. Garikapati	2018	U.S. Department of Energy Vehicle Technologies Office Annual Merit Review
Modelling Energy Consumption of Electric Freight Vehicles in Urban Pickup/Delivery Operations: Analysis and Estimation on a Real-World Dataset	C. Fiori and V. Marzano	2018	<i>Transportation Research Part D: Transport and Environment</i>
Modelling the Effect of Driving Events on Electrical Vehicles Energy Consumption Using Inertial Sensors in Smartphones	D. Jiménez, S. Hernández, J. Fraile-Ardanuy, J. Serrano, R. Fernández, and F. Alvarez	2018	<i>Energies</i>
Navigation Application Programming Interface Route Fuel Saving Opportunity Assessment on Large-Scale Real-World Travel Data for Conventional Vehicles and Hybrid Electric Vehicles	L. Zhu, J. Holden, and J. Gonder	2018	<i>Transportation Research Record</i>
Quantifying the Mobility and Energy Benefits of Automated Mobility Districts Using Microscopic Traffic Simulation	L. Zhu, V. Garikapati, Y. Chen, Y. Hou, H. Abdul Aziz, and S. Young	2018	International Conference on Transportation and Development: Connected and

Title	Authors	Year	Publication
			Autonomous Vehicles and Transportation Safety
Total Thermal Management of Battery Electric Vehicles	S. Chowdhury, L. Leitzel, M. Zima, M. Santacesaria, G. Titov, J. Lustbader, J. Rugh, J. Winkler, A. Khawaja, and M. Govindarajalu	2018	CO ₂ Reduction for Transportation Systems Conference
A Computationally Efficient Simulation Model for Estimating Energy Consumption of Electric Vehicles in the Context of Route Planning Applications	K. Genikomsakis and G. Mitrentsis	2017	<i>Transportation Research Part D: Transport and Environment</i>
A Study of Greenhouse Gas Emissions Reduction Opportunity in Light-Duty Vehicles by Analyzing Real Driving Patterns	K. Laberteaux and K. Hamza	2017	SAE World Conference
Green Routing Fuel Saving Opportunity Assessment: A Case Study on California Large-Scale Real-World Travel Data	L. Zhu, J. Holden, E. Wood, and J. Gonder	2017	IEEE Intelligent Vehicles Symposium
Highlighting the Differential Benefit in Greenhouse Gas Reduction via Adoption of Plug-In Hybrid Vehicles for Different Patterns of Real Driving	K. Laberteaux and K. Hamza	2017	SAE World Conference
In-Use Energy and CO₂ Emissions Impact of a Plug-In Hybrid and Battery Electric Vehicle Based on Real-World Driving	Y. Chen, K. Hu, J. Zhao, G. Li, J. Johnson, and J. Zietsman	2017	<i>International Journal of Environmental Science and Technology</i>
Modeling Control Strategies and Range Impacts for Electric Vehicle Integrated Thermal Management Systems with MATLAB/Simulink	G. Titov and J. Lustbader	2017	SAE World Congress
On-Road Validation of a Simplified Model for Estimating Real-World Fuel Economy	E. Wood, J. Gonder, and F. Jehlik	2017	<i>SAE International Journal of Fuels and Lubricants</i>
Plug-in Fuel Cell Electric Vehicles: A California Case Study	B. Lane, B. Shaffer, and G. Samuelsen	2017	<i>International Journal of Hydrogen Energy</i>
Technology Comparison for Spark Ignition Engines of New Generation	M. De Cesare, N. Cavina, and L. Paiano	2017	<i>SAE International Journal of Engines</i>

Title	Authors	Year	Publication
A Cluster Analysis Study of Opportune Adoption of Electric Drive Vehicles for Better Greenhouse Gas Reduction	K. Hamza and K. Laberteaux	2016	ASME Design Engineering Technical Conference
A Review of Computer Tools for Modeling Electric Vehicle Energy Requirements and Their Impact on Power Distribution Networks	K. Mahmud and G. Town	2016	<i>Applied Energy</i>
Aerodynamic Drag Reduction Technologies Testing of Heavy-Duty Vocational Vehicles and a Dry Van Trailer	A. Ragatz and M. Thornton	2016	National Renewable Energy Laboratory
An Energy Reallocation Model for Estimation of Equivalent Greenhouse Gas Emissions of Various Charging Behaviors of Plugin Hybrid Electric Vehicles	K. Hamza and K. Laberteaux	2016	<i>SAE International Journal of Alternative Powertrains</i>
An Opportunistic Wireless Charging System Design for an On-Demand Shuttle Service	K. Doubleday, A. Meintz, and T. Markel	2016	IEEE Transportation Electrification Conference and Expo
Analysis of Electric Vehicle Powertrain Simulators for Fuel Consumption Calculations	K. Davis and J. Hayes	2016	International Conference on Electrical Systems for Aircraft, Railway, Ship Propulsion, and Road Vehicles and International Transportation Electrification Conference
Analysis of In-Route Wireless Charging for the Shuttle System at Zion National Park	A. Meintz, R. Prohaska, A. Konan, A. Ragatz, T. Markel, and K. Kelly	2016	IEEE PELS Workshop on Emerging Technologies: Wireless Power Transfer
Assessing the Energy Impact of Traffic Management and Vehicle Hybridisation	D. Karbowski, N. Kim, J. Auld, and V. Sokolov	2016	<i>International Journal of Complexity in Applied Science and Technology</i>
Assessing the Stationary Energy Storage Equivalency of Vehicle-to-Grid Charging Battery Electric Vehicles	B. Tarroja, L. Zhang, V. Wifvat, B. Shaffer, and S. Samuelsen	2016	<i>Energy</i>
Design and Evaluation of Cyber Transportation Systems	Y. Hou	2016	State University of New York at Buffalo

Title	Authors	Year	Publication
Charging a Renewable Future: The Impact of Electric Vehicle Charging Intelligence on Energy Storage Requirements to Meet Renewable Portfolio Standards	K. Forrest, B. Tarroja, L. Zhang, B. Shaffer, and S. Samuelson	2016	<i>Journal of Power Sources</i>
Impacts of Adding Photovoltaic Solar System On-Board to Internal Combustion Engine Vehicles Toward Meeting 2025 Fuel Economy CAFE Standards	M. Abdelhamid, I. Haque, S. Pilla, Z. Filipi, and R. Singh	2016	<i>SAE International Journal of Alternative Powertrains</i>
Methodology to Evaluate the Operational Suitability of Electromobility Systems for Urban Logistics Operations	T. Teoh, O. Kunze, and C. Teo	2016	<i>Transportation Research Procedia</i>
Optimal Design and Techno-Economic Analysis of a Hybrid Solar Vehicle: Incorporating Solar Energy as an On-Board Fuel Toward Future Mobility	M. Abdelhamid, I. Haque, R. Singh, S. Pilla, and Z. Filipi	2016	ASME International Conference on Advanced Vehicle Technologies
Regression Based Emission Models for Vehicle Contribution to Climate Change	A. Pijoan, I. Oribe-Garcia, O. Kamara-Esteban, K. Genikomsakis, C. Borges, and A. Alonso-Vicario	2016	<i>Transport Systems, Theory and Practice</i>
The Evaluation of the Impact of New Technologies for Different Powertrain Medium-Duty Trucks on Fuel Consumption	L. Wang, A. Duran, K. Kelly, A. Konan, M. Lammert, and R. Prohaska	2016	SAE Commercial Vehicle Engineering Congress
A Cost Effectiveness Analysis of Quasi-Static Wireless Power Transfer for Plug-In Hybrid Electric Transit Buses	L. Wang, J. Gonder, E. Burton, A. Brooker, A. Meintz, and A. Konan	2015	IEEE Vehicle Power and Propulsion Conference
ADOPT: A Historically Validated Light-Duty Vehicle Consumer Choice Model	A. Brooker, J. Gonder, S. Lopp, and J. Ward	2015	SAE World Congress and Exhibition
Assessment of Alternative Fuel and Powertrain Transit Bus Options Using Real-World Operations Data: Life-Cycle Fuel and Emissions Modeling	Y. Xu, F. Gbologah, D. Lee, H. Liu, M. Rodgers, and R. Guensler	2015	<i>Applied Energy</i>

Title	Authors	Year	Publication
Combined Fluid Loop Thermal Management for Electric Drive Vehicle Range Improvement	D. Leighton	2015	SAE World Congress
Combining Agent-Based Modeling and Life Cycle Assessment for the Evaluation of Mobility Policies	Q. Florent and B. Enrico	2015	<i>Environmental Science & Technology</i>
Electric Vehicle Cost, Emissions, and Water Footprint in the United States: Development of a Regional Optimization Model	M. Noori, S. Gardner, and O. Tatari	2015	<i>Energy</i>
Evaluating the Impact of Road Grade on Simulated Commercial Vehicle Fuel Economy Using Real-World Drive Cycles	S. Lopp, E. Wood, and A. Duran	2015	SAE Commercial Vehicle Engineering Congress
Impact of Powertrain Electrification, Vehicle Size Reduction, and Lightweight Materials Substitution on Energy Use, CO2 Emissions, and Cost of a Passenger Light-Duty Vehicle Fleet	J. Palencia, T. Sakamaki, M. Araki, and S. Shiga	2015	<i>Energy</i>
Measuring the Benefits of Public Chargers and Improving Infrastructure Deployments Using Advanced Simulation Tools	E. Wood, J. Neubauer, and E. Burton	2015	SAE World Congress
Modeling Heavy/Medium-Duty Fuel Consumption Based on Drive Cycle Properties	L. Wang, A. Duran, J. Gonder, and K. Kelly	2015	SAE Commercial Vehicle Engineering Congress
Quantifying the Effect of Fast Charger Deployments on Electric Vehicle Utility and Travel Patterns via Advanced Simulation	E. Wood, J. Neubauer, and E. Burton	2015	SAE World Congress
Quantitative Effects of Vehicle Parameters on Fuel Consumption for Heavy-Duty Vehicle	L. Wang, K. Kelly, K. Walkowicz, and A. Duran	2015	SAE Commercial Vehicle Engineering Congress
Simulated Real-World Energy Impacts of a Thermally Sensitive Powertrain Considering Viscous Losses and Enrichment	F. Jehlik, E. Wood, J. Gonder, and S. Lopp	2015	<i>SAE International Journal of Materials and Manufacturing</i>
Suitability of Synthetic Driving Profiles from Traffic Micro-Simulation for Real-World Energy Analysis	Y. Hou, E. Wood, E. Burton, and J. Gonder	2015	ITS World Congress

Title	Authors	Year	Publication
The Importance of Grid Integration for Achievable Greenhouse Gas Emissions Reductions from Alternative Vehicle Technologies	B. Tarroja, B. Shaffer, and S. Samuelsen	2015	<i>Energy</i>
Thru-Life Impacts of Driver Aggression, Climate, Cabin Thermal Management, and Battery Thermal Management on Battery Electric Vehicle Utility	J. Neubauer and E. Wood	2015	<i>Journal of Power Sources</i>
Will Your Battery Survive a World with Fast Chargers?	J. Neubauer and E. Wood	2015	SAE World Congress
Contribution of Road Grade to the Energy Use of Modern Automobiles Across Large Datasets of Real-World Drive Cycles	E. Wood, E. Burton, A. Duran, and J. Gonder	2014	SAE World Congress
Optimization of Fuel Economy of Hybrid Electric Vehicles Using Set Based Dynamic Programming	N. Ramaswamy and N. Sadegh	2014	ASME Dynamic Systems and Control Conference
Updating United States Advanced Battery Consortium and Department of Energy Battery Technology Targets for Battery Electric Vehicles	J. Neubauer, A. Pesaran, C. Bae, R. Elder, B. Cunningham	2014	<i>Journal of Power Sources</i>
Assessing the Battery Cost at Which Plug-In Hybrid Medium-Duty Parcel Delivery Vehicles Become Cost-Effective	L. Ramroth, J. Gonder, and A. Brooker	2013	SAE World Congress
Lightweighting Impacts on Fuel Economy, Cost, and Component Losses	A. Brooker, J. Ward, and L. Wang	2013	SAE World Congress
Overcoming the Range Limitation of Medium-Duty Battery Electric Vehicles Through the Use of Hydrogen Fuel Cells	E. Wood, L. Wang, J. Gonder, and M. Ulsh	2013	<i>SAE International Journal of Commercial Vehicles</i>
Sensitivity of Plug-In Hybrid Electric Vehicle Economics to Drive Patterns, Electric Range, Energy Management, and Charge Strategies	J. Neubauer, A. Brooker, and E. Wood	2013	<i>Journal of Power Sources</i>
Quantifying Uncertainty in Vehicle Simulation Studies	B. Geller and T. Bradley	2012	<i>SAE International Journal of Passenger Cars – Mechanical Systems</i>

Title	Authors	Year	Publication
Sensitivity of Battery Electric Vehicle Economics to Drive Patterns, Vehicle Range, and Charge Strategies	J. Neubauer, A. Brooker, and E. Wood	2012	<i>Journal of Power Sources</i>
Variability of Battery Wear in Light-Duty Plug-In Electric Vehicles Subject to Ambient Temperature, Battery Size, and Consumer Usage	E. Wood, J. Neubauer, A. Brooker, J. Gonder, and K. Smith	2012	International Battery, Hybrid, and Fuel Cell Electric Vehicle Symposium 26
Technology Improvement Pathways to Cost-Effective Vehicle Electrification	A. Brooker, M. Thornton, and J. Rugh	2010	SAE World Congress

Appendix C: Supplemental Plots

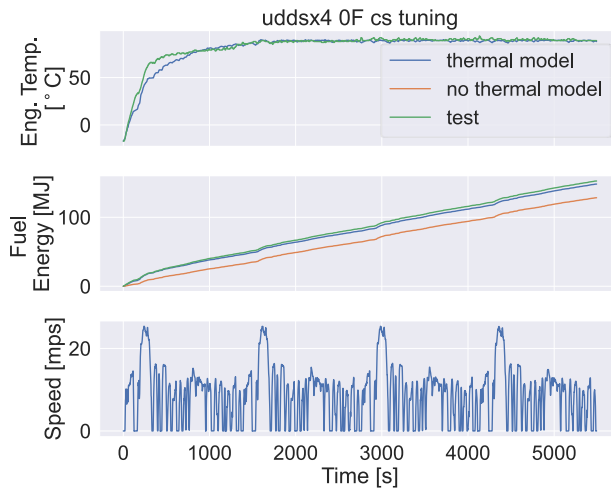


Figure C-1. Four repeated UDDS cycles with 0°F ambient/start temperature

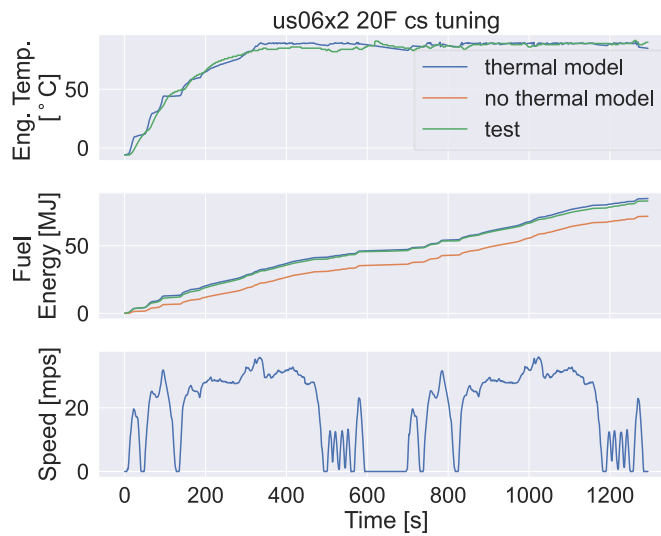


Figure C-2. Two repeated US06 cycles with 20°F ambient/start temperature

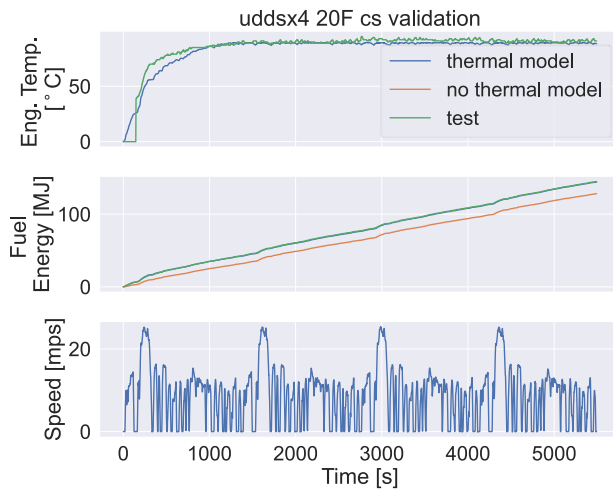


Figure C-3. Four repeated UDDS cycles with 20°F ambient/start temperature

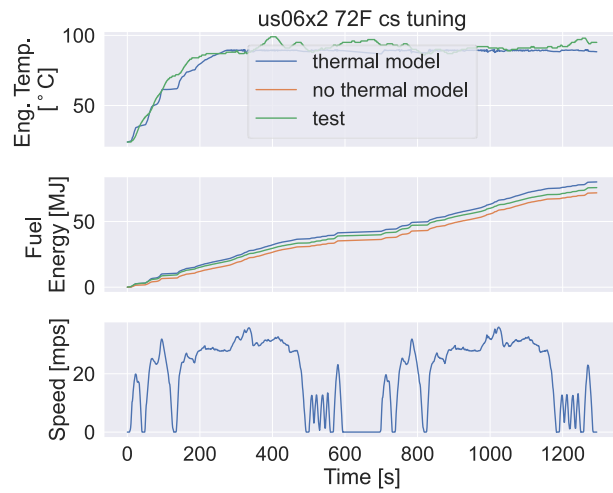


Figure C-4. Two repeated UDDS cycles with 72°F ambient/start temperature

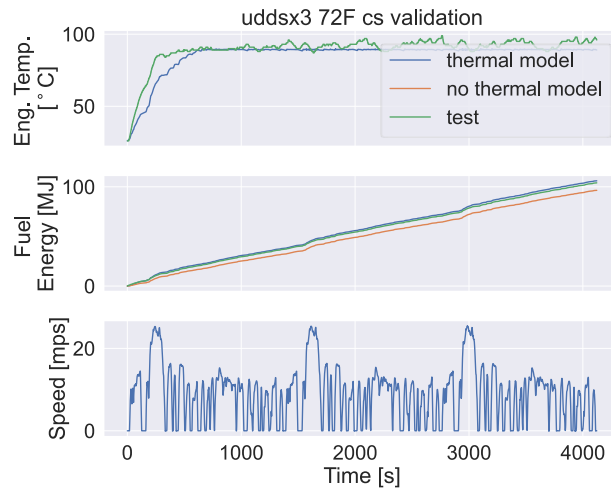


Figure C-5. Three repeated UDDS cycles with 72°F ambient/start temperature